Friedrich-Alexander-Universität
Erlangen-Nürnberg

Erlangen Centre for Astroparticle Physics

Gamma-Ray Astronomy

II – Galactic Sources

Dr Alison Mitchell
Junior Research Group Leader,
FAU Erlangen-Nürnberg

Astroparticle School, Obertrubach-Bärnfels
12th October 24

Emmy Noether-Programm
DFG Deutsche Forschungsgemeinschaft

Funded by
DFG Deutsche Forschungsgemeinschaft
German Research Foundation

Cosmic Ray sources

Transition between galactic and extragalactic accelerators starts at ~10^{15}eV and ends at the ankle ~10^{18}eV.

Recent growth in the number of known sources at UHE (≥100 TeV) - mainly thanks to HAWC & LHAASO

“PeVatrons” = accelerators of particles to energies ≥ 10^{15} eV

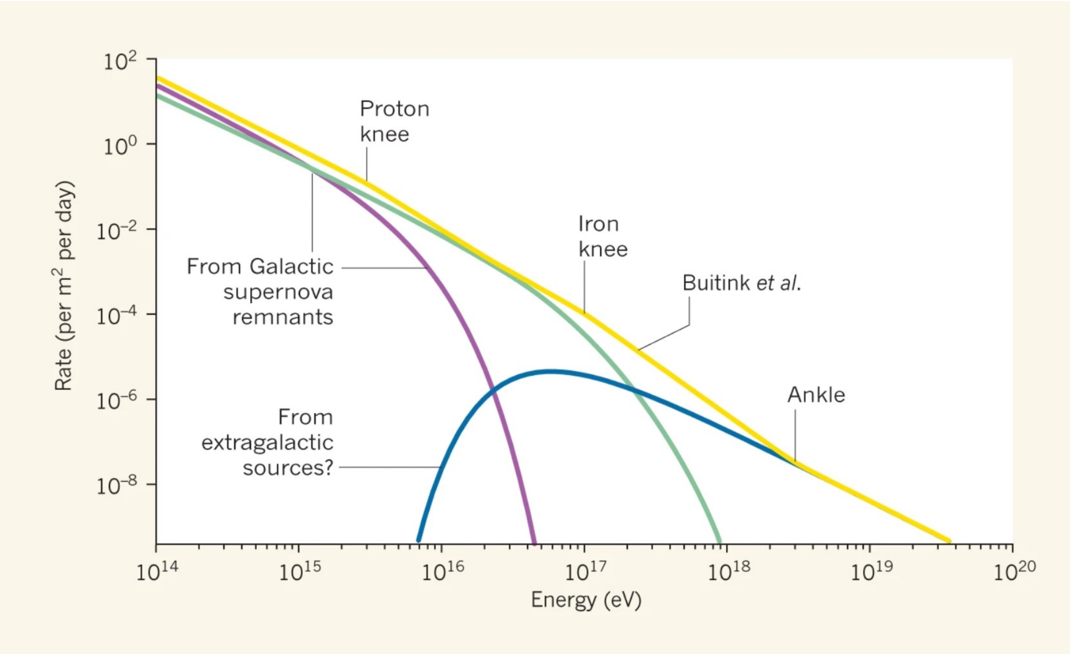

Taylor, Nature **531** 43-44 (2016)

Kifune plot (Credit: Stephen Fegan) + UHE γ rays

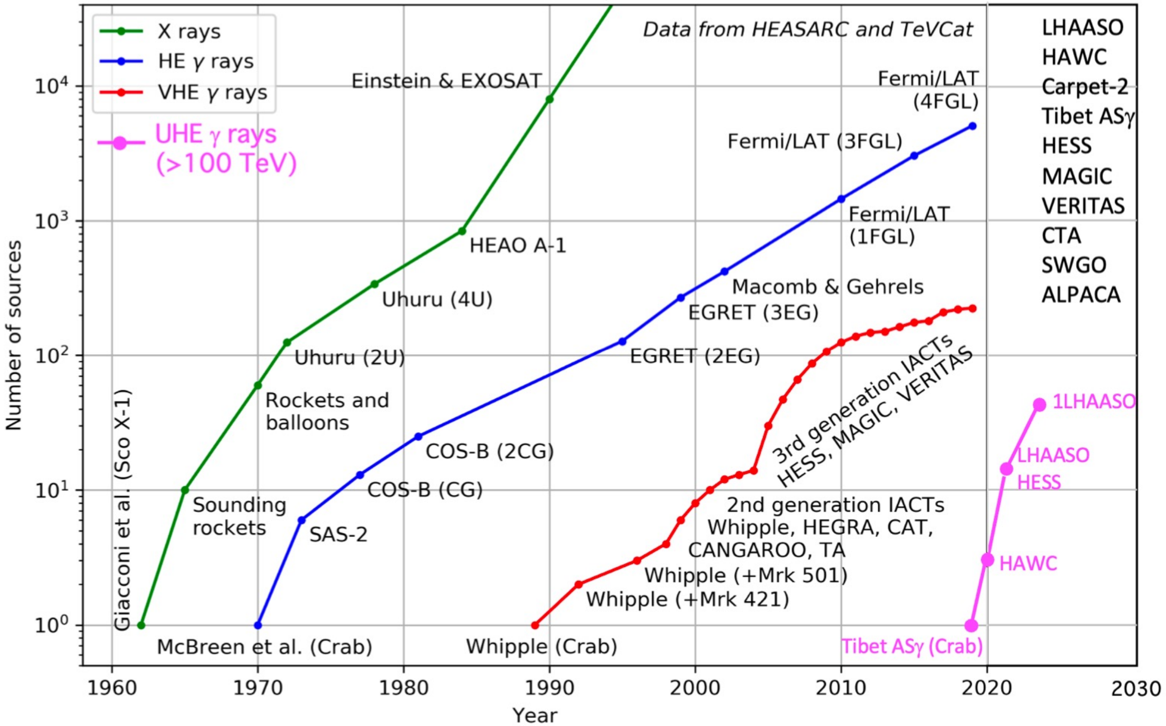

For the production of cosmic rays, we are mostly interested in the end stages of stellar evolution

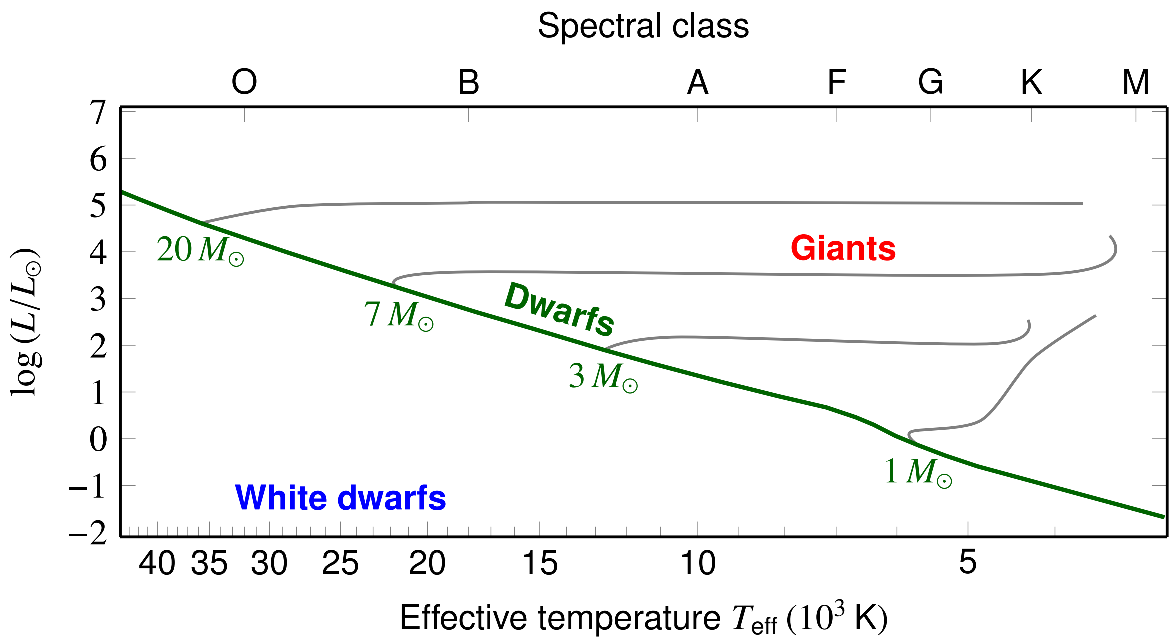

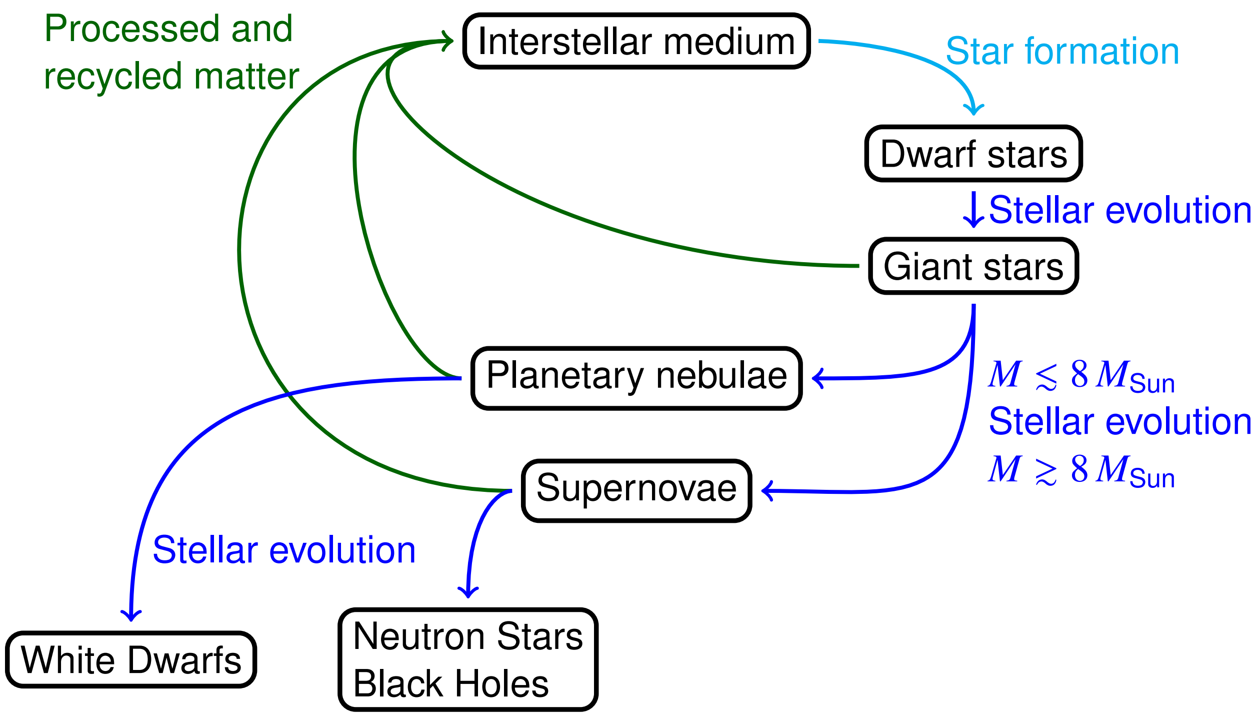

Core-collapse Supernovae

1. Nuclear burning ceases – core (Fe) contracts
2. Electron gas becomes degenerate
3. Mass surpasses Chandrasekhar limit → electron pressure cannot oppose self-gravity → rapid contraction.
4. Heavy nuclei capture electrons, temperature increases rapidly
5. Photons disintegrate heavy nuclei, e.g. $^{56}Fe + \gamma \rightarrow 13\ ^{4}He + 4n$
6. High density: free protons capture free electrons and turn into neutrons
7. Matter ”rains” onto proto-neutron star and is reflected at high density core
8. Outward moving shock front forms
9. Additional energy input from neutrino wind
10. → inversion of direction of movement → **Supernova explosion**

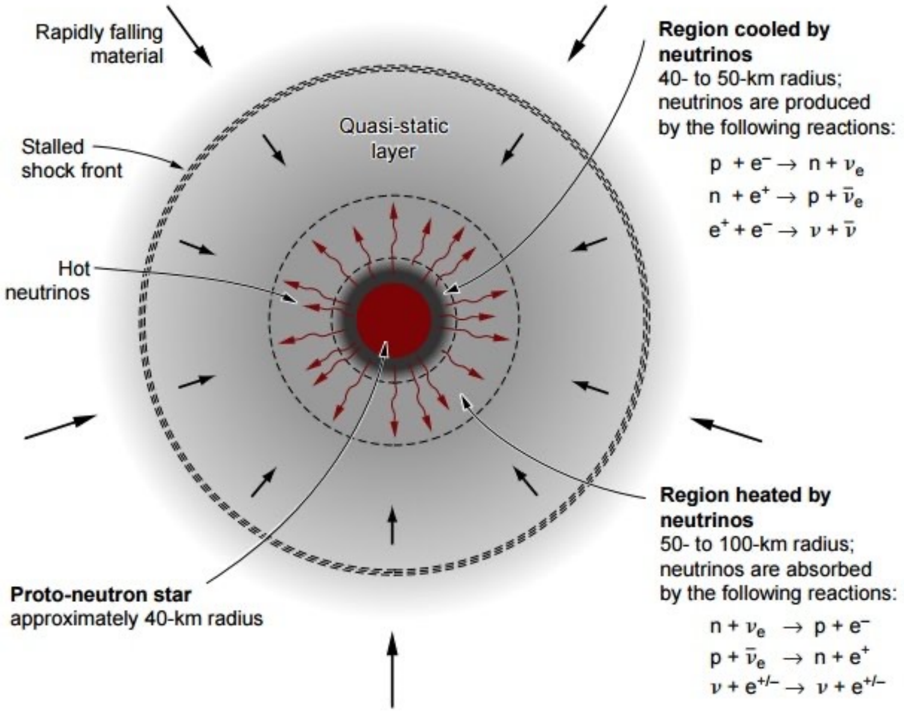

Supernovae classification

SN type I : No Hydrogen Balmer lines

Type Ia: Strong Si II absorption at 6150 Å

Type Ib/c: no Si II absorption, Ca, O emission lines.

SN type II : Strong hydrogen Balmer lines

Type II-L : “linear” light curve

Type II-P : “plateau” light curve

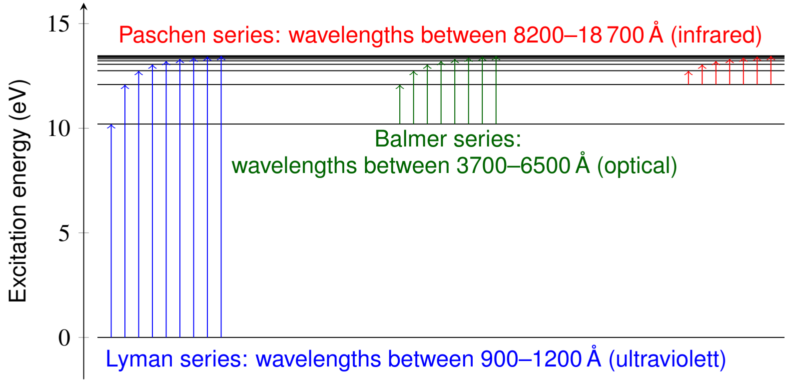

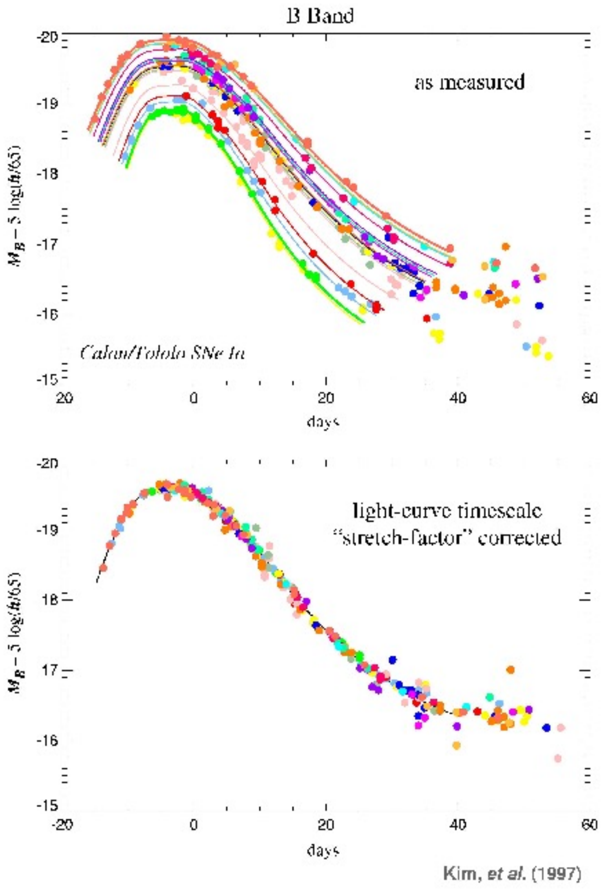

Only type SN Ia are observed from both young and old stellar populations

→ different origin

→ White Dwarfs in binary systems accreting matter from companion (see later)

Near uniform light curve evolution → can be used to measure distances

Supernova Remnants

– Acceleration at shock fronts of SNRs:
  – ~10^{51} erg per SN explosion
  – ~10% into proton / CR acceleration
  – ~ 3 events per century in Milky Way

→ Would be sufficient to power Cosmic Rays

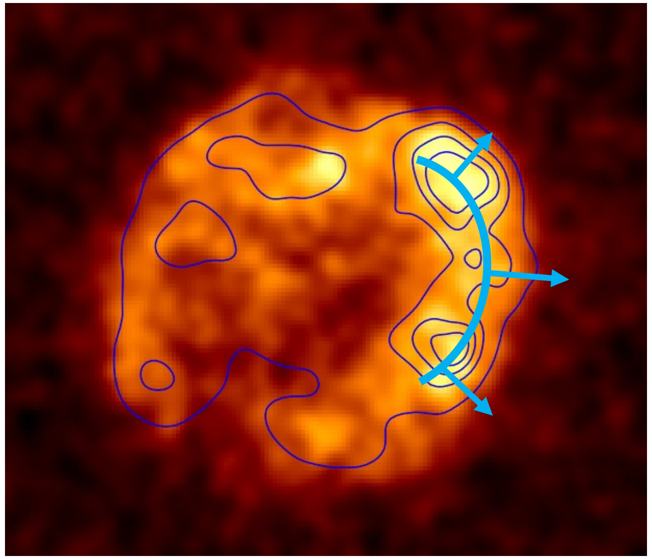

- Cosmic rays: deflected by magnetic fields
- Interactions produce neutral messengers: gamma-rays & neutrinos point to source
- Motivation for gamma-ray astronomy
  → high energy particles

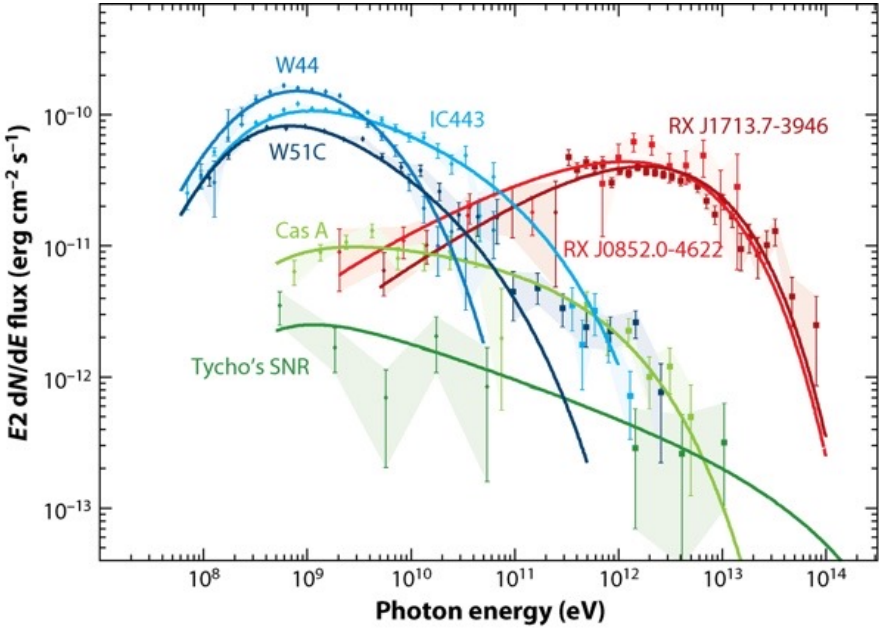

1 erg = 10^{-7} J = 0.62 TeV

Funk S. 2015.
Annu. Rev. Nucl. Part. Sci. 65:245–77

Galactic sources: Supernova Remnants

Evidence for characteristic pion bump with gamma-ray observations

Supernova Remnants interacting with nearby molecular clouds

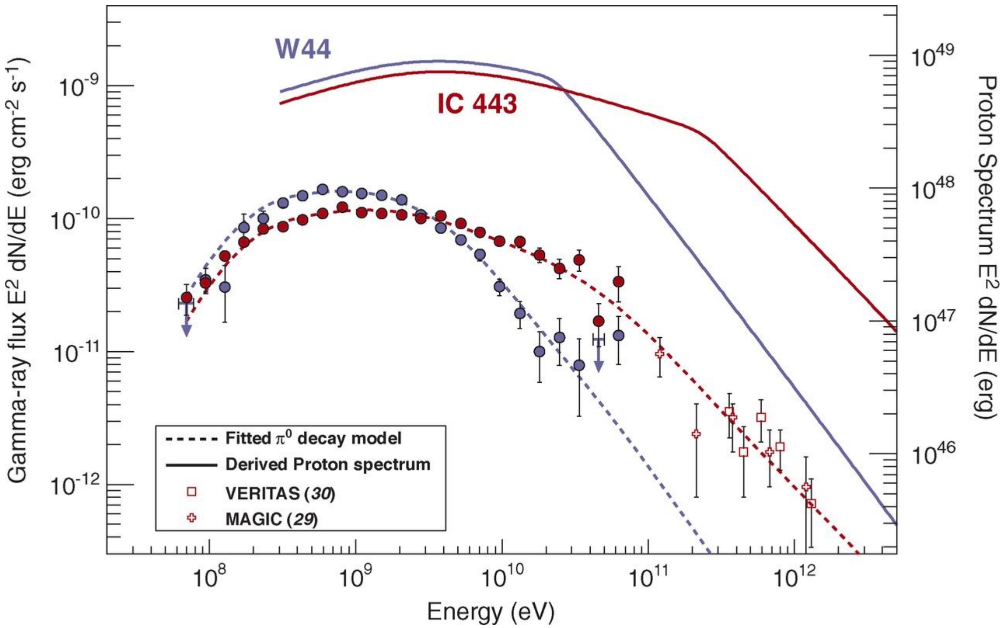

Fermi-LAT, Science, (2013)

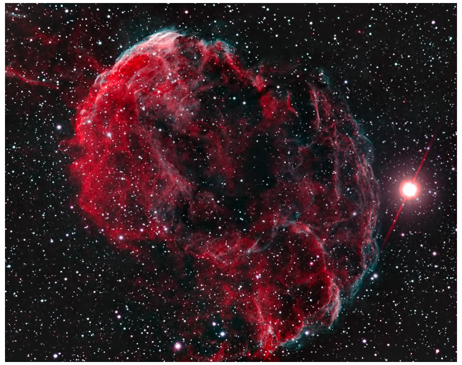

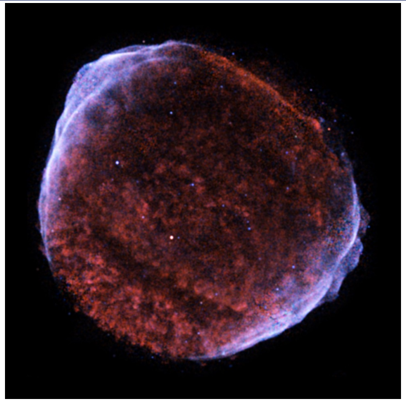

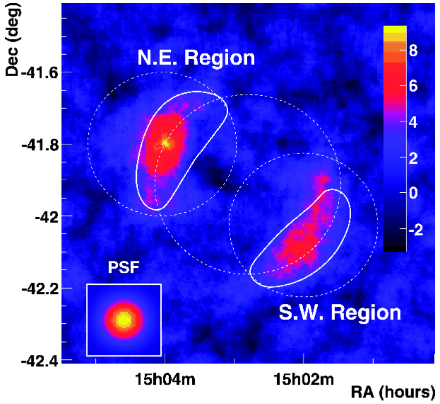

H.E.S.S. A&A 516 (2010) A62

Very High Energy Gamma-ray Sky

de Naurois Universe **7** (2021) 421
http://tevcat2.uchicago.edu/

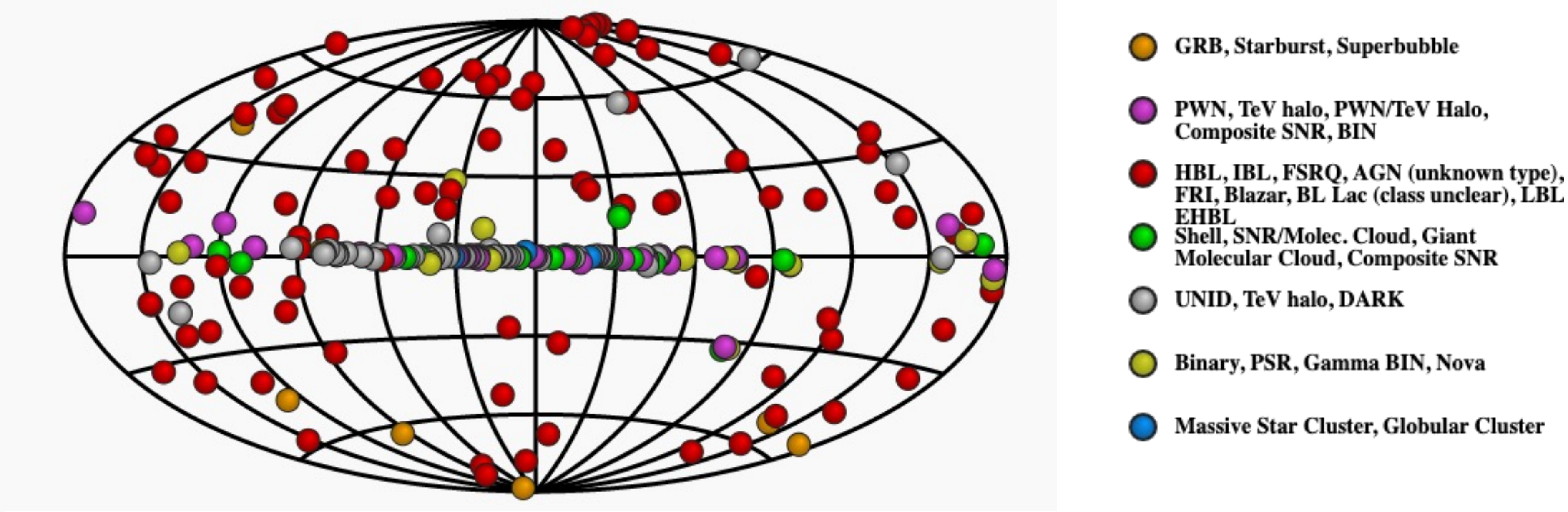

Galactic Sources

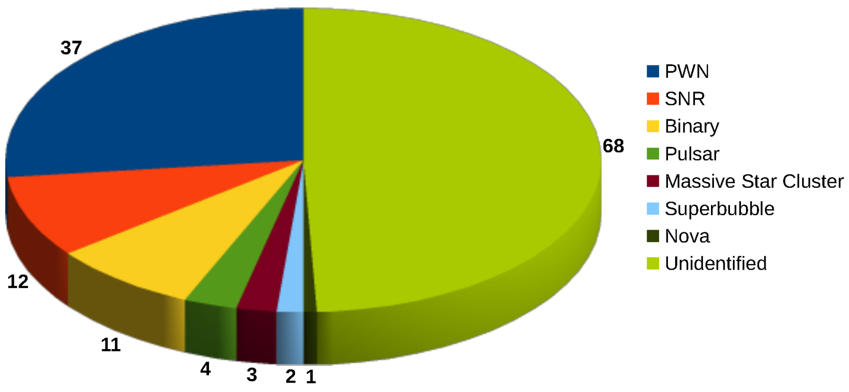

Extragalactic Sources

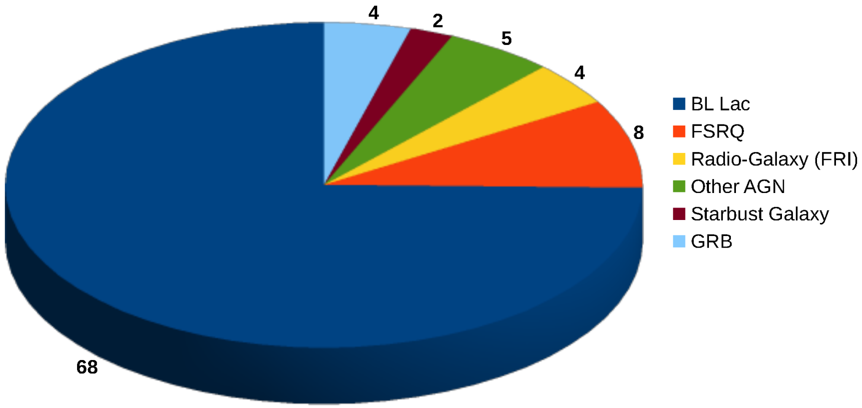

Very High Energy Gamma-ray Sky

H.E.S.S. Galactic Plane Survey

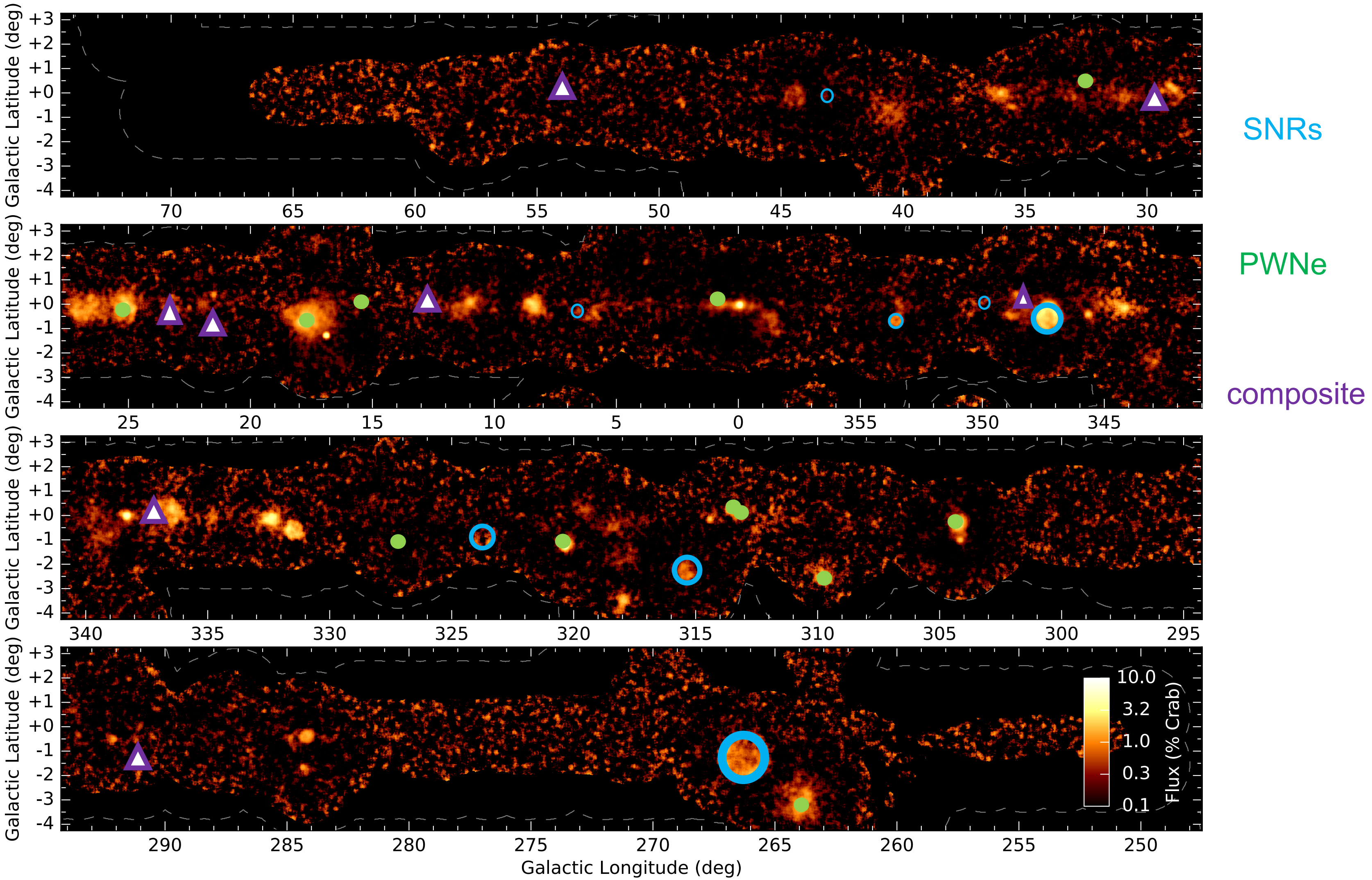

What are Pulsars?

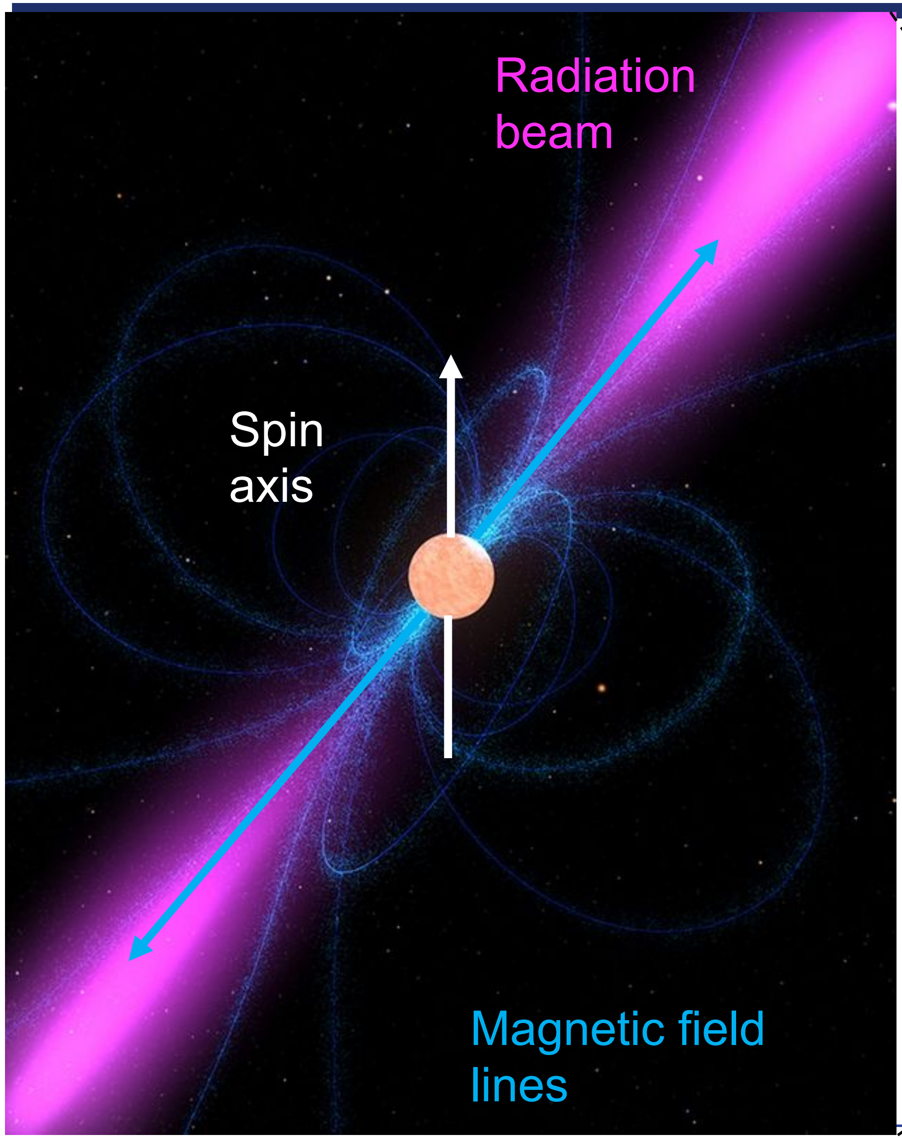

<u>Pulsar</u>: Rotating neutron star

Formed during collapse of a stellar core, sustained against gravity via neutron degeneracy pressure

Angular momentum conserved → very rapid rotation

Magnetic flux conserved → very strong and variable B field ~$10^{11} - 10^{14}$ Gauss

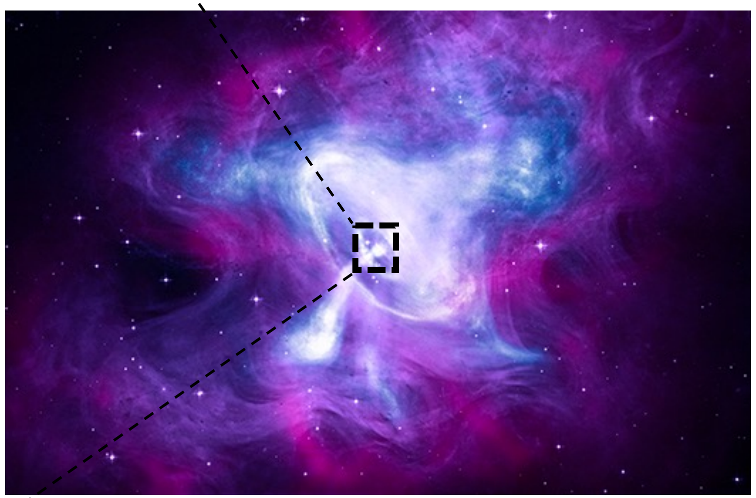

Crab pulsar: X-ray, infrared & optical
Credit: NASA/CXC/SAO/STScI

$$L = I\omega = \frac{2}{5}MR^2\omega \propto \frac{MR^2}{P}$$

$$\Phi = BR^2$$

$$B_{NS} = B_* \left(\frac{R_*}{R_{NS}}\right)^2$$

Pulsars

https://www.jb.man.ac.uk/~pulsar/Education/Sounds/sounds.html

Discovered in 1967 – astrophysical signal with very short periods

Rotation velocity at surface must be less than the speed of light, c: $R < \frac{Pc}{2\pi}$

“Light cylinder” = radius at which particles would have to travel at c to co-rotate

Typical size R ~10 km

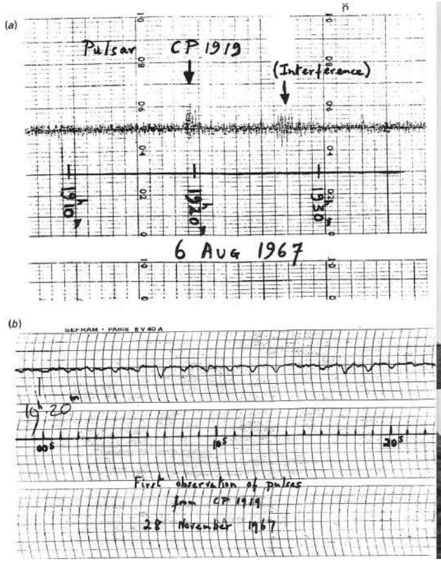

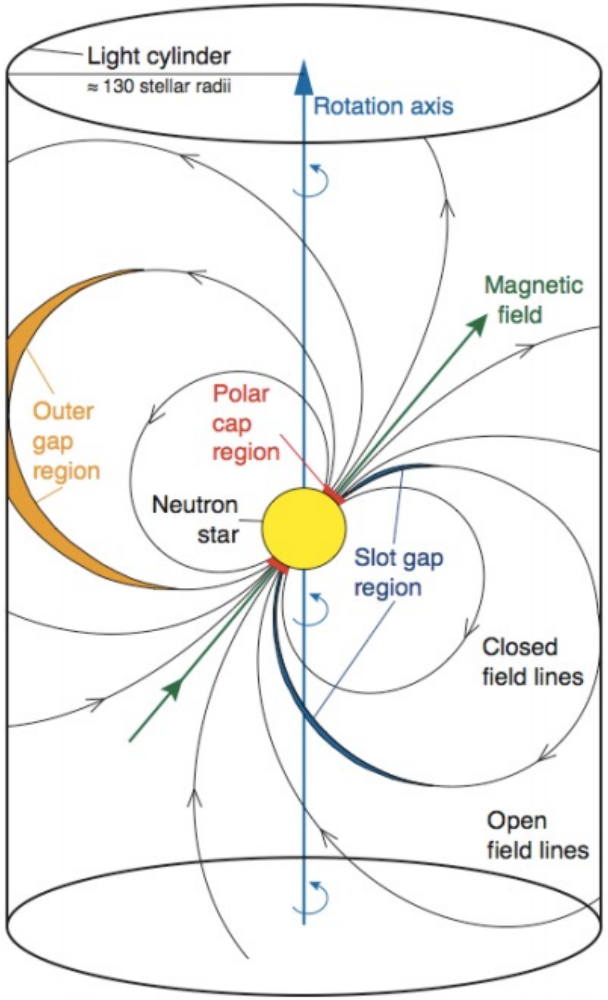

Pulsar energy loss

Change in spin frequency over time: $\dot{\Omega} = -k\Omega^n$ where n is the braking index

$$P = P_0\left(1 + \frac{t}{\tau_0}\right)^{\frac{1}{n-1}}$$

Assume pure magnetic dipole radiation (n = 3) corresponding to the loss in kinetic energy

Pulsars are precise astronomical clocks

e.g. Crab pulsar: P = 33 ms = 0.0333924123 ± 1.2×10^{-9} s and Pdot = 4.20972×10^{-13} s/s ± 3.0×10^{-18} s/s

Energy loss: $\frac{dE}{dt} = -\frac{32\pi^5 B^2 R^6 \sin\theta^2}{3\mu_0 c^3 P^4}$ $\qquad \dot{E} \equiv 4\pi^2 I \frac{\dot{P}}{P^3}$

Near constant until a time τ_0 has elapsed.

$$\dot{E} = \dot{E}_0\left(1 + \frac{t}{\tau_0}\right)^{-\frac{(n+1)}{(n-1)}}$$

$$\tau_0 \equiv \frac{P_0}{(n-1)\dot{P}_0} = \frac{2\tau_c}{n-1} - t$$

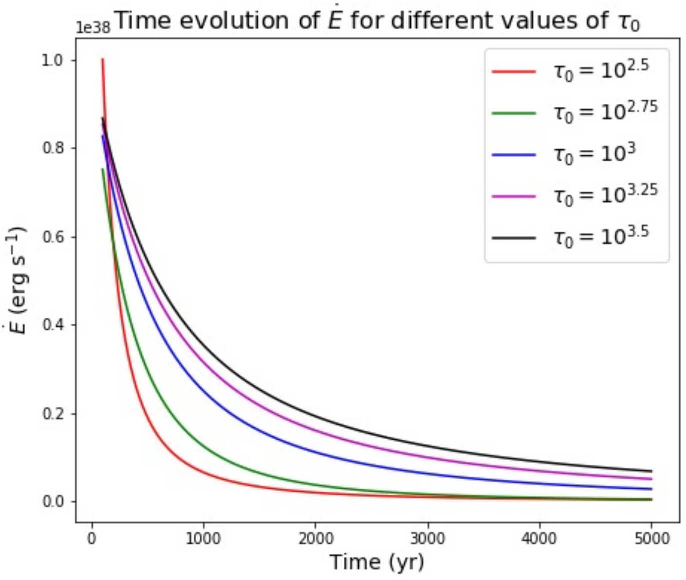

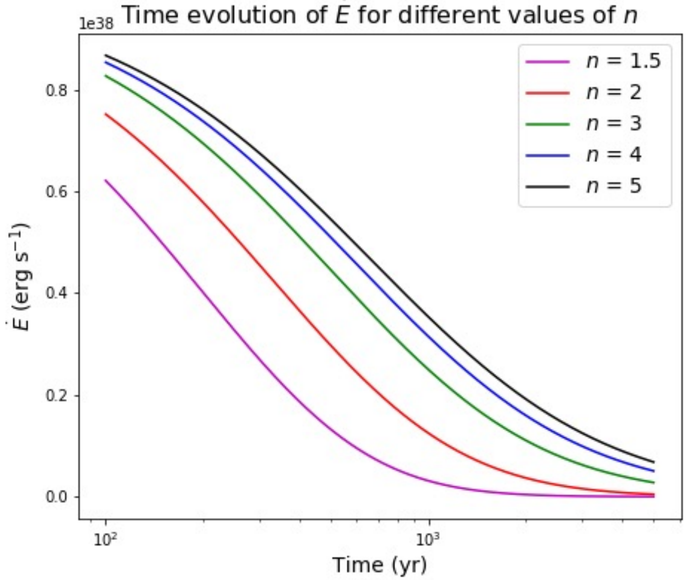

Pulsar Population

Consider the known pulsar population

Typically shown on a “p-pdot” diagram,
i.e. period vs period derivative

Blue lines = characteristic timescale $\tau_c = \frac{P}{(n-1)\dot{P}}$

Red lines = spin-down luminosity

Green lines = magnetic field

Lower left = millisecond pulsars

Black line = “death line” → pulsed signals are typically not observed beyond this line.

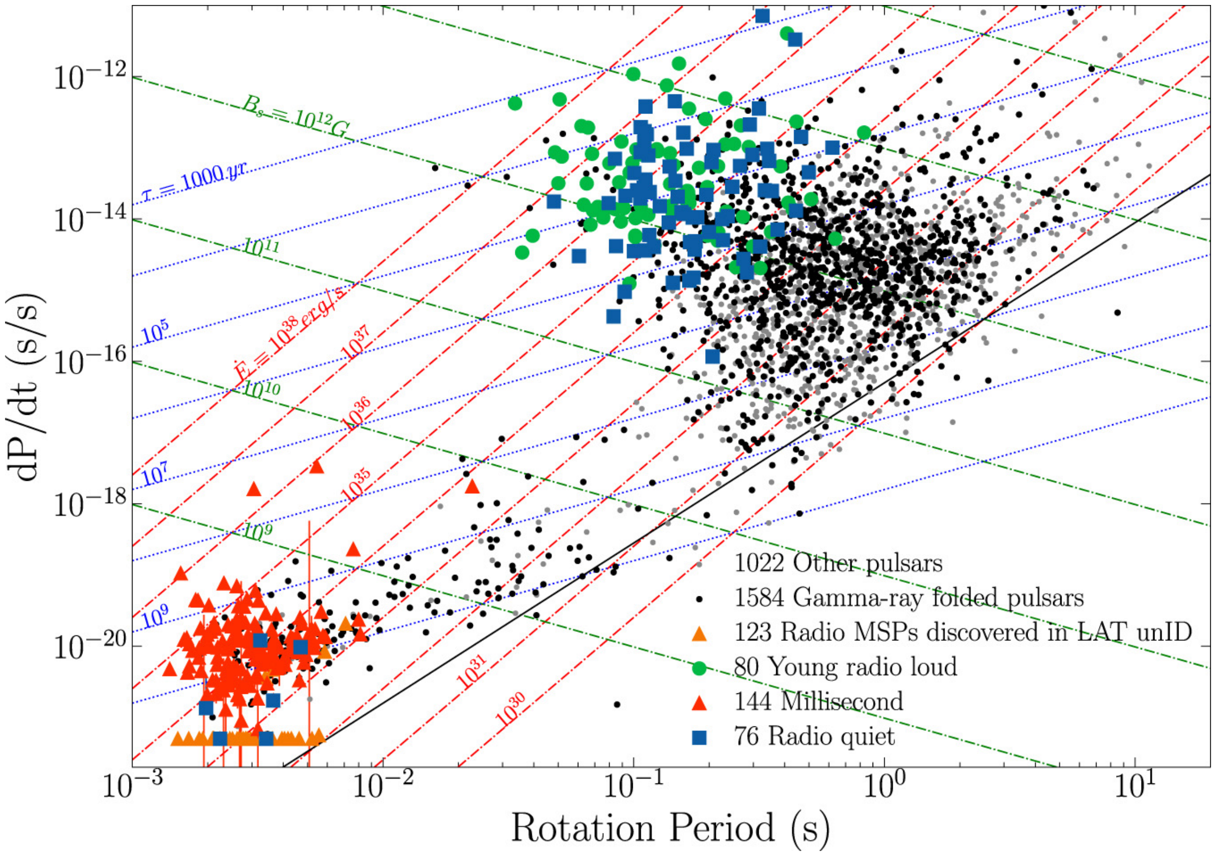

3PC Fermi-LAT Collaboration, Smith et al. ApJ **958** (2023) 191

Energetic pulsar environments

Pulsars listed in the ATNF

More energetic or closer pulsars dominate TeV detections

Some outliers – likely poor distance estimate or misattributed

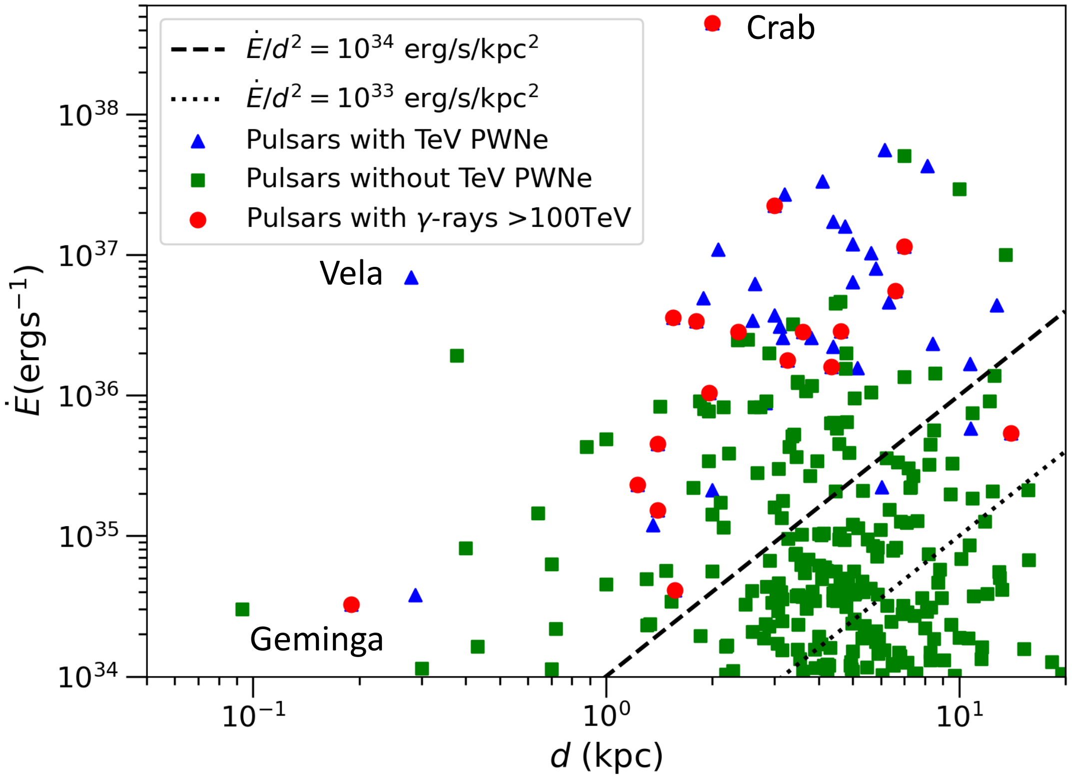

Pulsar – Pulsar Wind – Pulsar Wind Nebula

→ Charged particles accelerated in magnetic fields radiate

→ Radiation produces $e^+ - e^-$ pairs

Nebula of high energy particles → Mainly $e^\pm$

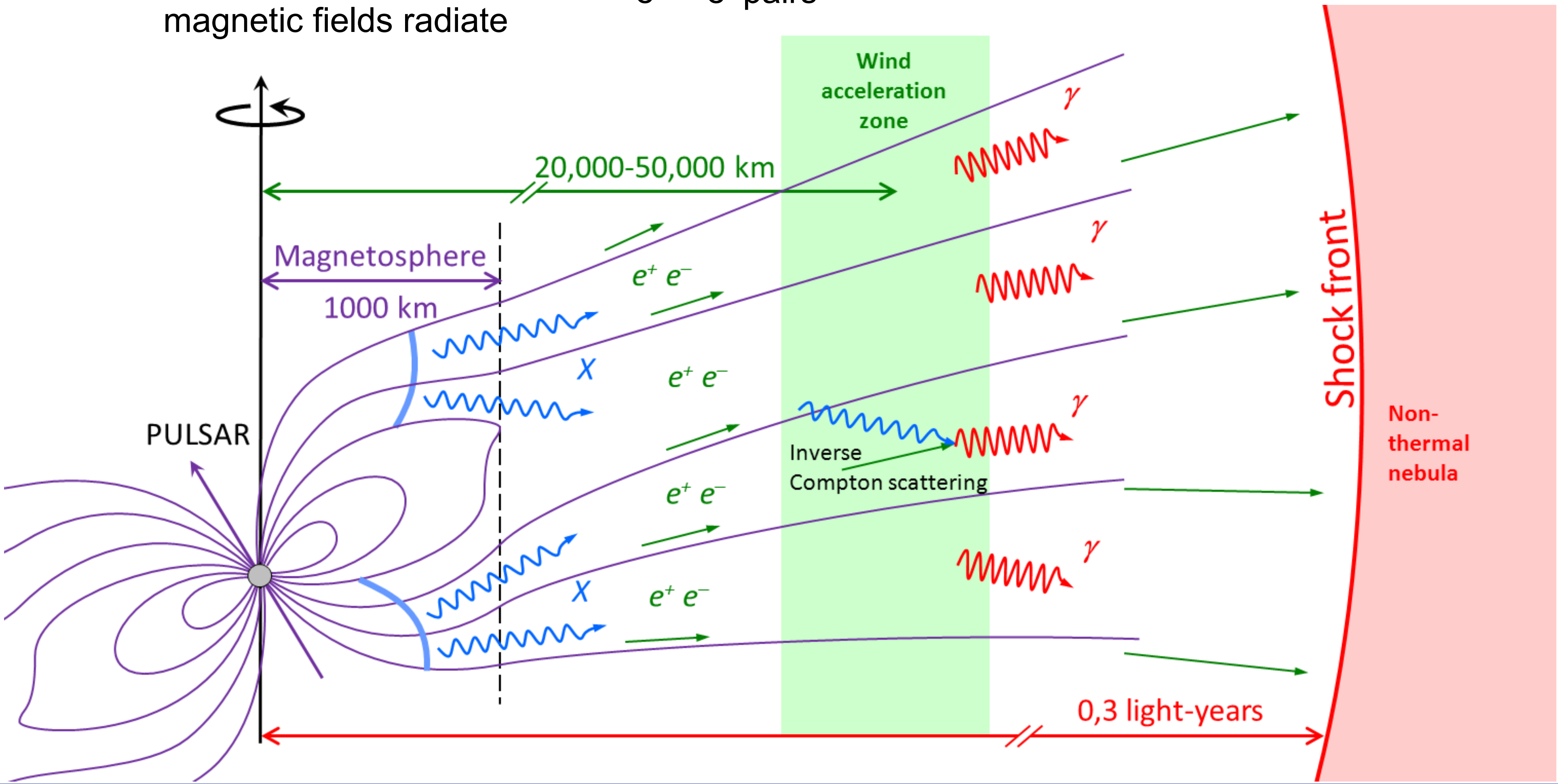

Evolutionary stages of pulsar environments

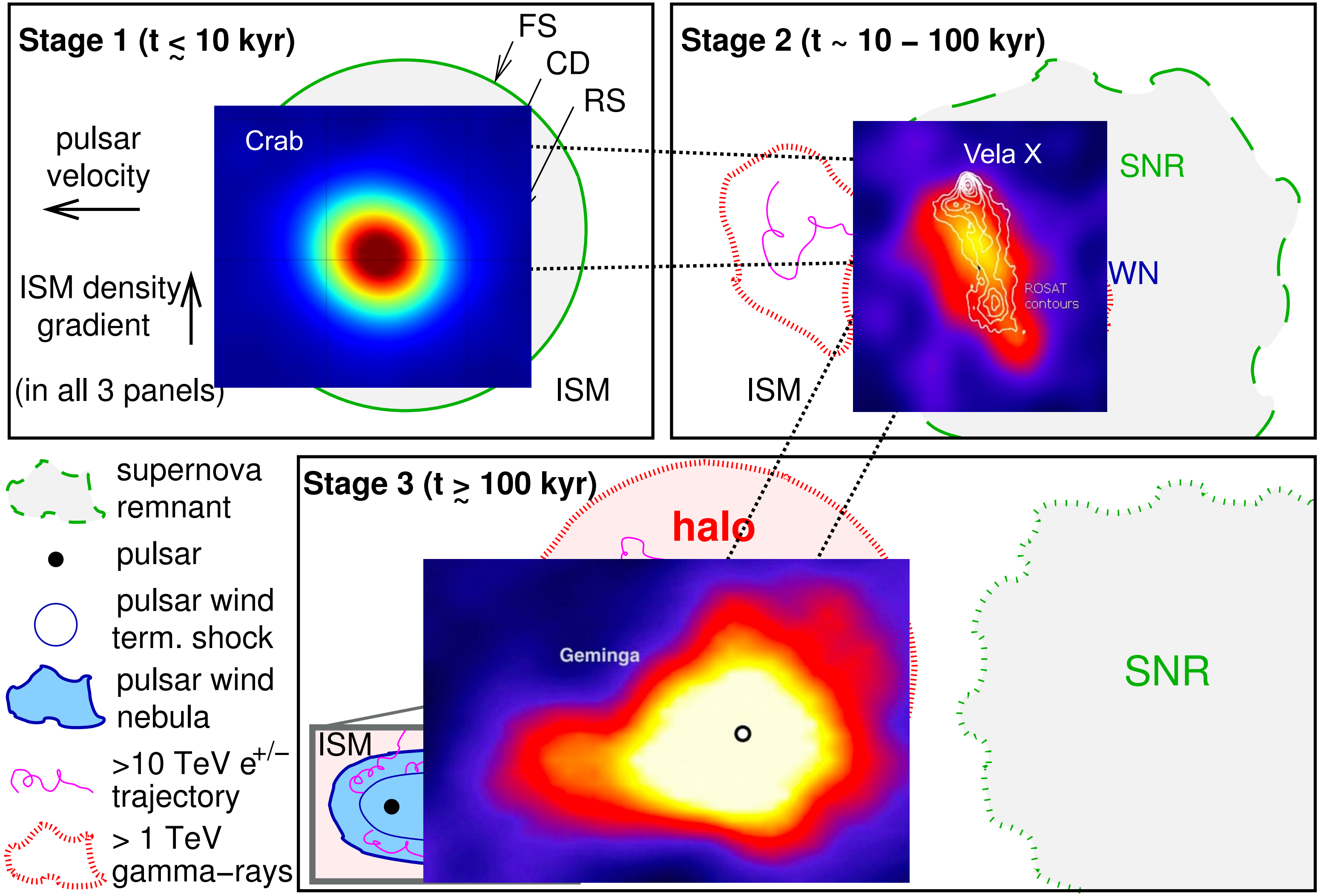

Pulsar Wind Nebulae (PWN)

→ **Pulsar Halos**

Giacinti, AM, Lopez-Coto et al, A&A **636**, A113 (2020)

Crab Nebula

Pulsar Wind Nebula – “Standard candle” of TeV gamma-ray astronomy

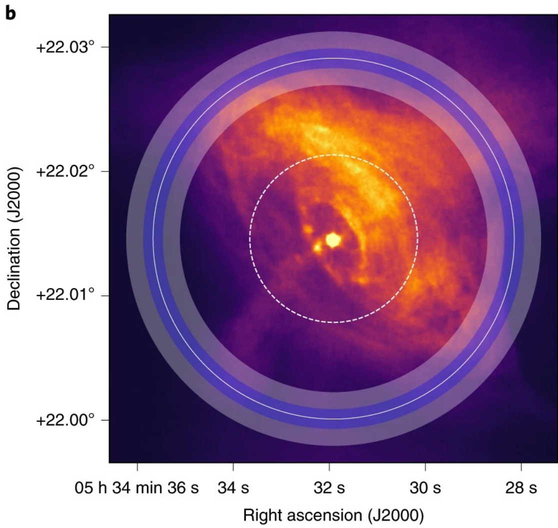

- First TeV source: Whipple 1989
- Highest energy photons > 1 PeV
- Brightest VHE gamma-ray source → ”Crab” units
- t = 0.94 kyr, $\dot{E}$ = 4.5x10^{38} erg/s, d = 2 kpc

VHE extension: 52”

H.E.S.S. collaboration,
Nature Ast. **4**, 167-173 (2020)

Joint Fermi & HESS analysis
A&A **686** (2024) A308

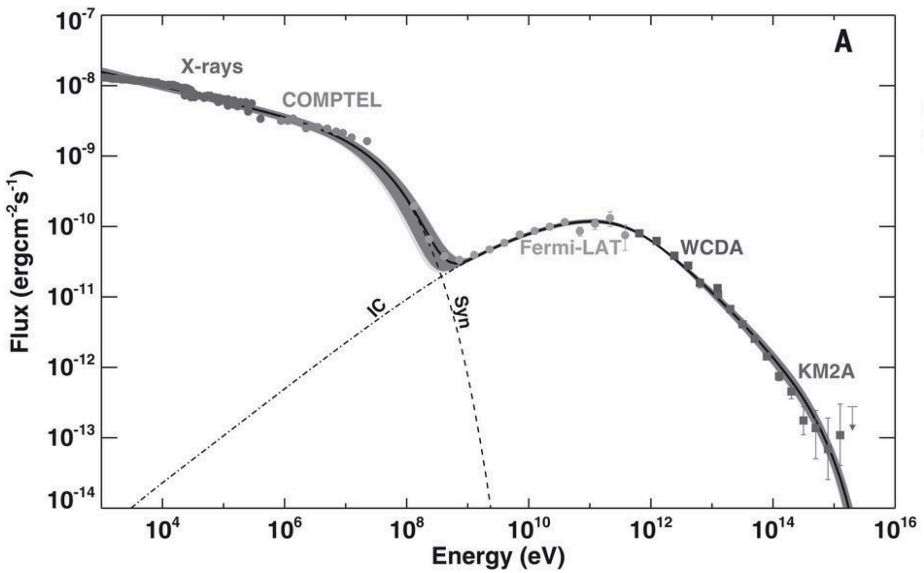

Z. Cao et al. LHAASO collaboration, Science **373**, 425-430 (2021)

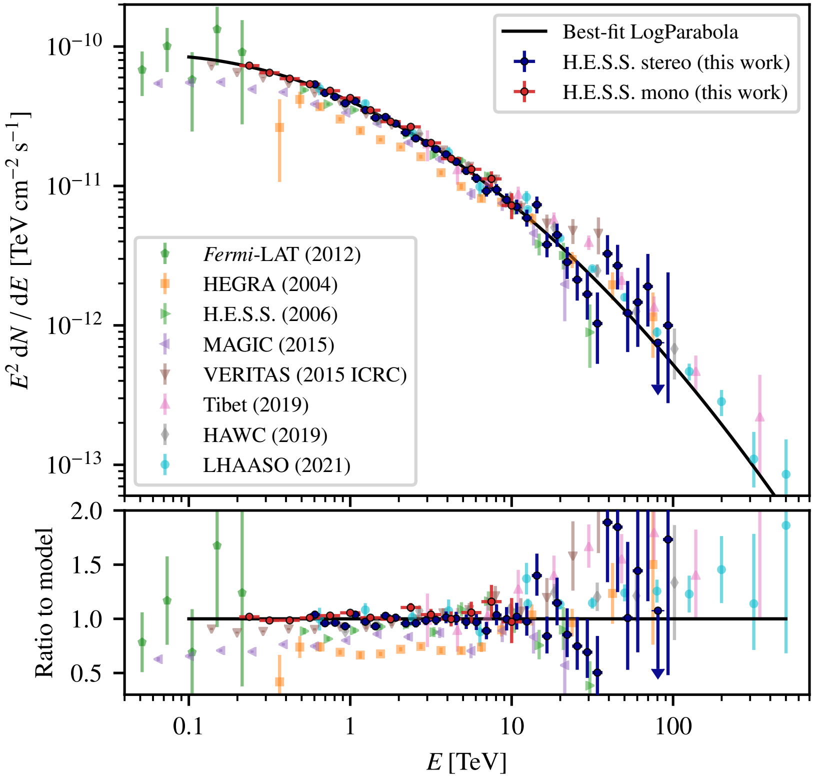

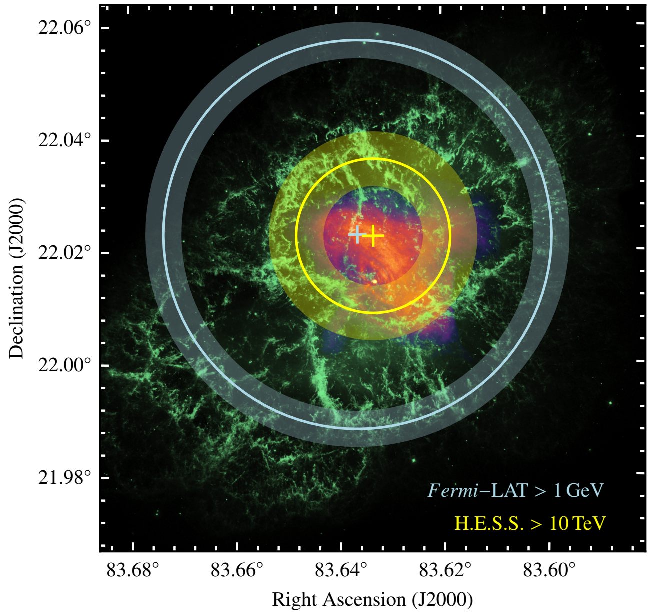

Pulsed emission from pulsars

Pulse profile depends mainly on the angle of the beam with respect to Earth

Opening angle may be different depending on the wavelength

Typical profile includes P1, P2 and bridge emission

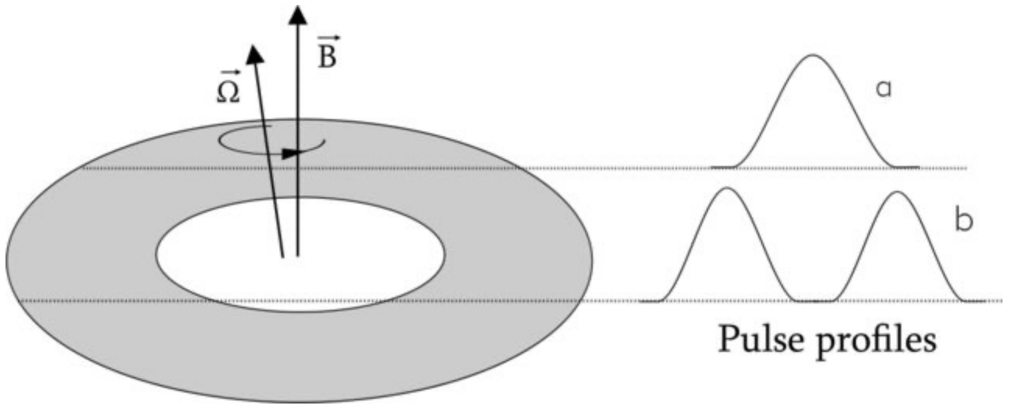

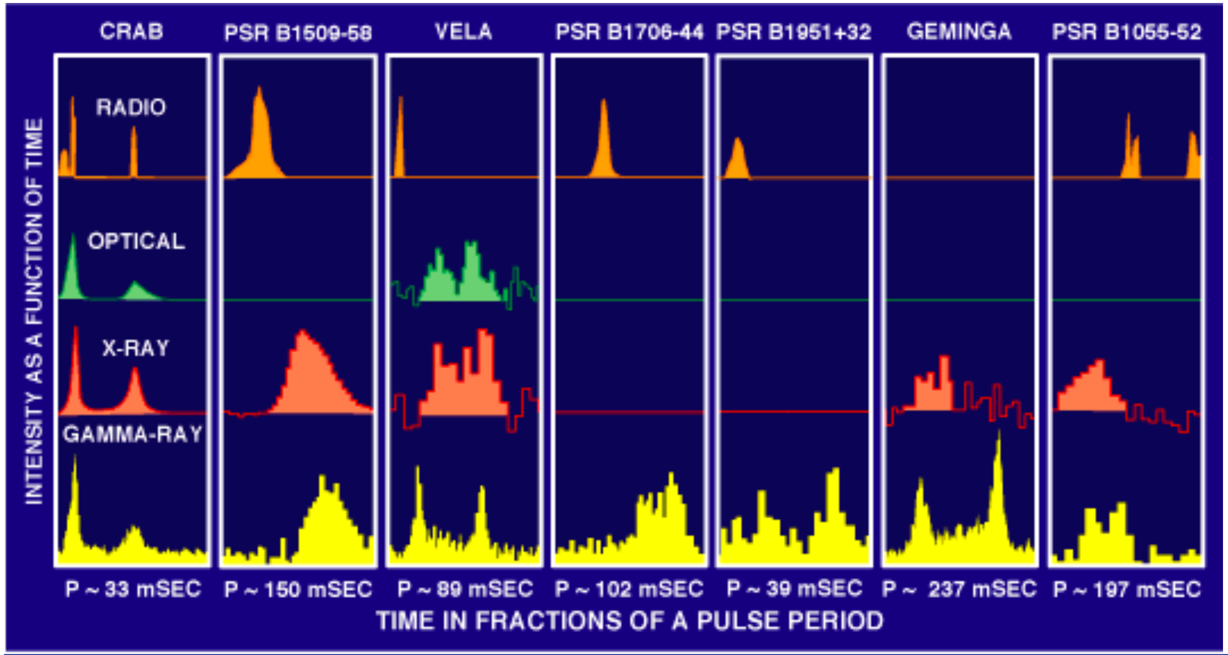

Vela Pulsar

H.E.S.S. collaboration, Nature Astronomy, **7**, 1341-1350 (2023)

- Pulsed emission detected up to 20 TeV
- Predominantly from the P2 pulse
- t = 11 kyr, $\dot{E}$ = 7x10^{36} erg/s, d = 287 pc

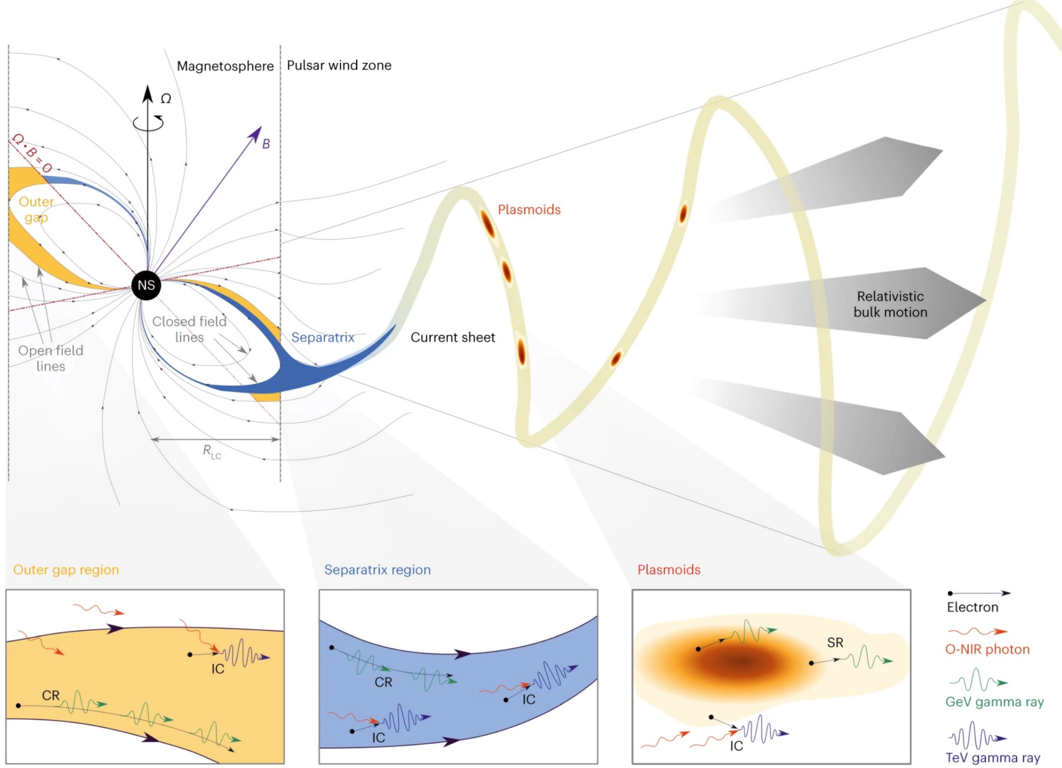

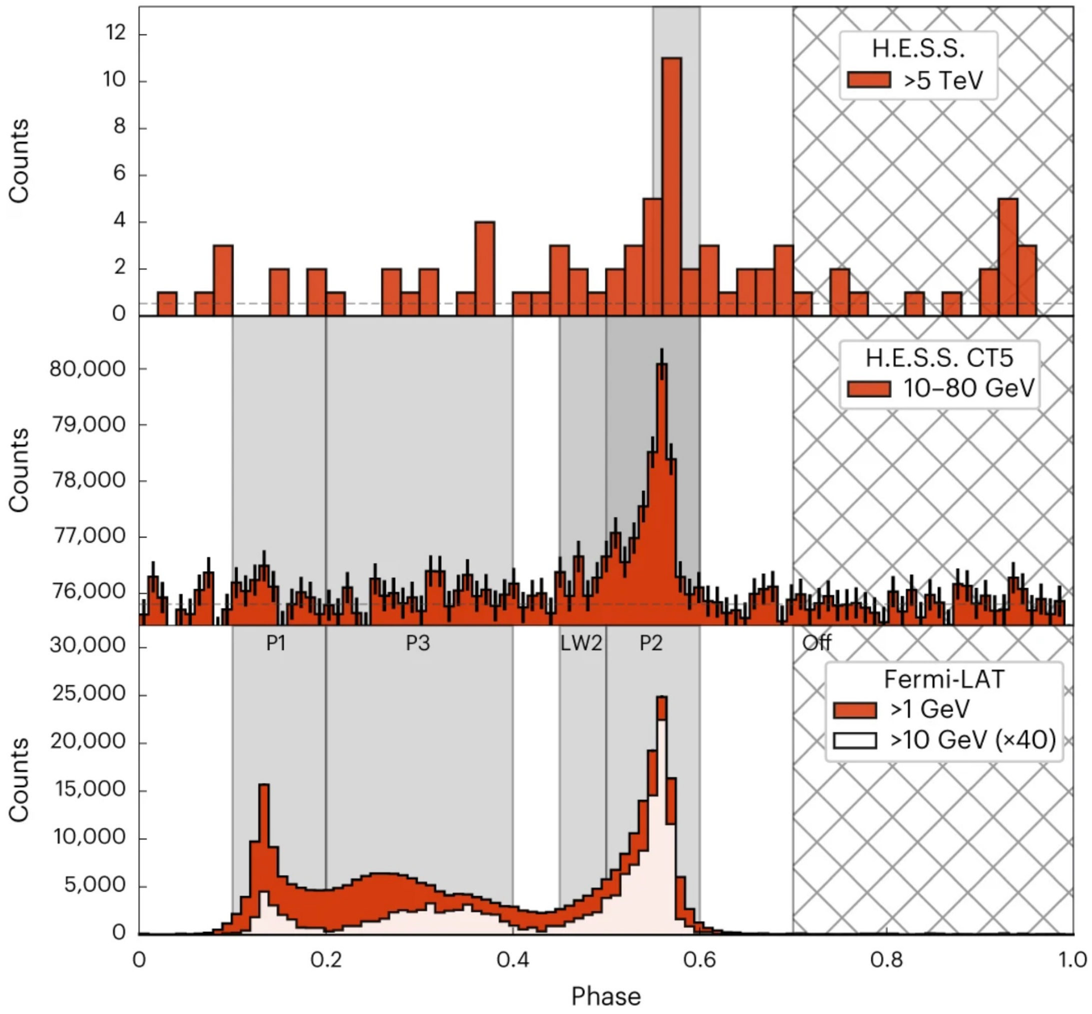

Pulsar Wind Nebulae

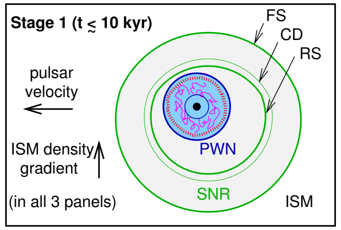

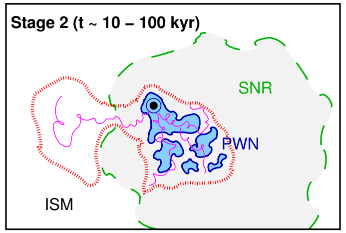

- Most numerous source class in the VHE gamma-ray sky

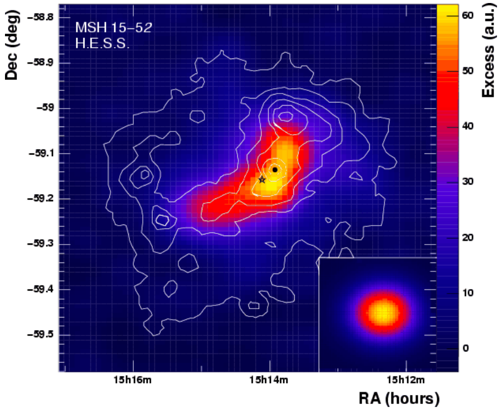

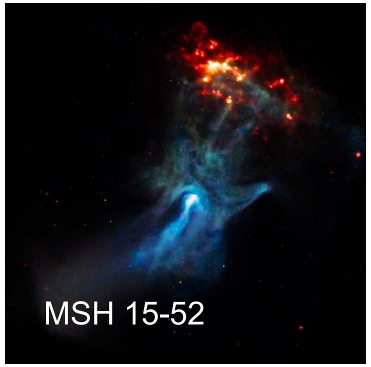

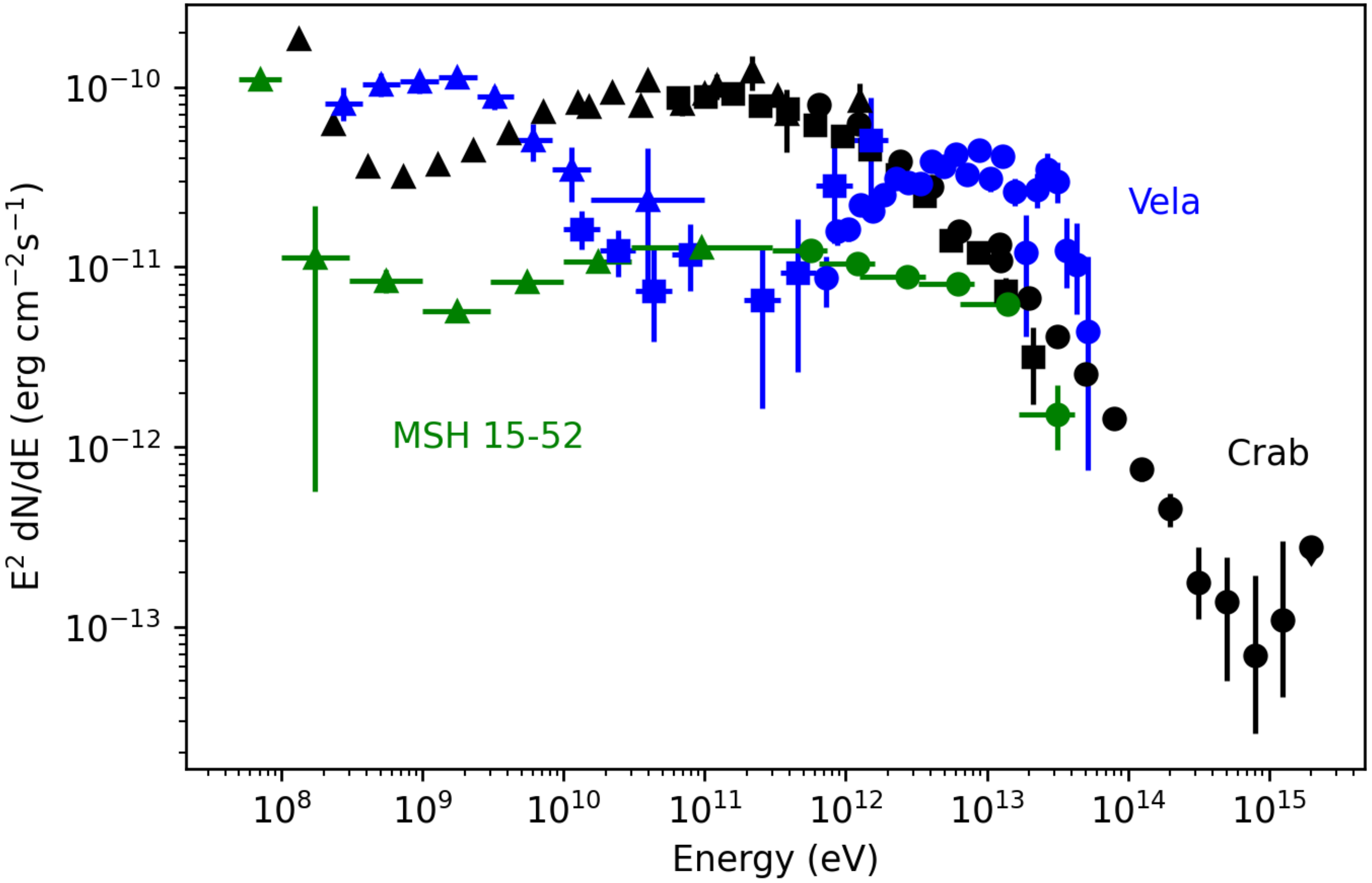

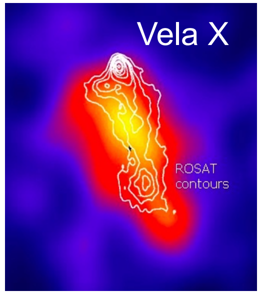

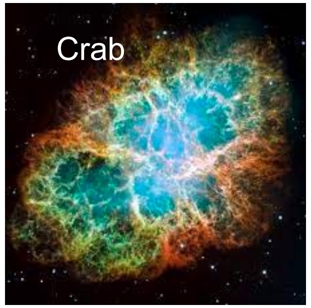

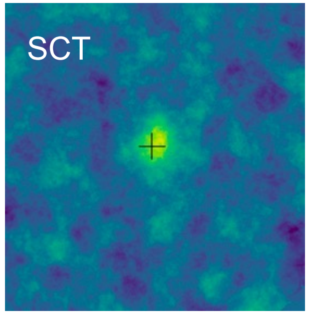

A&A **435**, L17-L20 (2005) https://news.ucsc.edu/2020/06/crab-nebula.html

Example Stage 2: Vela X

Pulsar Wind Nebula

- Age = 11.3 kyr
  Energy output = 6.9x10^{36} erg/s
  Distance = 0.28 kpc
- R: radio = 12.2 pc
  X-ray = 3.08 pc
  TeV = 2.9 pc

Hinton et al. ApJ **7**, 1-5 (2011)

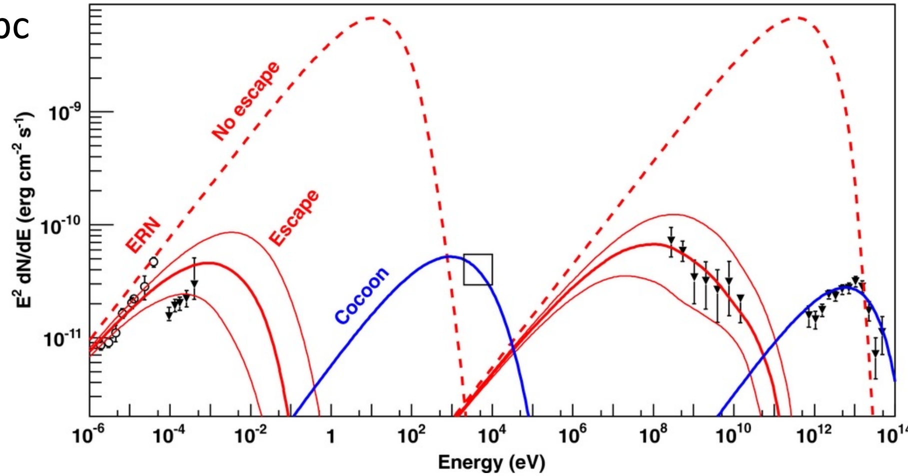

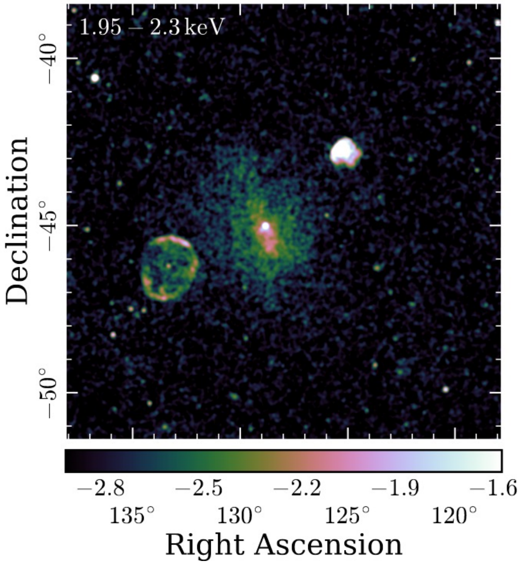

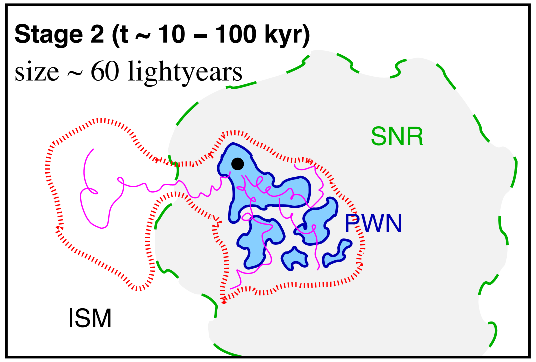

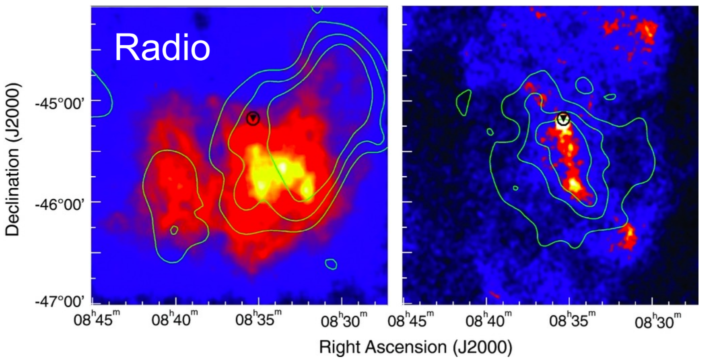

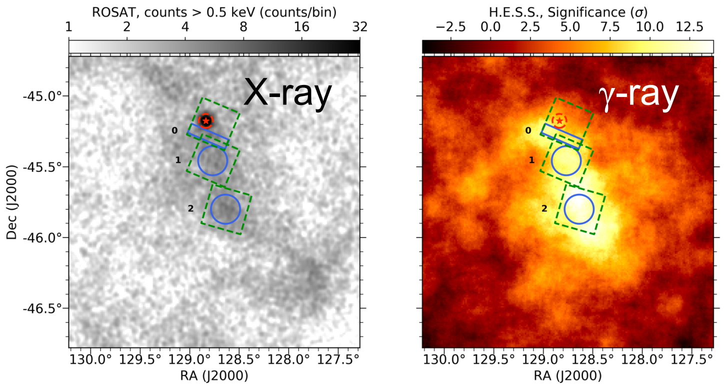

H.E.S.S. Collaboration, A&A 627, (2019) A100

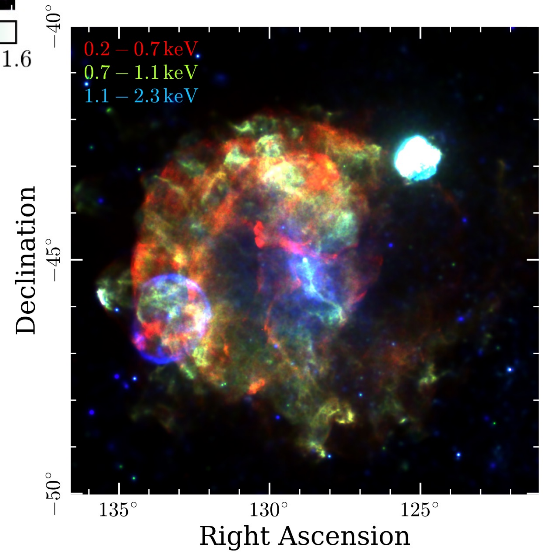

eROSITA, Mayer et al. A&A **676**, A68 (2023)

Pulsar Wind Nebulae

HESS J1825-137

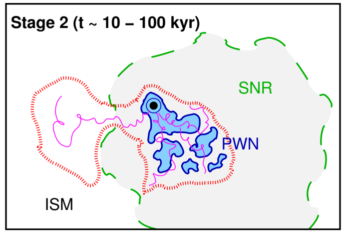

- Age = 21.4 kyr
  Energy output = 2.8x10^{36} erg/s
  Distance = 3.9 kpc
- R: radio = ? pc
  X-ray = 9.1 pc
  TeV = 50 pc

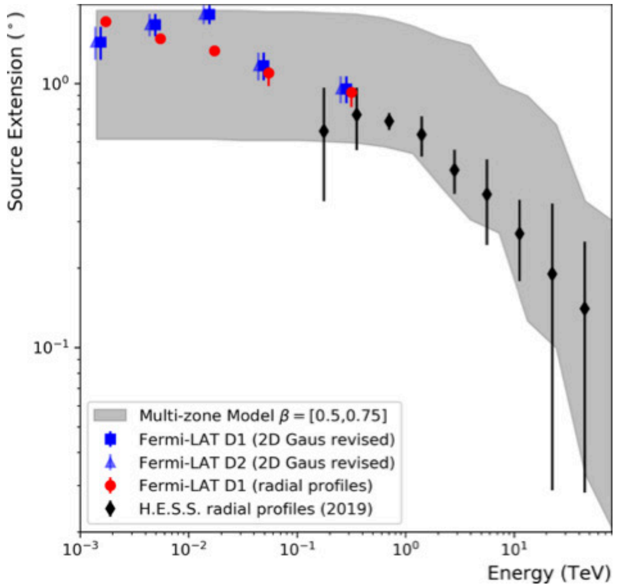

Principe et al. A&A **640** (2020) A76

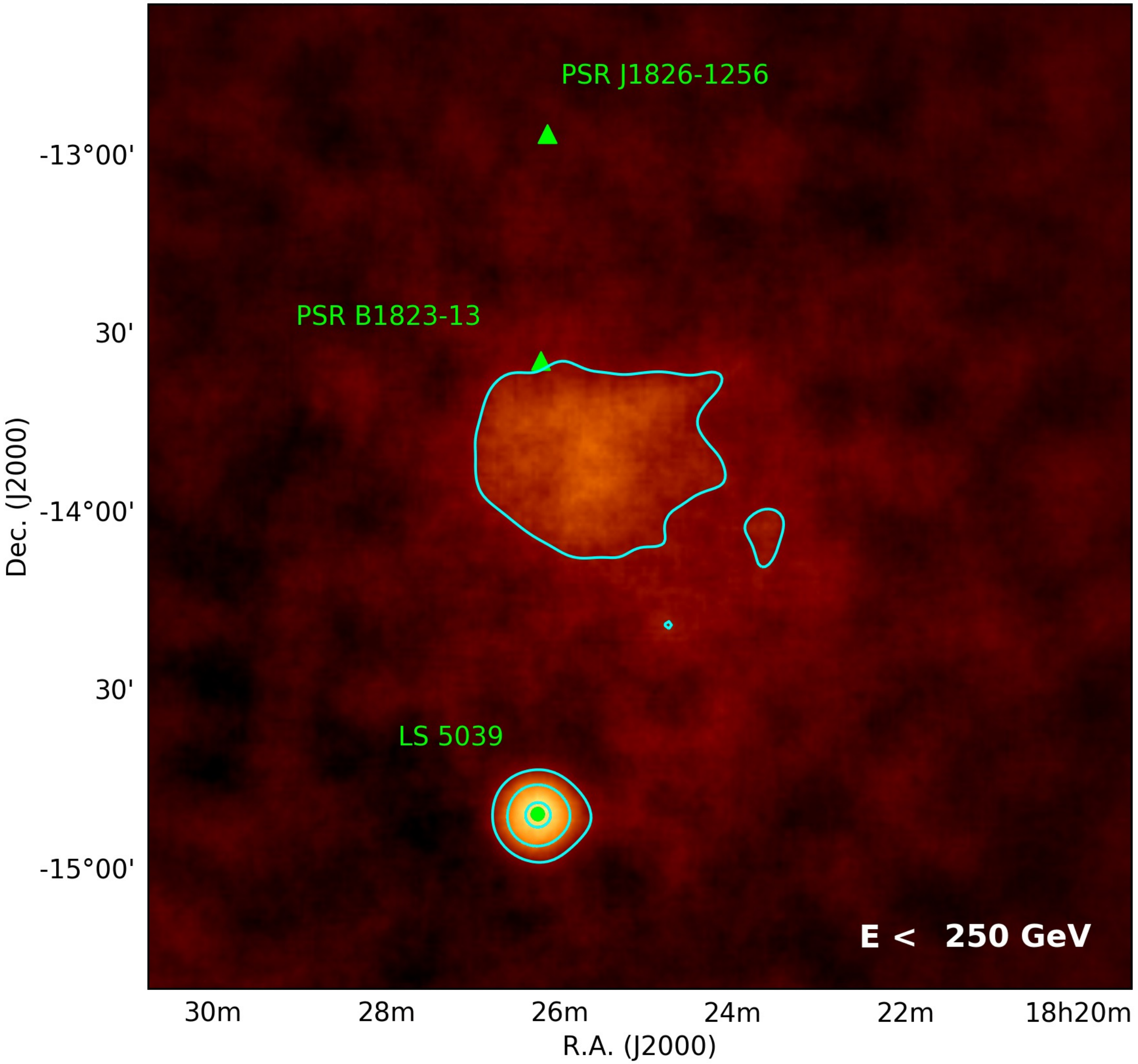

H.E.S.S. collaboration et al. A&A **621** (2019) A116

Example transition: HESS J1813-178

Joint fit to Fermi-LAT and H.E.S.S. data yielded a core component A and extended component B

Modelled as electron populations of different ages released from the pulsar

Energy density is PWN-like and halo-like respectively

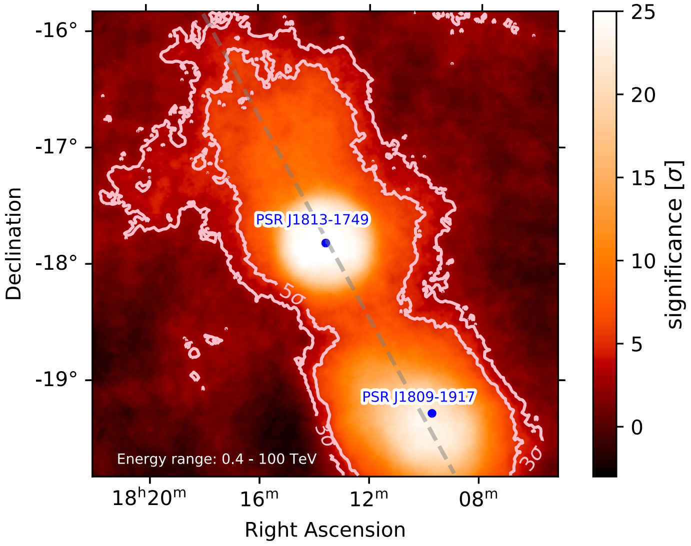

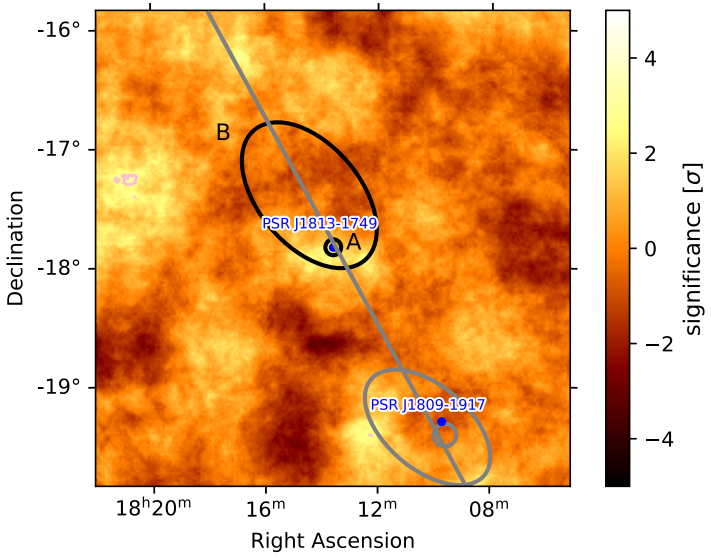

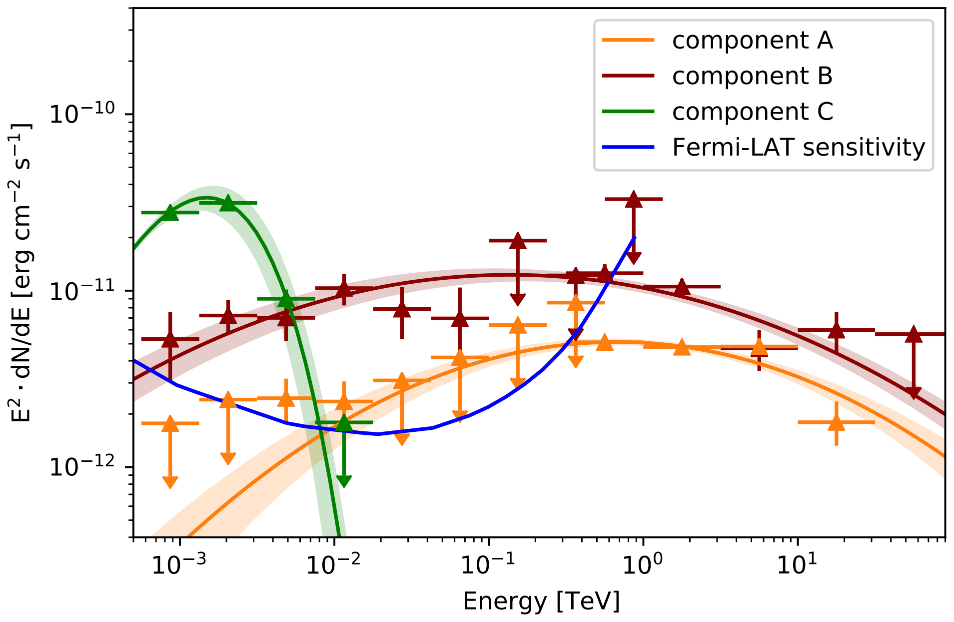

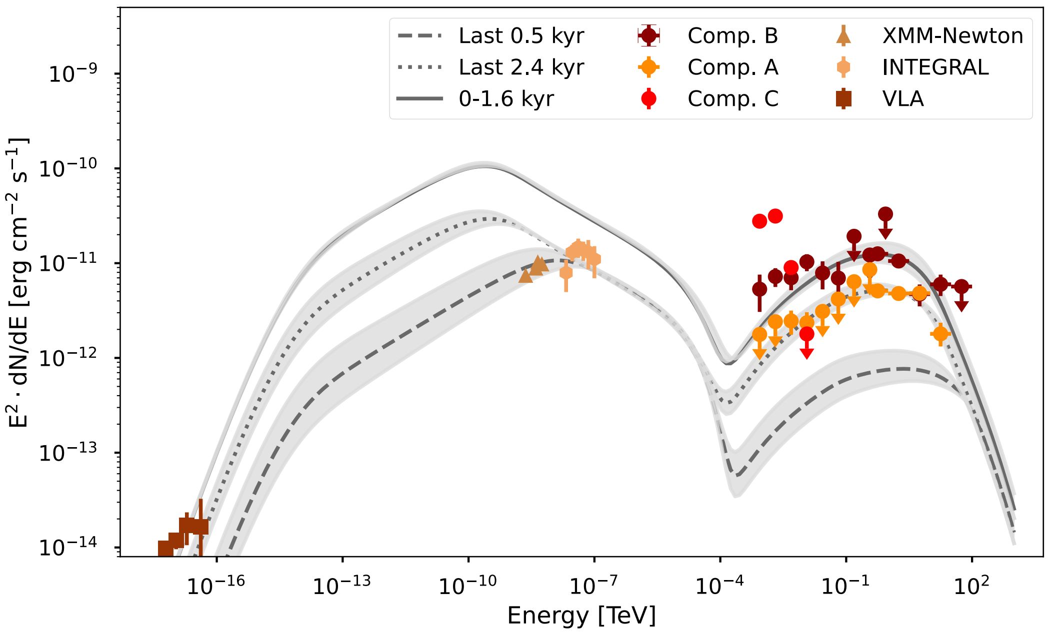

T. Wach, H.E.S.S. (A&A submitted)

Particle transport – electron cooling

Size decreases with increasing energy

→ Due to cooling losses as particles are transported away from the pulsar

→ Increasing spectral index – less high energy particles

→ Combined X-ray and gamma-ray: constrain magnetic field strength

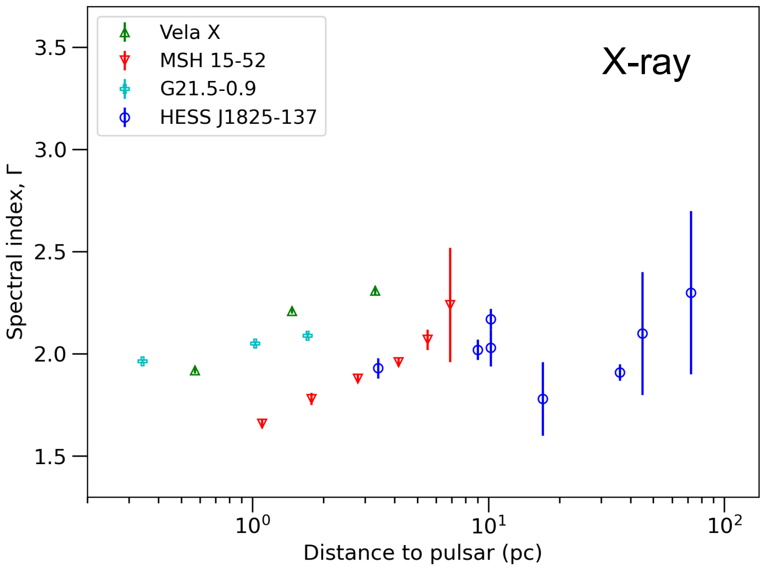

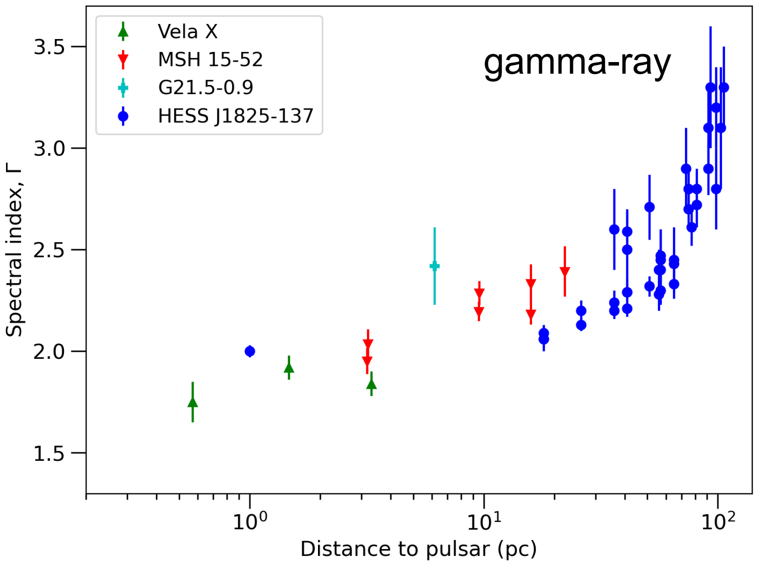

Gelfand & AM, Handbook of X-ray and gamma-ray astrophysics arXiv:2208.11026

Pulsar halos

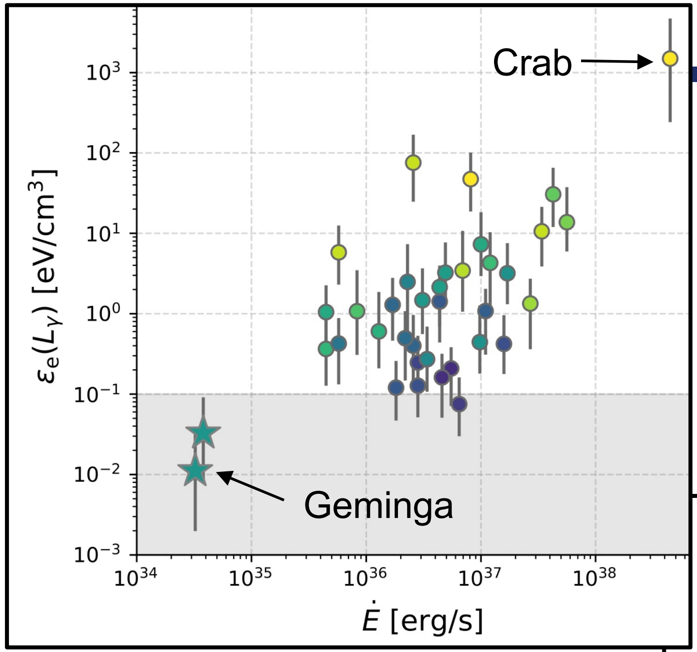

← Low energy density in electrons compared to the ISM

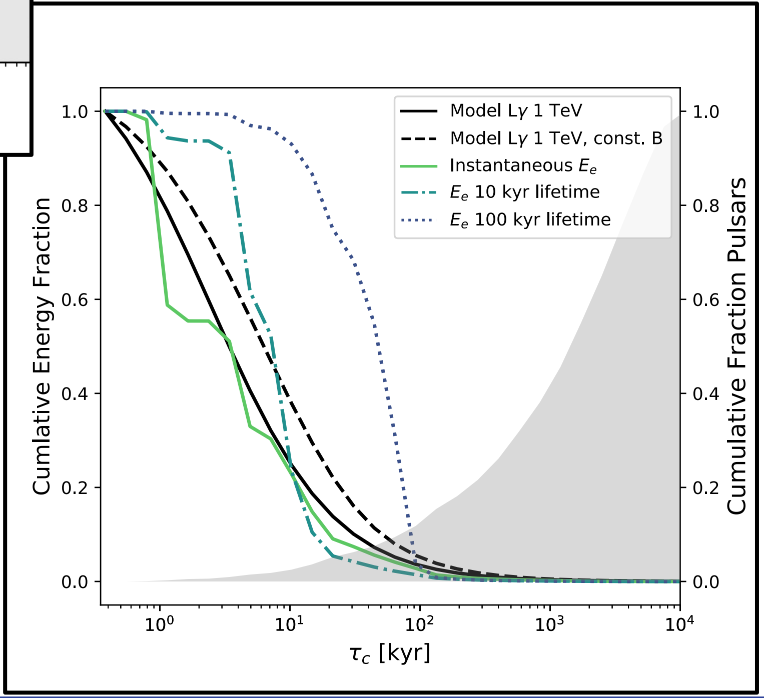

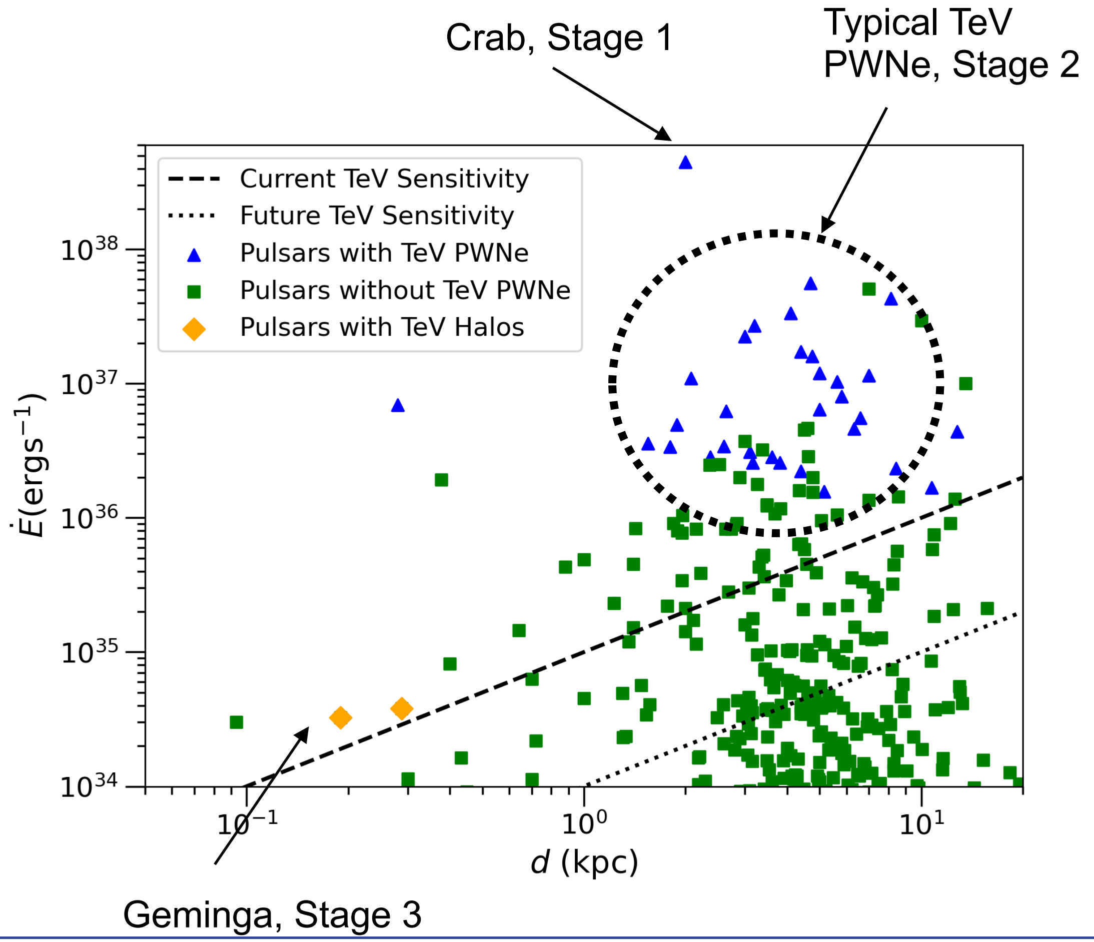

A small number of energetic pulsars dominate the CR electrons. →

Can be a large number of halos, yet contribute less to the CR electrons

Giacinti, AM, Lopez-Coto et al, A&A **636**, A113 (2020)

Pulsar halos: e.g. Geminga

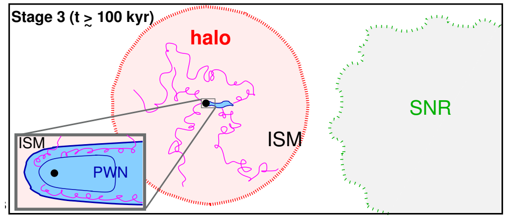

- First identified at TeV energies by Water Cherenkov Detector HAWC
  Larger field-of-view → less angular size bias
- IACTs such as H.E.S.S. have since put effort into improving analysis sensitivity to extended sources
  - Consistent view of the Galactic Plane (H.E.S.S. & HAWC, ApJ, **917**, 2021, 6)
    → several extended sources seen by HAWC now detected in H.E.S.S. data

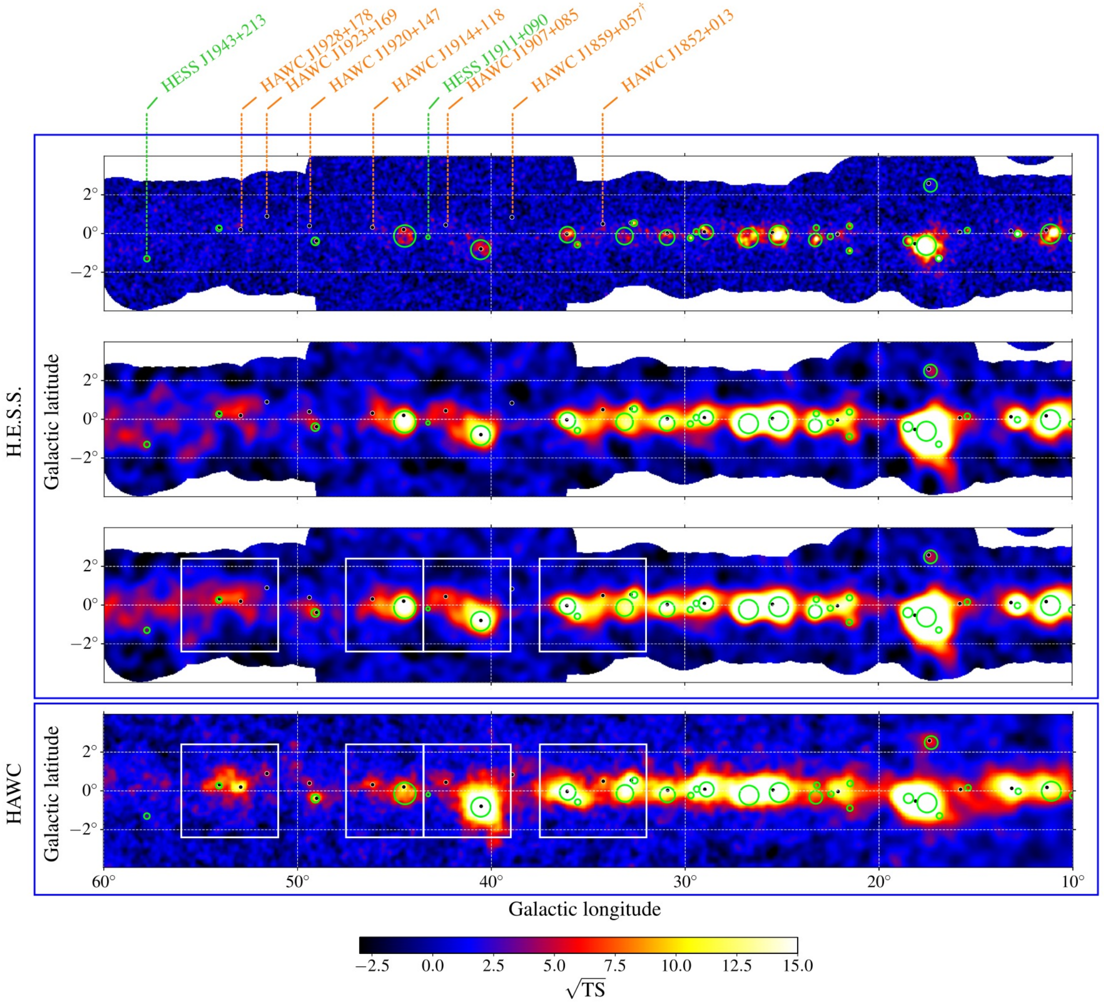

H.E.S.S. & HAWC Collaborations, ApJ **917** (2021) 6

Pulsar halos: e.g. Geminga

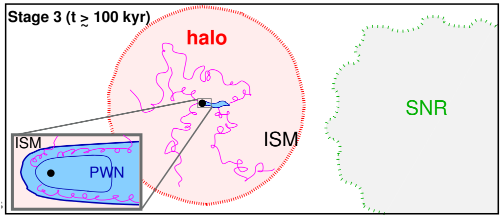

- First identified at TeV energies by Water Cherenkov Detector HAWC
  Larger field-of-view → less angular size bias
- IACTs such as H.E.S.S. have since put effort into improving analysis sensitivity to extended sources
  - Consistent view of the Galactic Plane (H.E.S.S. & HAWC, ApJ, **917**, 2021, 6)
    → several extended sources seen by HAWC now detected in H.E.S.S. data
  - Detection of the canonical halo around the Geminga pulsar
  - t = 342 kyr, $\dot{E}$ = 3.2x10^{34} erg/s, d = 0.25 kpc

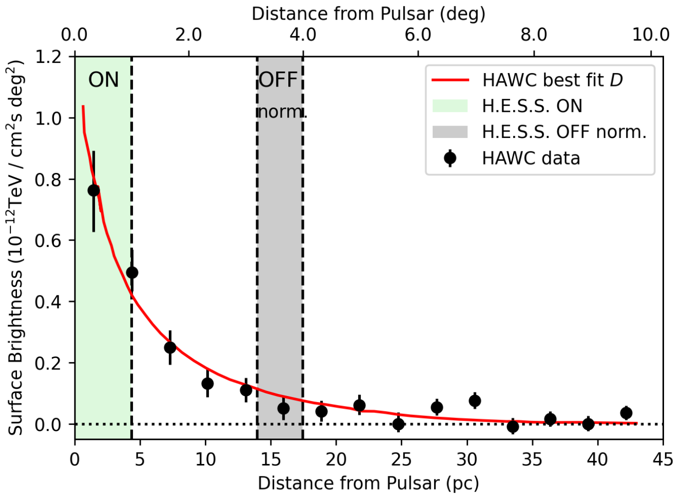

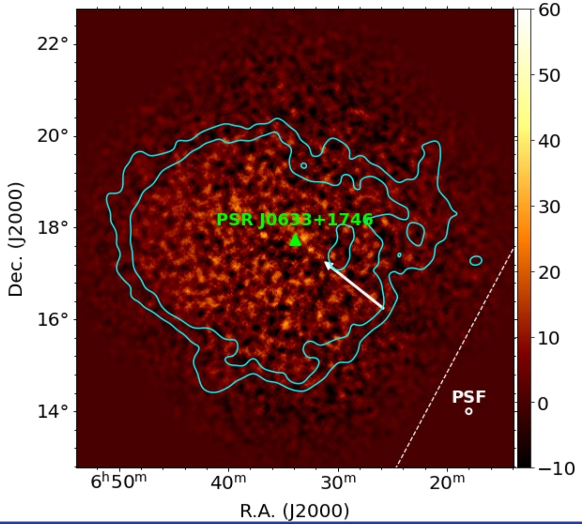

HESS A&A (2023)

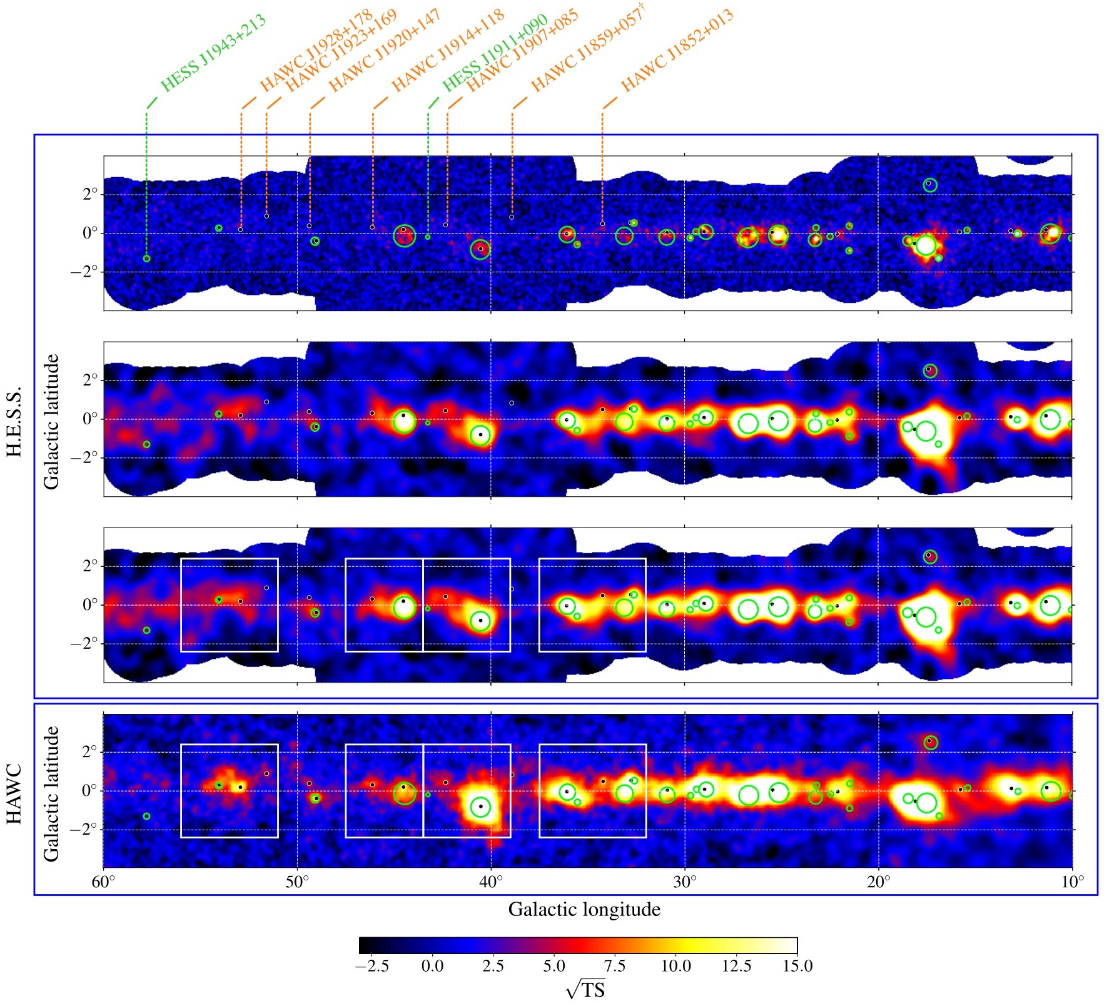

H.E.S.S. & HAWC Collaborations, ApJ **917** (2021) 6

Electron Diffusion in the Geminga Halo

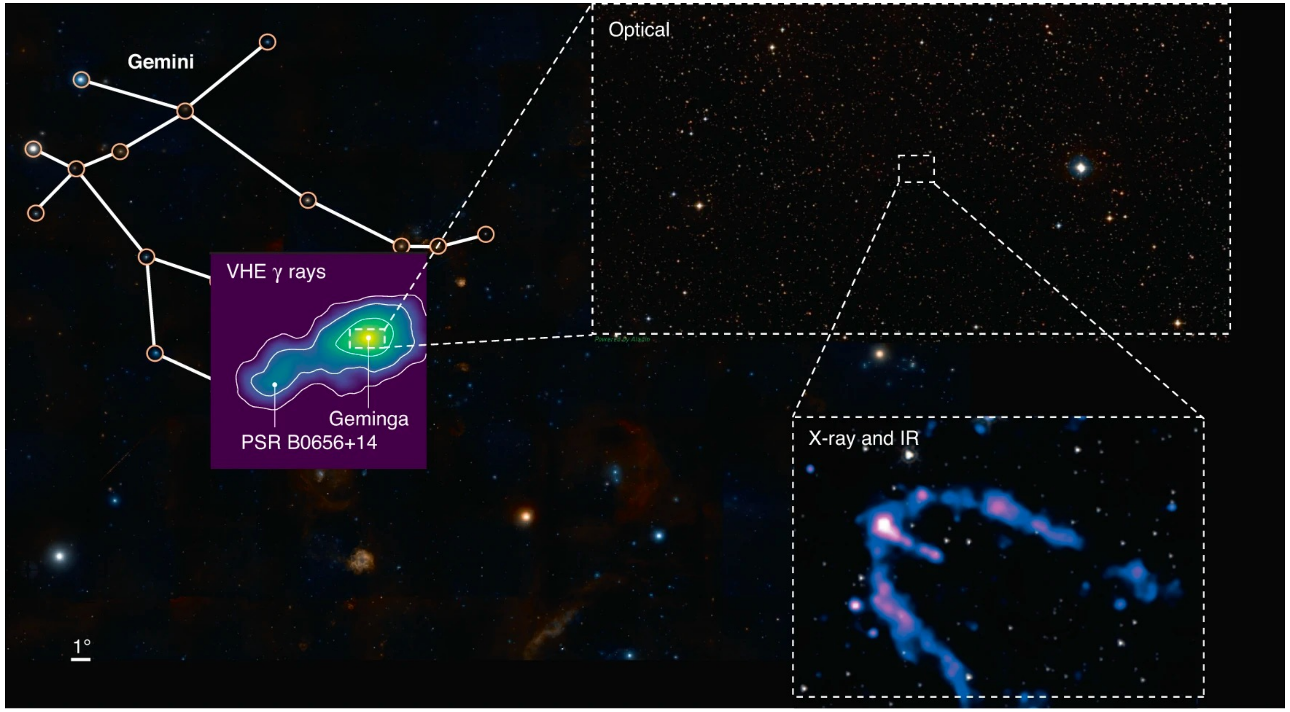

Lopez-Coto et al. Nat. Ast. **6** (2022) 199-206

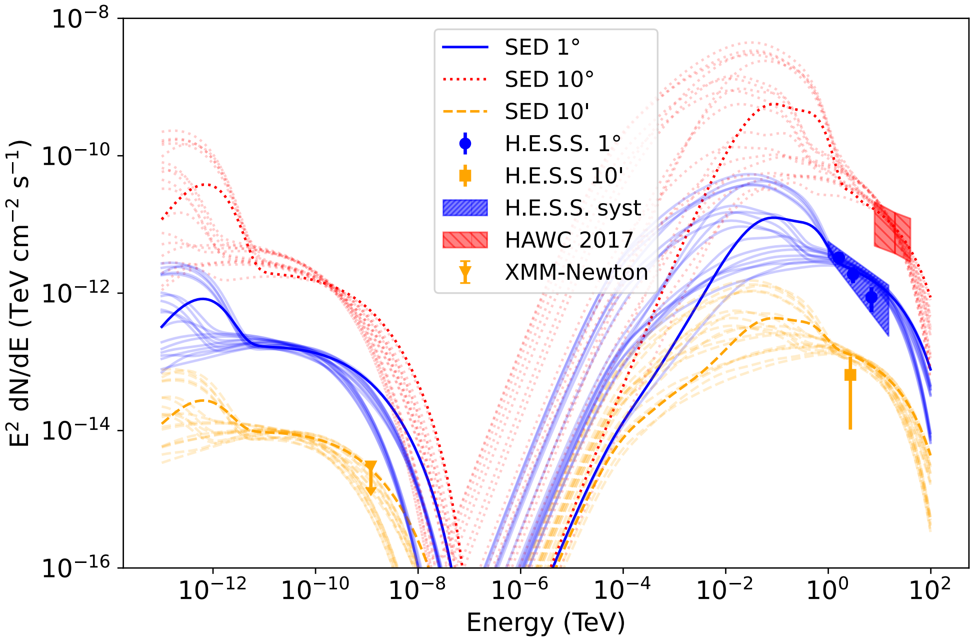

H.E.S.S. Collaboration A&A (2023)

- VHE gamma-ray emission extended scales >> X-ray size
- Emission profile indicates diffusion far below the Galactic average → not expected for particles escaped into the ISM
- H.E.S.S. results can be consistently described with MWL data under a slow diffusion model

Diffusion modelling of the Geminga pulsar halo

- Model of continuous electron injection by the pulsar and diffusion through the halo
- Peak diffusion radius corresponds to the age of the system via electron cooling losses
- Parameter scan: varied n, δ, α, η, B & E_c
  → 243 possible combinations

- Diffusion Coefficient normalisations significantly below galactic average values are preferred

$$D(E_e) = D_0(E_e/10\,GeV)^{\delta}$$
$$r_d = 2\sqrt{D(E_e)t_E} \quad \text{(S6).}$$

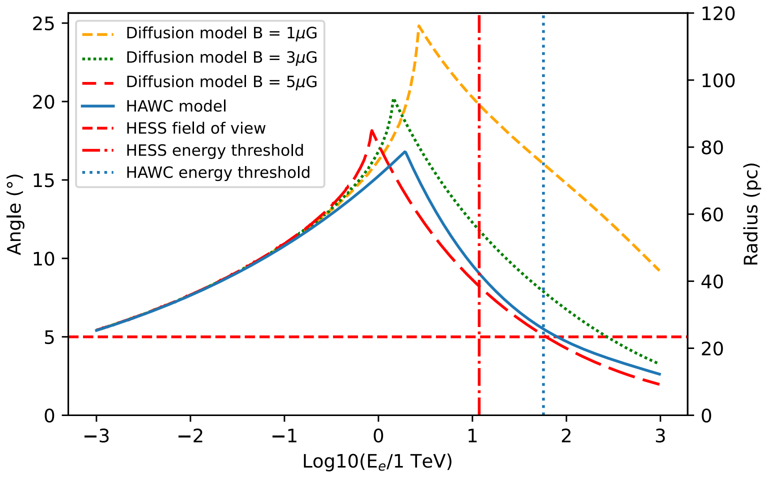

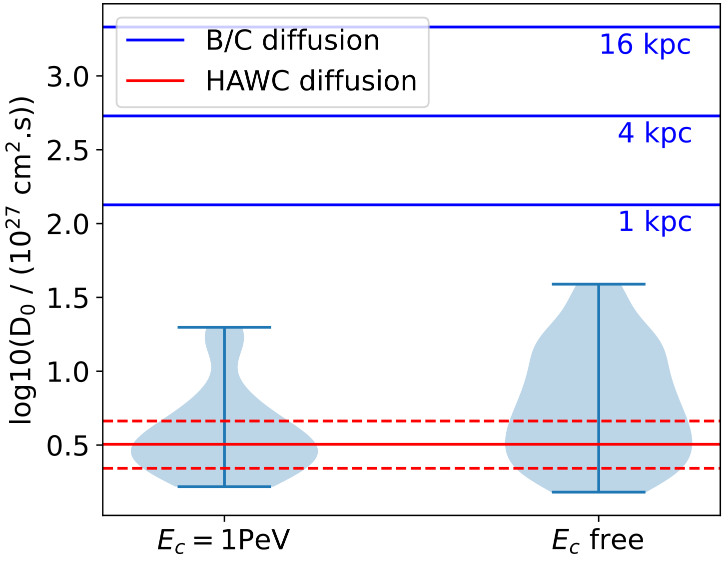

Cosmic Ray Electron Spectrum

- Recent measurements of slow diffusion in accelerator vicinity
- Generally need a local source contribution to explain the high energy CR electron spectrum
- Nature unclear: local SNR, local pulsar....

$\Delta E \pm 15\%$ due to hadronic interaction model uncertainties

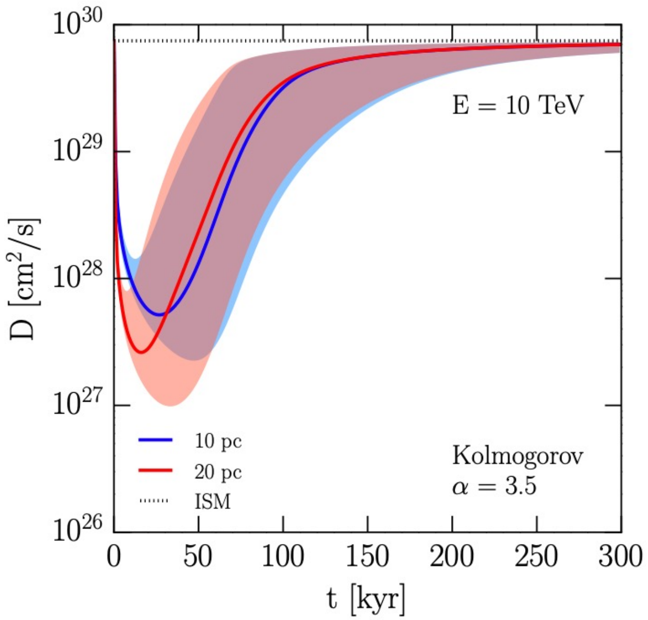

Evoli et al PRD **98**, 063017 (2018)

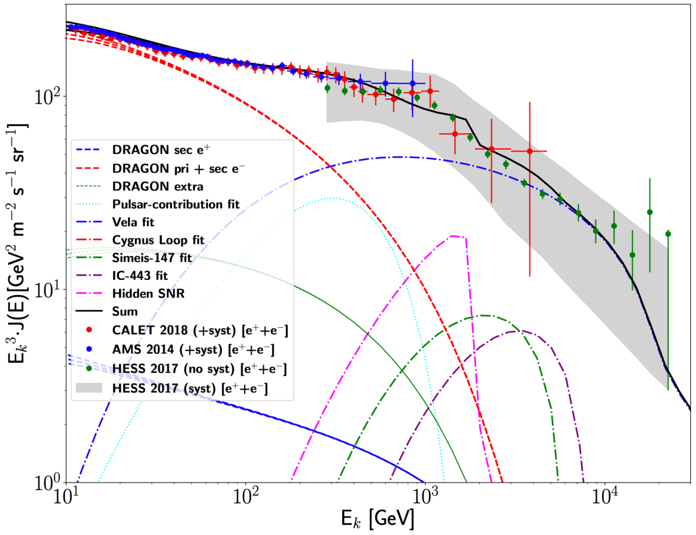

Fornieri et al. JCAP **02** (2020) 009

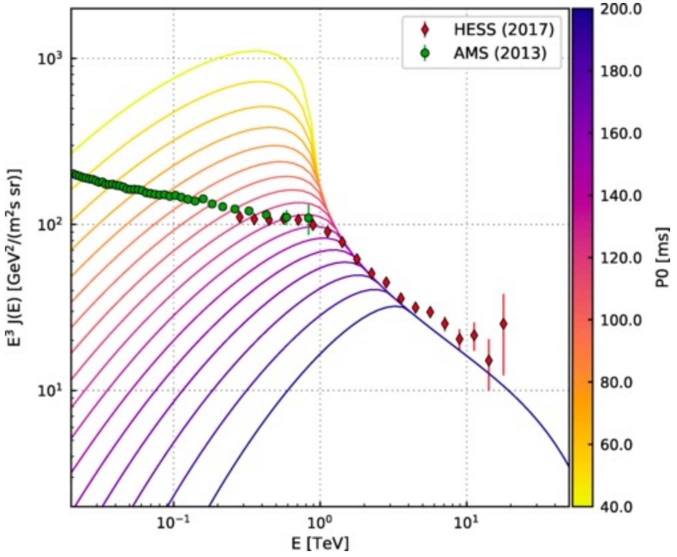

Lopez-Coto et al. PRL **121** (2018) 251106

PeVatron candidates

Recall: galactic Cosmic Rays must reach at least “knee” energies of ~3 PeV

→ Search for accelerators of hadronic particles: “PeVatrons”

→ Gamma-ray signatures are roughly a factor 10 lower energy, i.e. around 100 TeV

Potential source classes:

– supernova remnants?
– Galactic Centre region?
– stellar clusters?
– escaping CRs interacting with clouds?
– Unidentified sources?

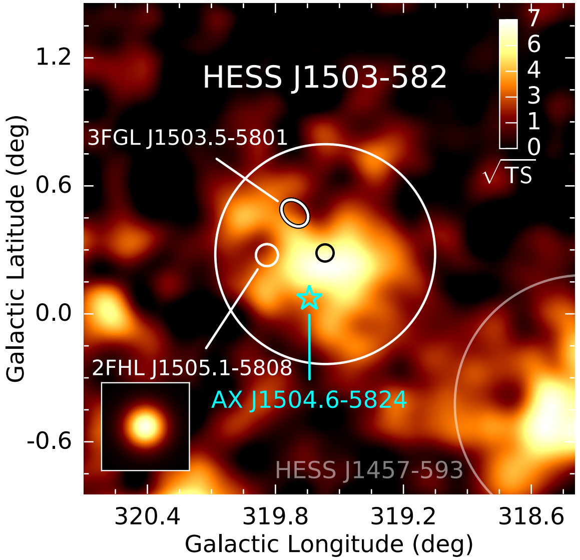

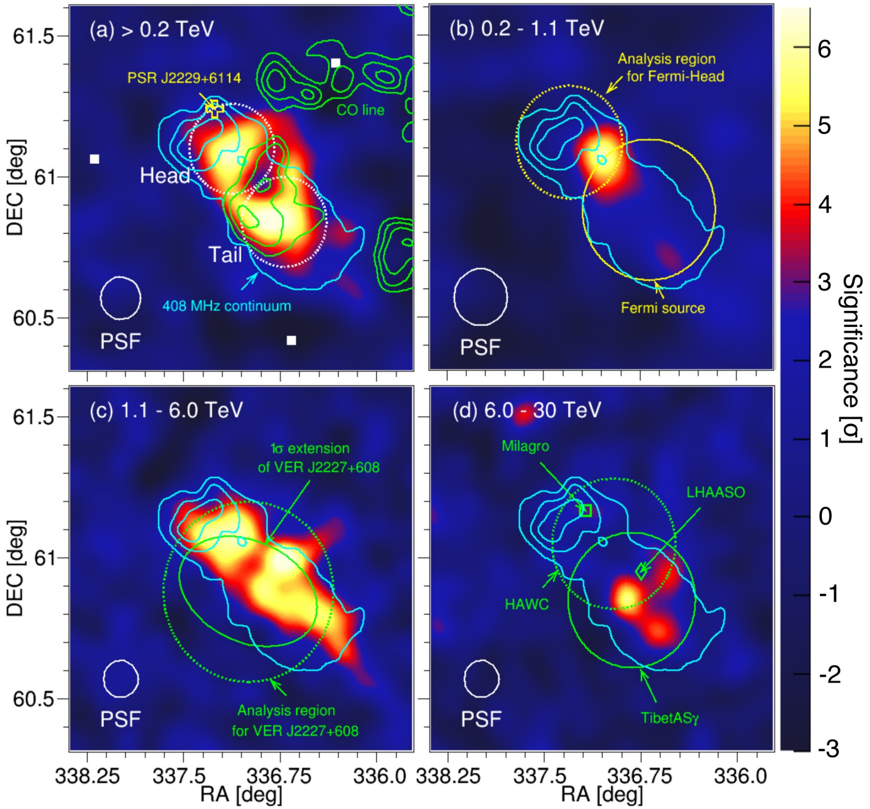

G106.3+2.7 / Boomerang nebula
MAGIC collaboration A&A **671**, A12 (2023)

Dark sources

Incl. Globular clusters

Dark → no known counterparts

Unidentified → acceleration method unclear

(e.g. multiple counterparts)

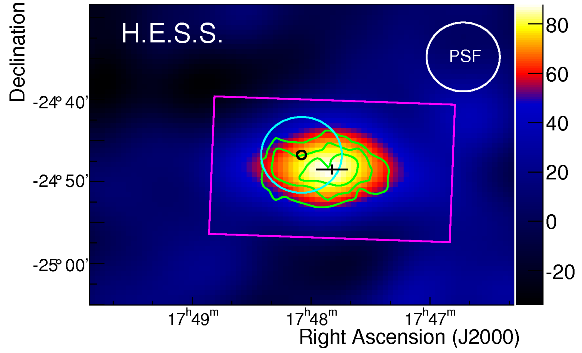

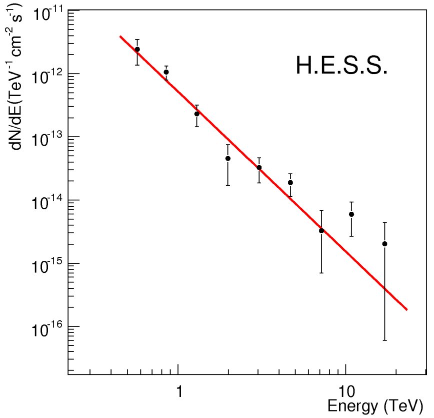

H.E.S.S. Collaboration A&A **531** L18 (2011)

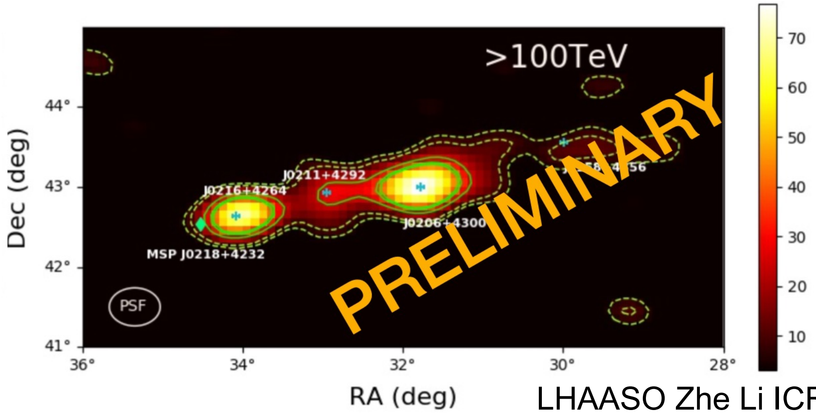

LHAASO Zhe Li ICRC(2023)

"Very-high-energy gamma-ray emission from the direction of the Galactic globular cluster Terzan 5"

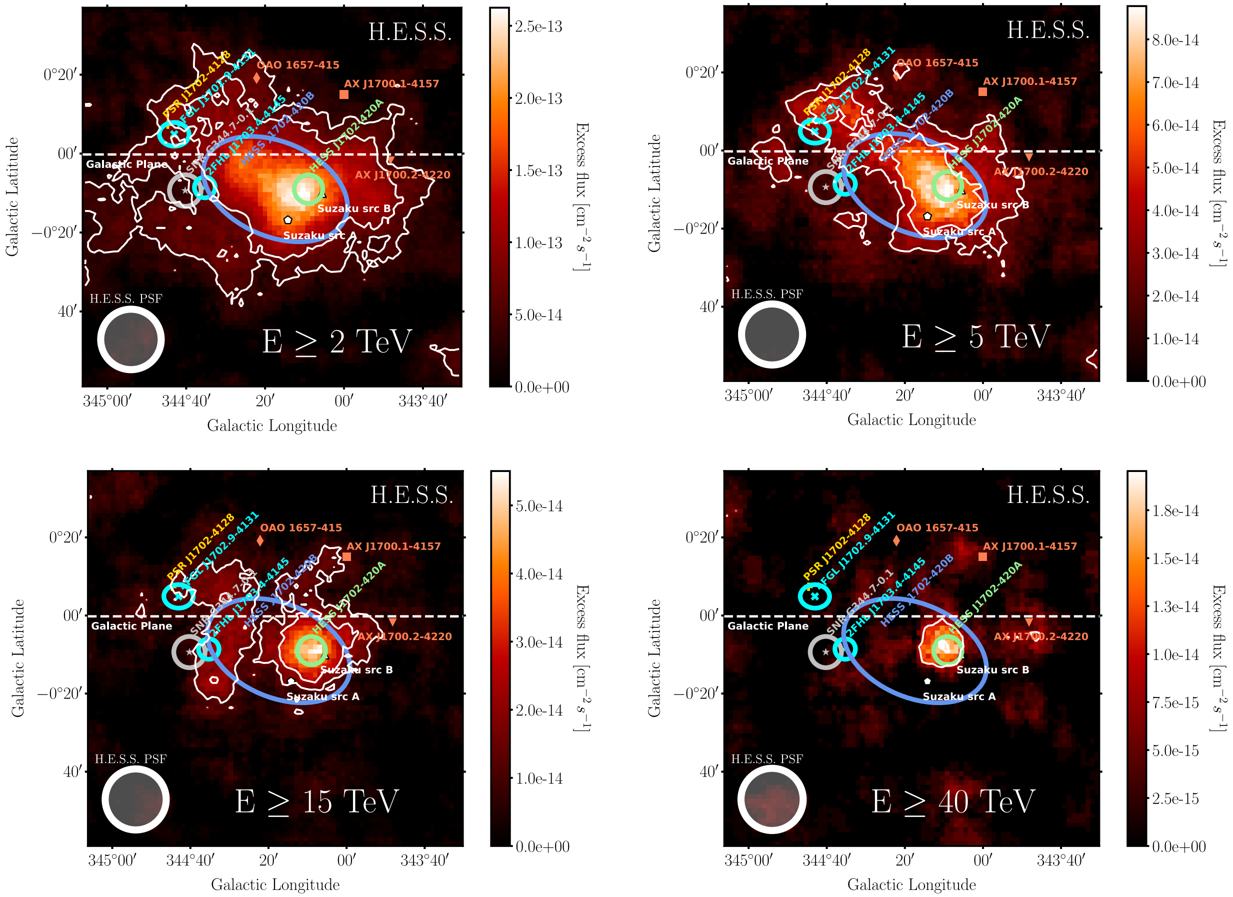

HESS J1702-420

H.E.S.S. Collaboration A&A **653** A152 (2021)

Stellar clusters

Groups of stars that are formed at approximately the same time from the same cloud of gas and dust.

→ All members have roughly the same age and initial chemical composition

→ All members are located at approximately the same distance from Earth

→ All members are gravitationally bound to other cluster members

Types:

- Young, massive stellar clusters (~Myr)
- Open clusters (~Myr – 100Myr)
- Globular clusters (~10s Gyrs)

Westerlund 1, young massive stellar cluster, JWST

Messier 3, globular cluster, University of Arizona

Stellar Clusters and Cygnus Superbubble

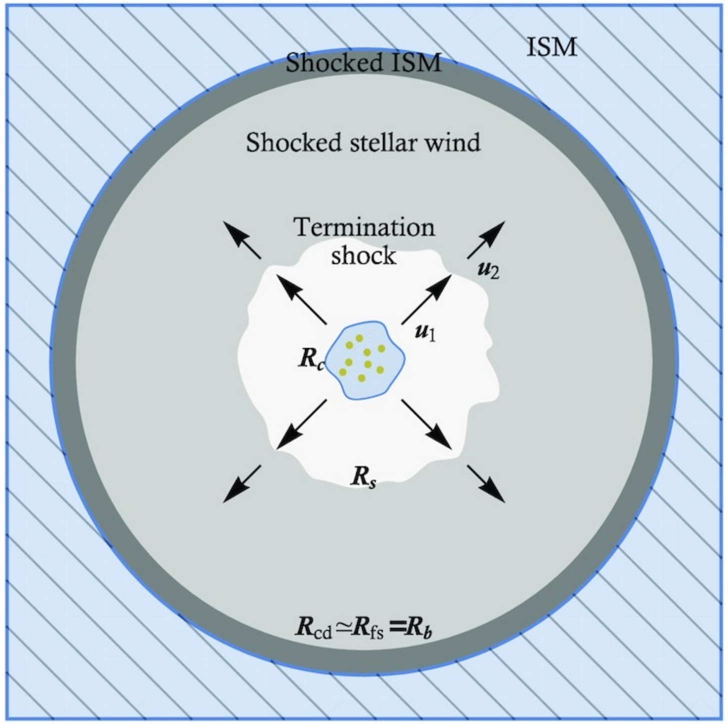

Morlino et al. MNRAS **504** (2021) 6096-6105

- Collective stellar winds drive a shock in the interstellar medium
- Requires typically young stellar clusters / massive star forming regions
- Highest energy photon measured to date: 1.42 ± 0.13 PeV → from Cygnus region? LHAASO J2032+4102 (Cao et al. Nature **594** (2021) 33-36)
- HAWC Cygnus cocoon (Nature Astro. **5** (2021) 465-471)

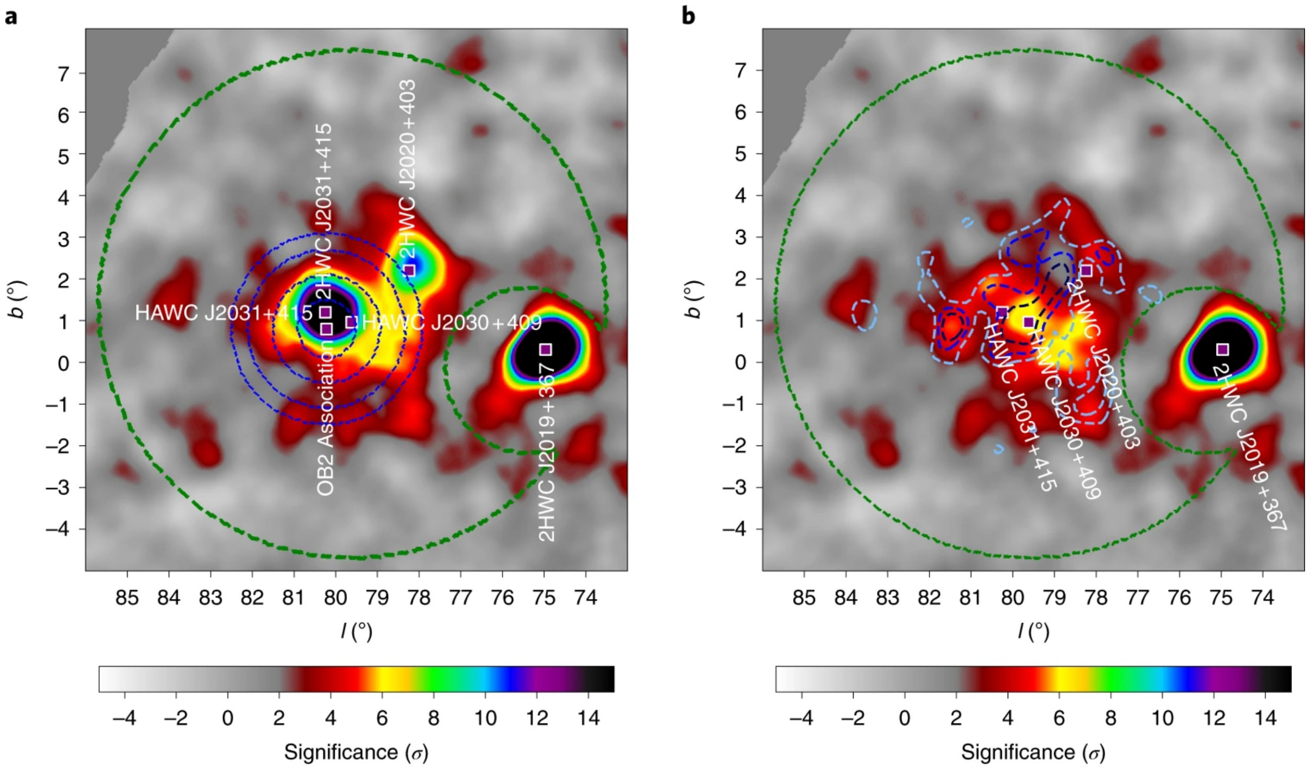

Which stellar clusters are PeVatrons?

- Most promising clusters identified based on Gaia catalogue
- Caveat: cluster bubbles have a large angular size (1º - 10º) → low surface brightness

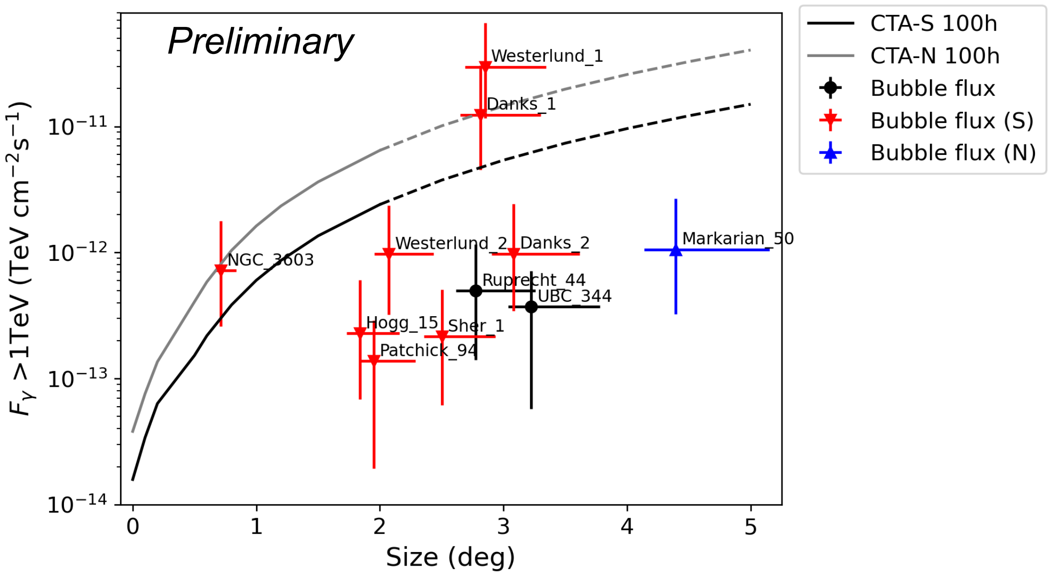

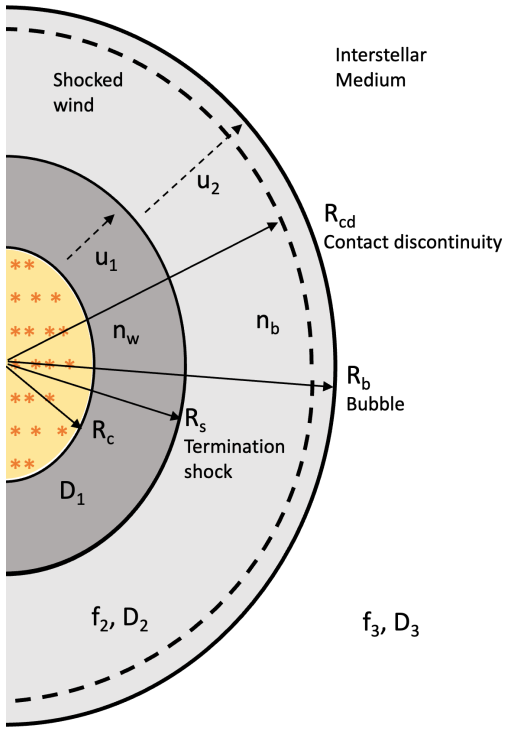

S. Celli, AM, A. Specovius, G. Morlino, S. Menchiari (ICRC2023)

Stellar Clusters

- Collective stellar winds drive a shock in the interstellar medium
- Requires typically young stellar clusters / massive star forming regions
- Member stars with strong individual winds

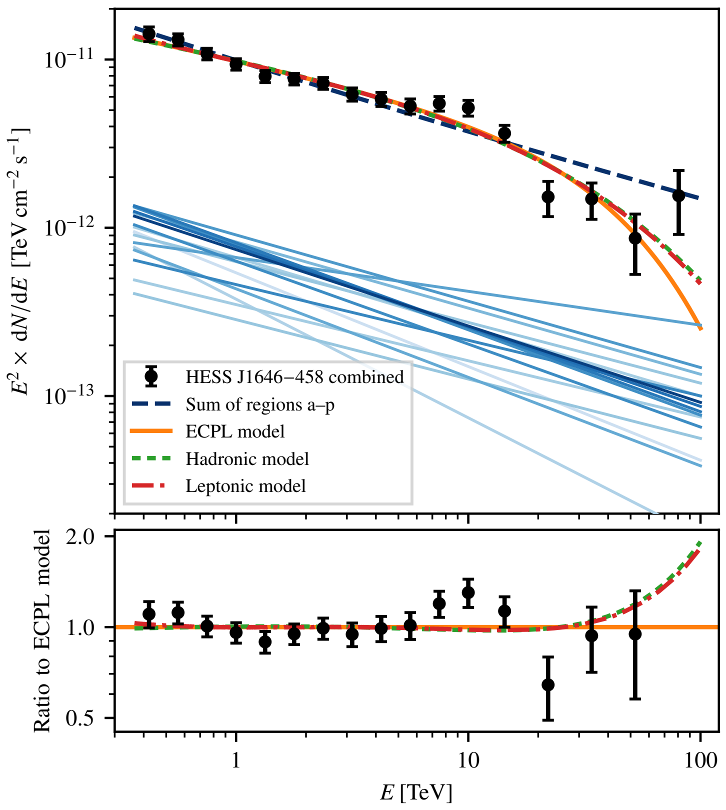

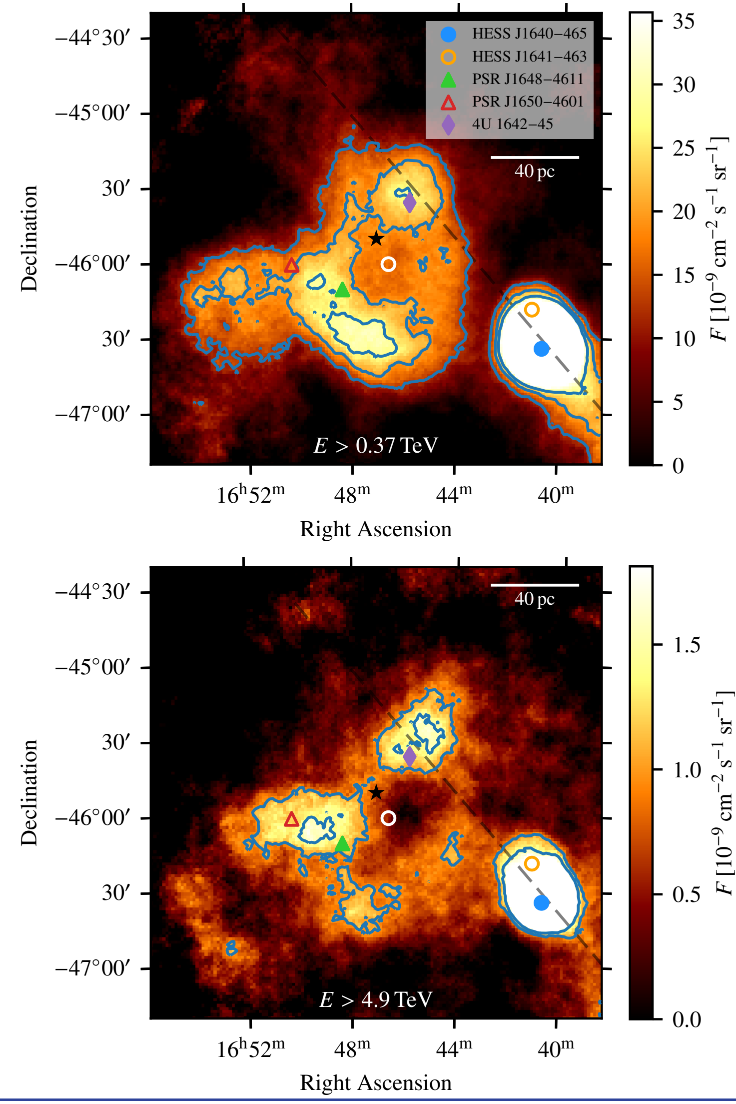

Westerlund 1
HESS Collaboration A&A **666** A124 (2022)

Highest energy gamma-ray sky > 100 TeV

- Sky maps by LHAASO, Tibet-ASγ and HAWC:
- $E_\gamma > 100$ TeV   ($E_p \sim 1$ PeV; $E_e \sim 183$ TeV)
  → ~12 sources
- Cao et al. Nature **594** (2021) 33-36

Source	Location (l,b)	Detected > 100 TeV by	Possible Origin
Crab Nebula	(184.557, -5.784)	HAWC, MAGIC, LHAASO, Tibet-ASγ	PSR
HESS J1702-420	(344.304, -0.184)	H.E.S.S.	?
Galactic Centre	(0-1.2, -0.1– +0.1)	H.E.S.S.	SMBH?
eHWC J1825-134	(18.116, -0.46)	HAWC, LHAASO	PSR
LHAASO J1839-0545	(26.49, -0.04)	LHAASO	PSR
LHAASO J1843-0338	(28.722, 0.21)	LHAASO	SNR
LHAASO J1849-0003	(32.655, 0.43)	LHAASO	PSR, YMC
eHWC J1907+063	(40.401, -0.70)	HAWC, LHAASO	SNR, PSR
LHAASO J1929+1745	(52.94, 0.04)	LHAASO	PSR, SNR
LHAASO J1956+2845	(65.58, 0.10)	LHAASO	PSR, SNR
eHWC J2019+368	(75.017, 0.283)	HAWC, LHAASO	PSR, H II/YMC
LHAASO J2032+4102	(79.89, 0.79)	LHAASO	YMC, PSR, SNR?
LHAASO J2108+5157	(92.28, 2.87)	LHAASO	?
TeV J2227+609	(106.259, 2.73)	Tibet-ASγ, LHAASO	SNR, PSRs

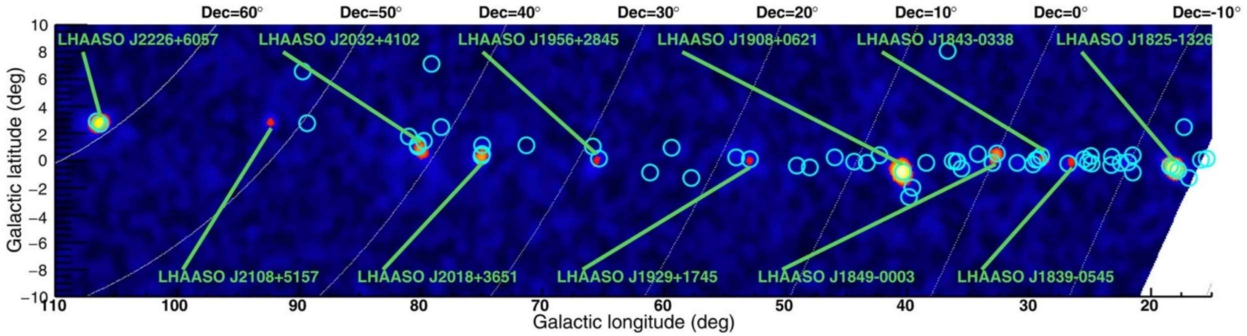

- Most associated with pulsars
- Generally, pulsars are associated with leptonic emission (e^+ & e^-)

Highest energy gamma-ray sky

- Sky maps by LHAASO, Tibet-ASγ and HAWC: $E_\gamma > 100$ TeV → ~12 sources

  (E_p~1 PeV; E_e~183 TeV)
  Cao et al. Nature **594** (2021) 33-36

- **2023**: ~ 75 gamma-ray sources above 25 TeV, 43 above 100 TeV
  → all located in our Galaxy
  1st LHAASO Catalogue,
  Cao et. al. arXiv:2305.17030v1

- Many unassociated – no known counterpart

- Most common identified counterparts are pulsars

- Generally, pulsars are associated with leptonic emission (e^+ & e^-)

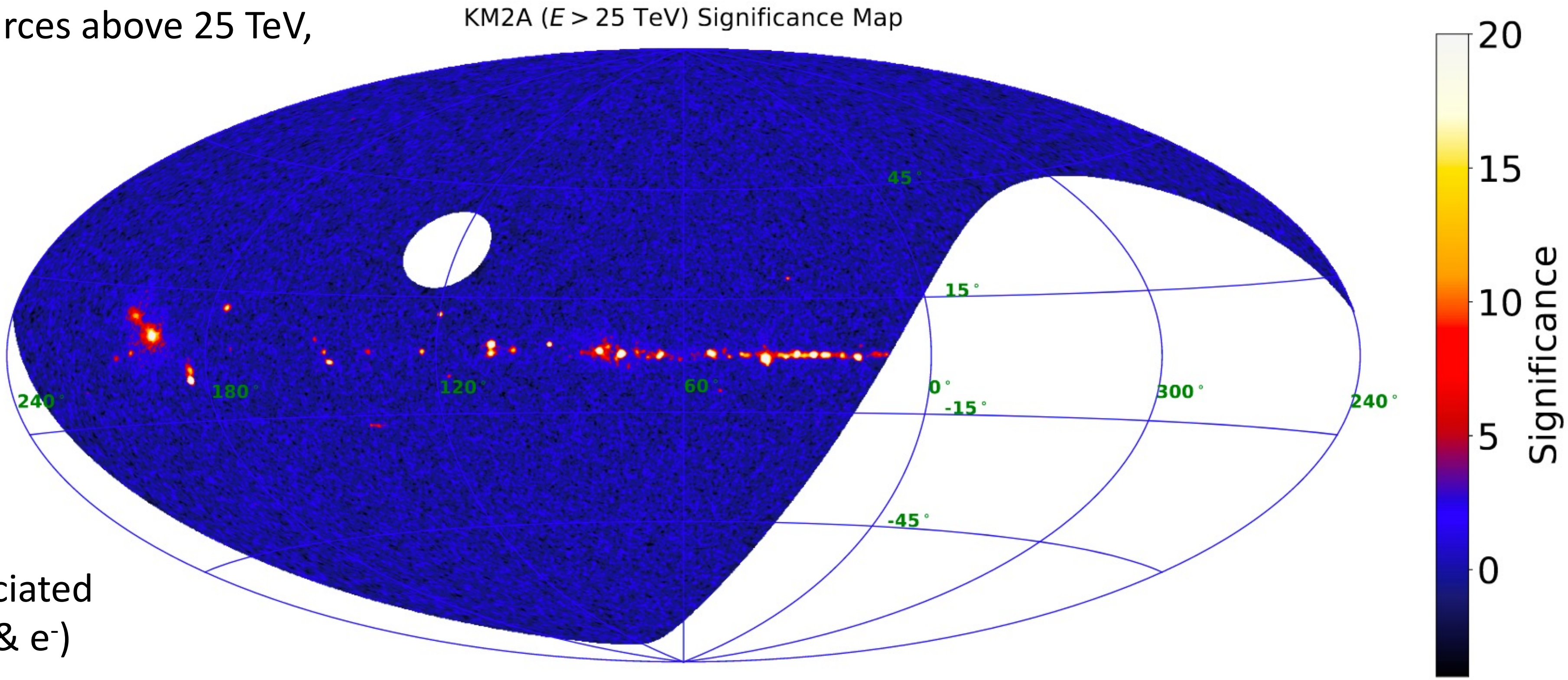

UHE leptonic emission & Klein-Nishina effect

Inverse Compton proceeds in two regimes: Thomson regime & Klein-Nishina regime in which an electron loses a small or large fraction of its energy respectively.

$$\Xi_{IC} \equiv {}^{U_{rad}}/_{U_B}$$

- In high radiation environments, synchrotron cooling dominates over IC losses, even into Klein-Nishina regime. (IC cross-section suppressed)
- Resulting spectrum is harder / cut-off is less pronounced.
- Leptonic spectra out to PeV energies can be observed

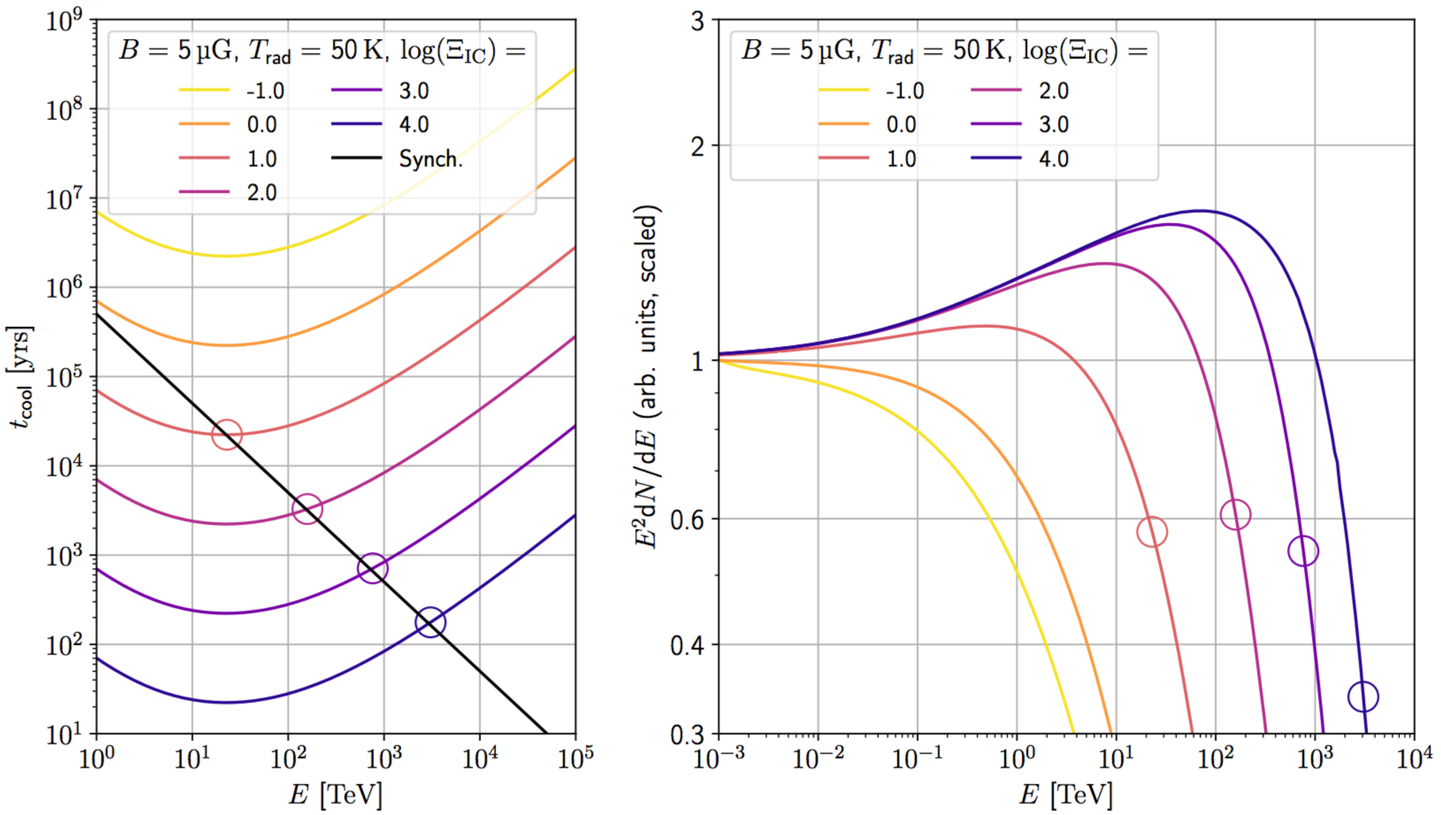

Breuhaus et al. ApJL **908** L49 (2021)

Klein-Nishina cut-off → sub-dominant hadronic component

e.g. Crab Nebula

A sub-dominant hadronic component could be revealed at the highest energies, beyond the Klein-Nishina cut-off

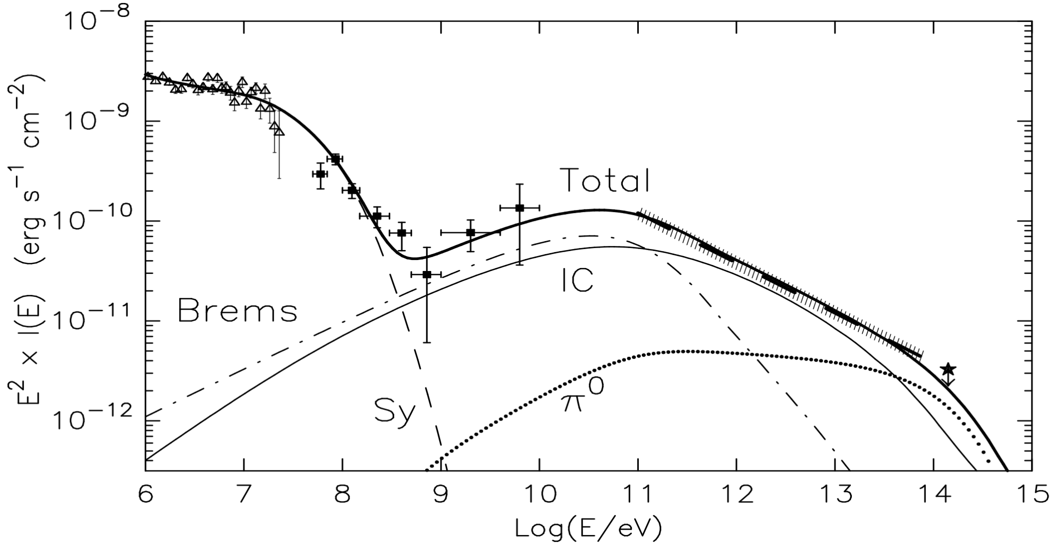

Aharonian & Atoyan, proc. "Neutron Stars and Pulsars" 439 (1998)

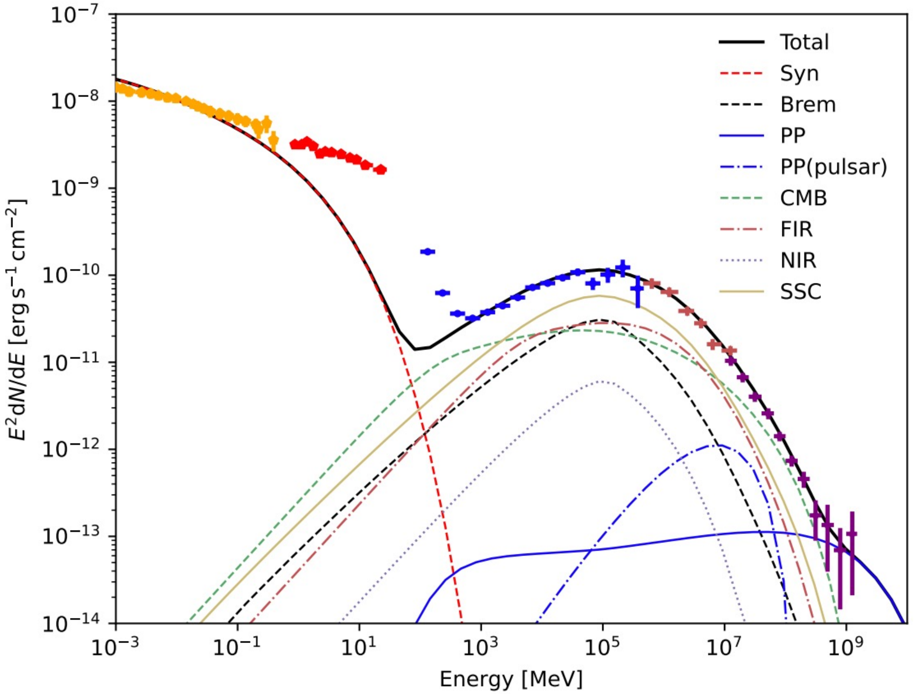

Nie et al, ApJ 924, 42 (2022)

Gamma-ray signatures of cosmic rays

→Protons (and heavier nuclei) escape from accelerator – will interact with nearby clouds

→Predict and search for gamma-rays from clouds identified in radio

→Can use clouds in vicinity of accelerators to probe escape of protons and constrain their presence

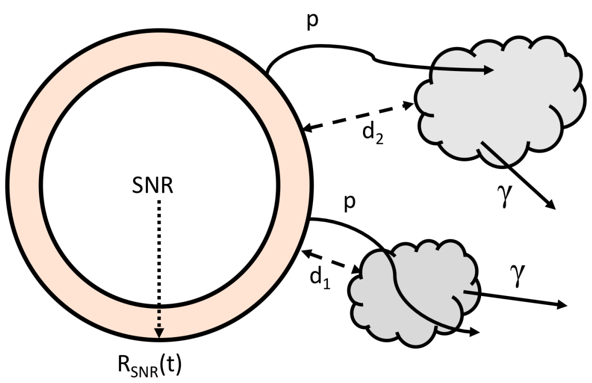

AM et al. MNRAS ***503*** *3522-3539 (2021)*

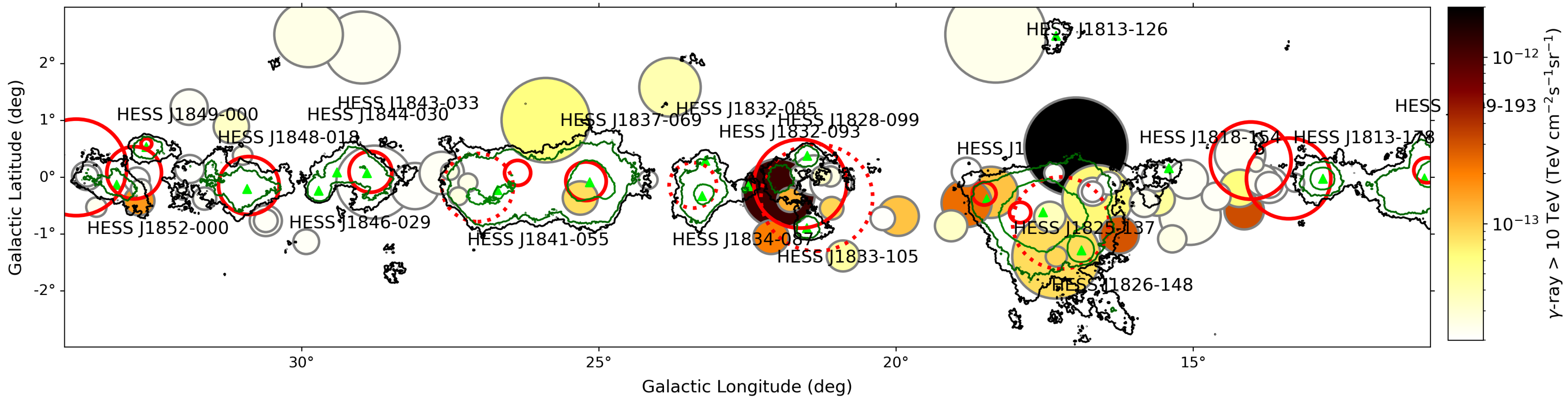

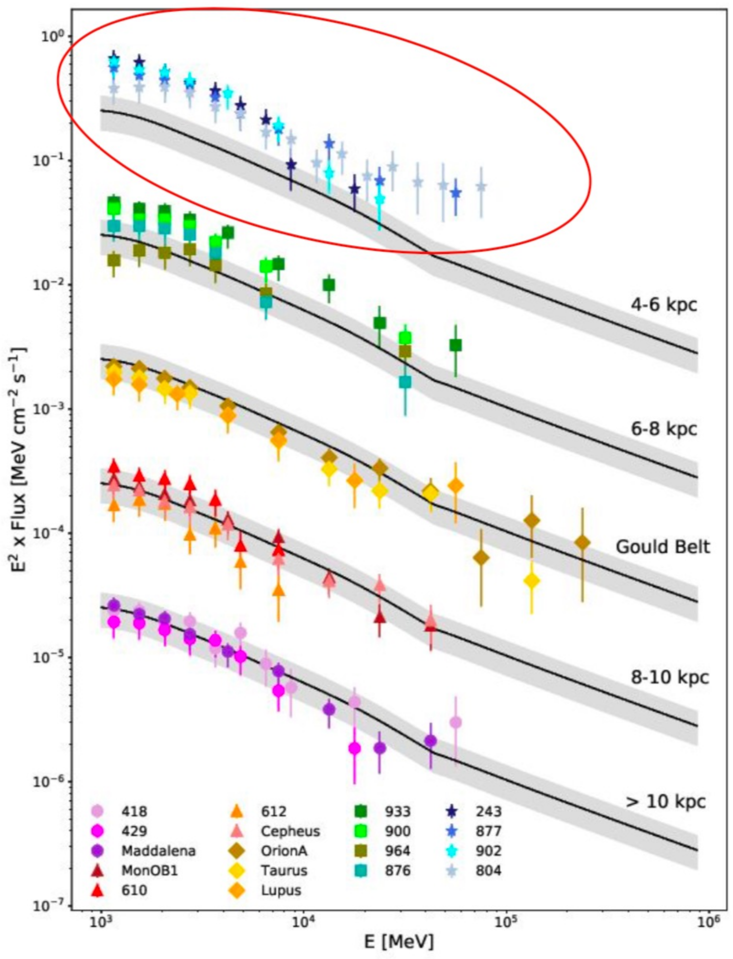

Aharonian et al, PRD **101**, 083018 (2020)

SNR + Cloud Model: particle and gamma-ray flux

Particle flux from an impulsive accelerator, α = 2 (Aharonian & Atoyan '96)

$$f(E,r,t) \approx f_0 \frac{N_0 E^{-\alpha}}{\pi^{3/2} R_d^3} \exp\left(-\frac{(\alpha-1)t}{\tau_{pp}} - \frac{R^2}{R_d^2}\right)$$

Gamma-ray flux Φ_γ produced by interactions with a target cloud (Kelner et al 2006)

$$\Phi_\gamma(E_\gamma) = c n_H \int_{E_\gamma}^{\infty} \sigma_{\mathrm{inel}}(E_p) f(E_p,r,t) F_\gamma\left(\frac{E_\gamma}{E_p}, E_p\right) \frac{dE_p}{E_p}$$

If particles fully traverse cloud, observable flux is normalised based on the cloud volume.

Otherwise, a cell-based integration is performed over the partial cloud volume that the particles have traversed.

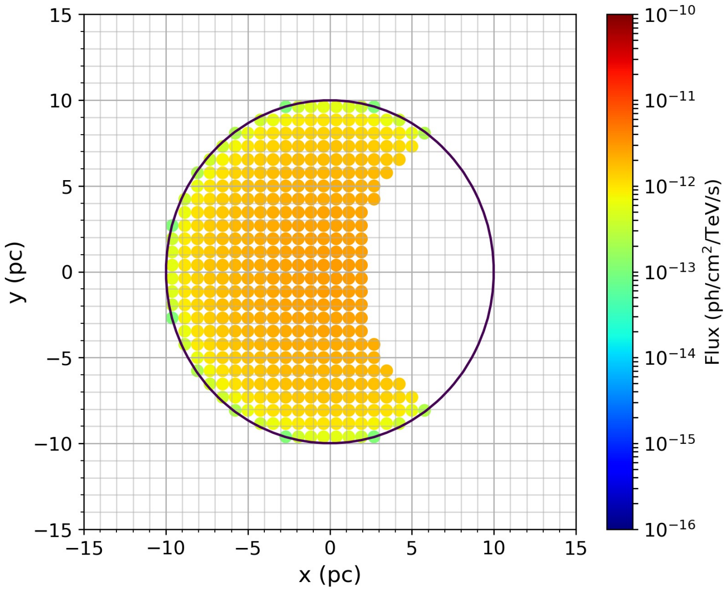

SNR evolution and particle escape

Particles of different energies are released at different times during the evolution of the SNR.

$$t_{\rm esc} = t_{\rm sed}\left(\frac{p}{p_M}\right)^{-1/\beta} \ {\rm yr}$$

Assume all SNR considered to be in the Sedov-Taylor phase (~ 100yr – 50kyr), Sedov time = 1.6kyr (type II), β = 2.5

Meanwhile, the SNR radius also expands.

$$R_{\rm SNR}(t) = 0.31\left(\frac{(E_{SN}/10^{51}{\rm erg})}{(n/1{\rm cm}^{-3})(\mu_1/1.4)}\right)^{1/5} (t/{\rm yr})^{2/5} \ {\rm pc}$$

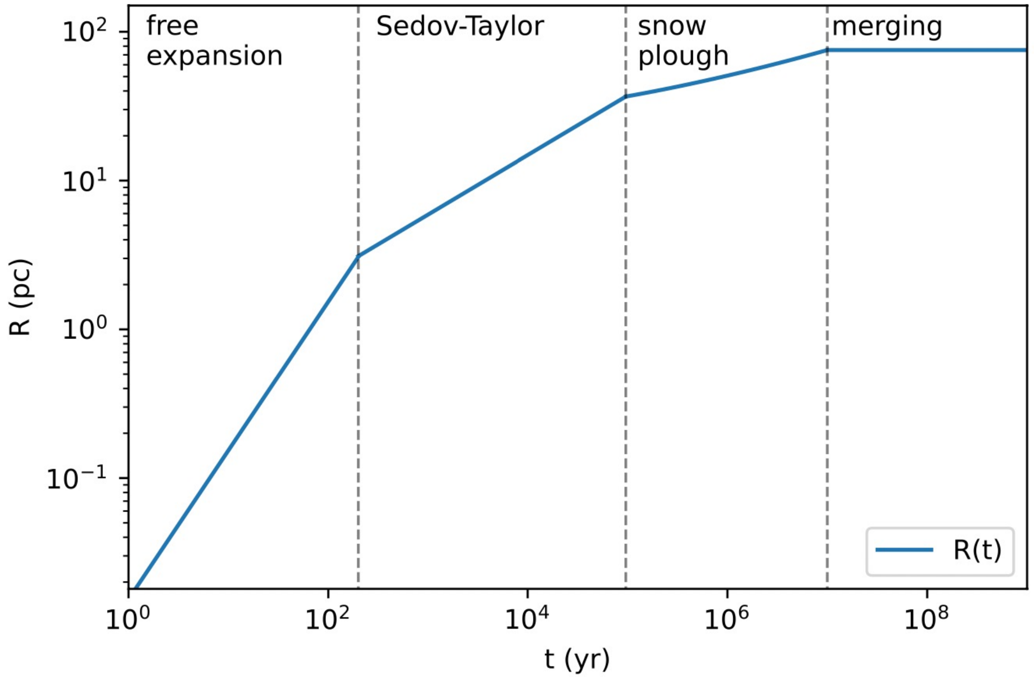

Then:
- diffuse through ISM to reach cloud
- particle interactions with cloud

SNRs as PeVatrons

If all SNRs act as PeVatrons for a short time (i.e. Emax at the Sedov time), how many should be detectable now?

Explore parameter phase space of model

Fit to data where possible (e.g. RX J1713...)

Once particles have been accelerated by the SNR:
– diffuse through ISM to reach cloud
– particle interactions with cloud

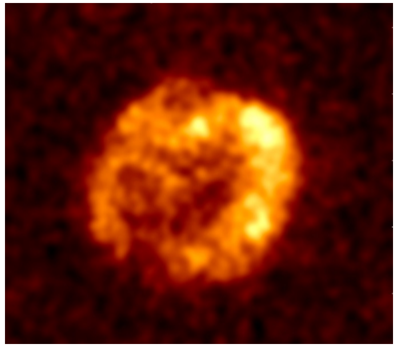

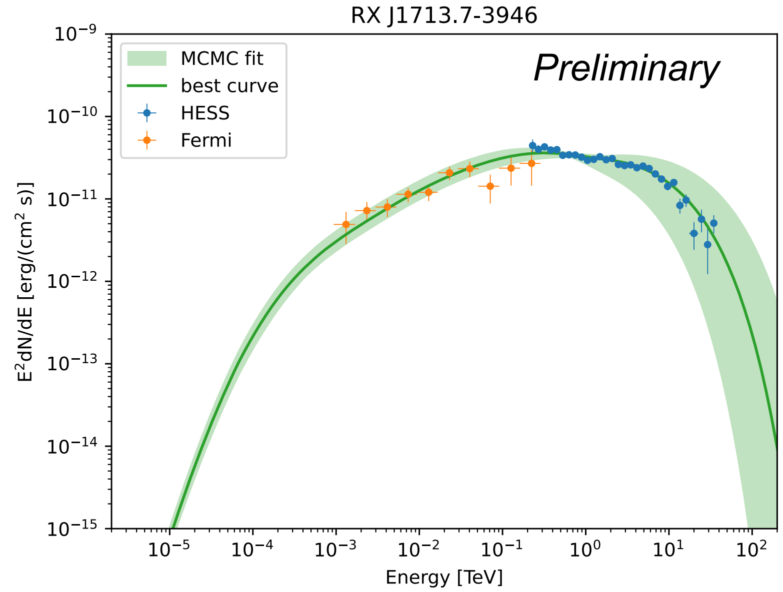

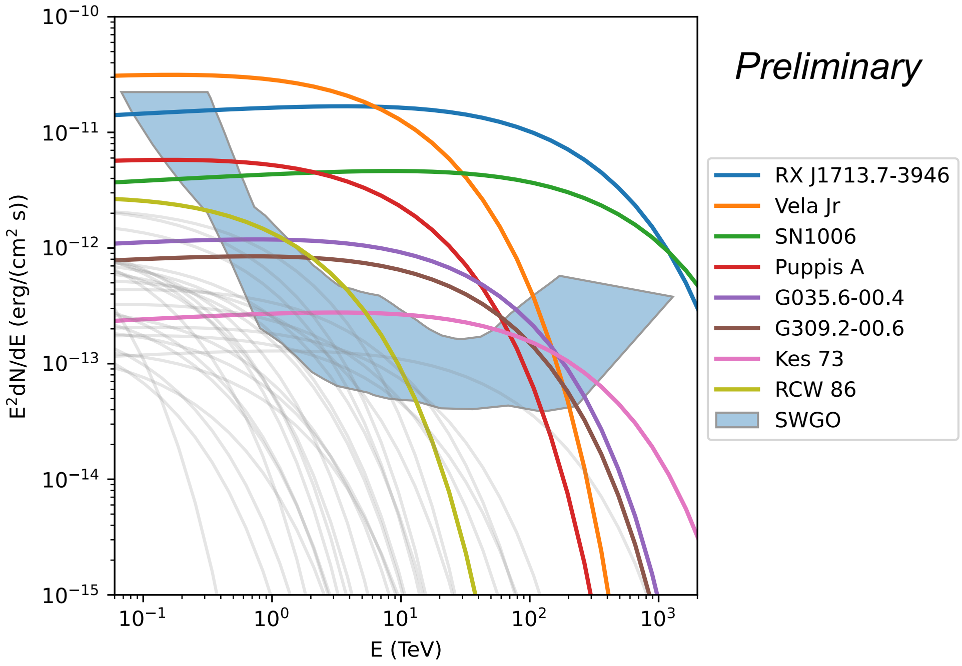

N. Scharrer, V. Joshi, S. Spencer, AM

Cloud – SNR properties: example spectra

Primary variables (aside from model assumptions) are:

- SNR age (t): peak shifts to lower energies for older SNRs
- Cloud density (n): higher density = more flux
- SNR-cloud separation distance (d):
  it takes more time for lower energy particles to arrive

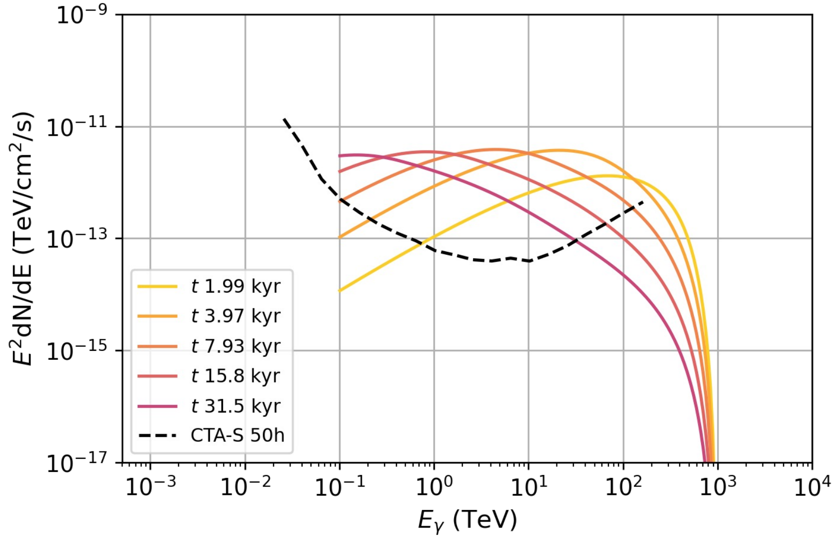

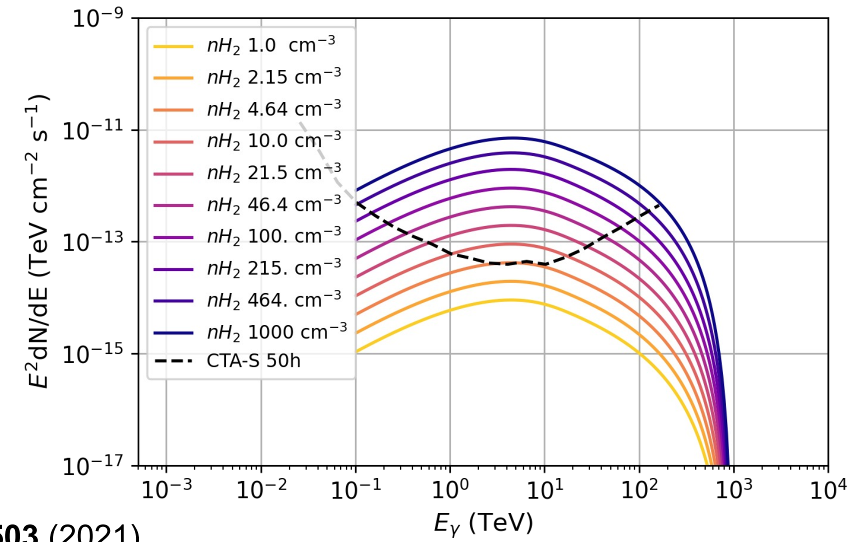

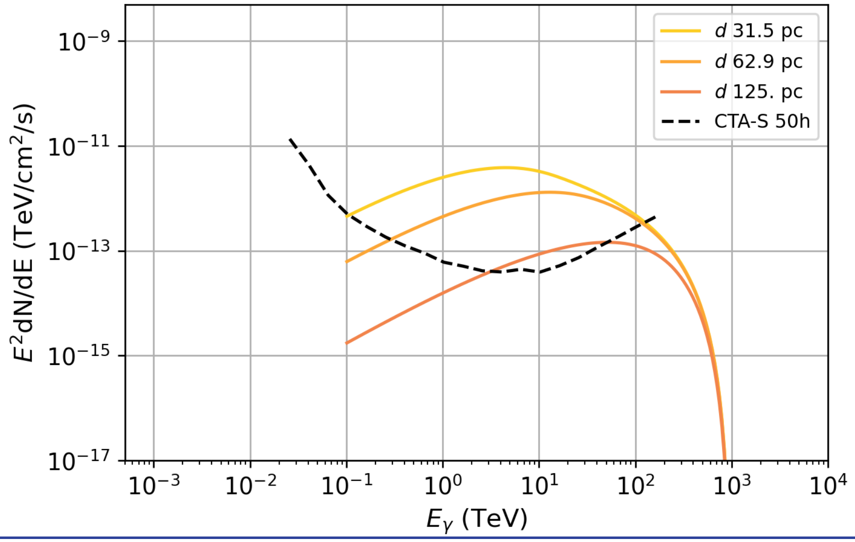

AM, Rowell, Celli, Einecke MNRAS **503** (2021)

LHAASO J2108+5157

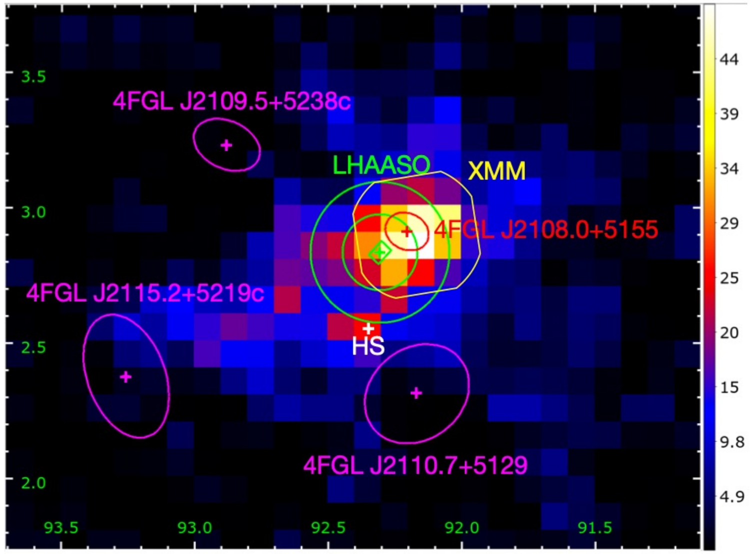

Figure 2: *Fermi*-LAT TS map above 2 GeV

An intriguing dark source, discovered at UHE (Cao et al. Nature 2021)

Coincident with a molecular cloud, yet no clear accelerator nearby

HAWC detection, Veritas upper limits (Kumar et al, ICRC2023, 941)
Fermi-LAT detection

Constrain properties of molecular clouds → scan parameter space to constrain potential SNR properties

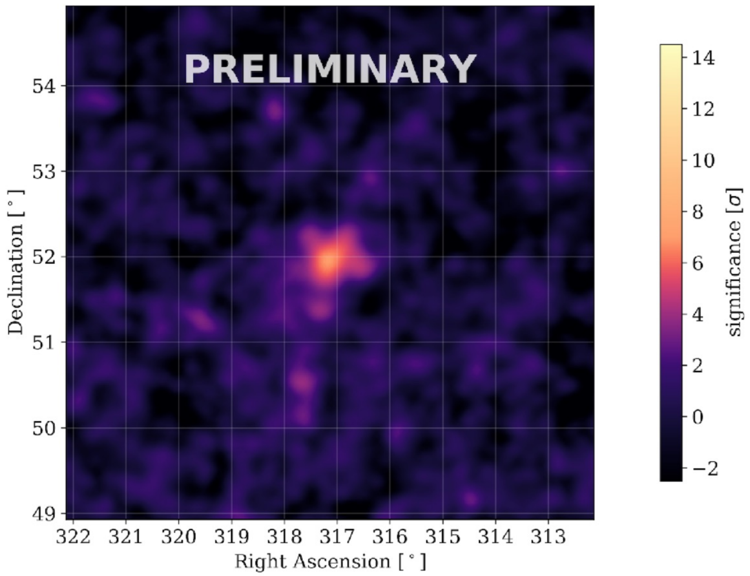

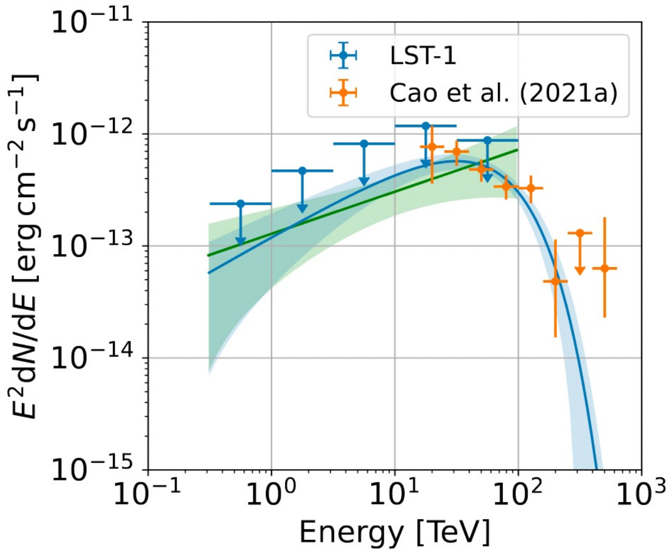

Abe et al. A&A **673** (2023) A75

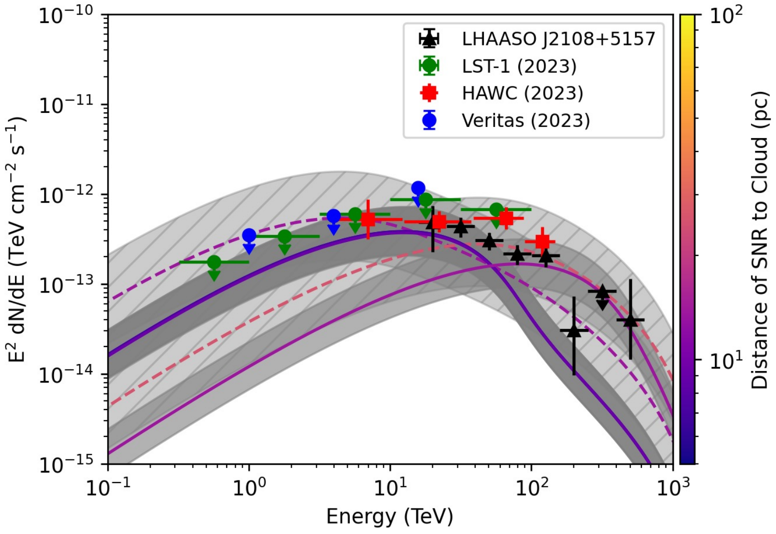

AM A&A **684** A66 (2024)

Galactic Centre Region

HESS J1745-290 is a point-like source consistent with Sgr A* at the centre of our galaxy, yet the emission mechanism remains unknown.

G0.9+0.1 is a compact pulsar wind nebula

Two bright point-like sources – contributions removed via modelling

A bright ridge of emission remains, consistent with CO gas contours

→ Evidence for diffuse emission in the central 200 pc of our Galaxy

An iterative fitting procedure can characterise the different components

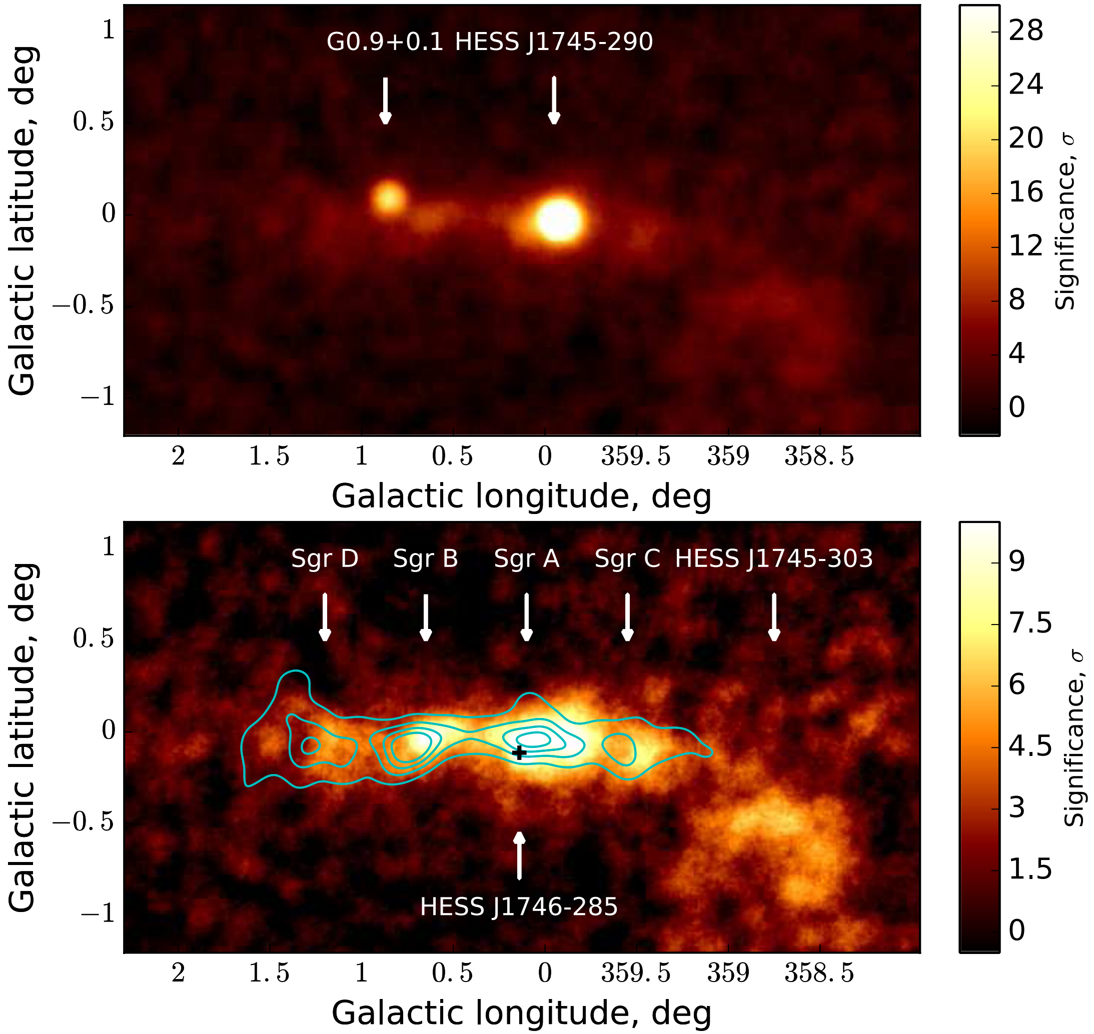

Galactic Centre PeVatron?

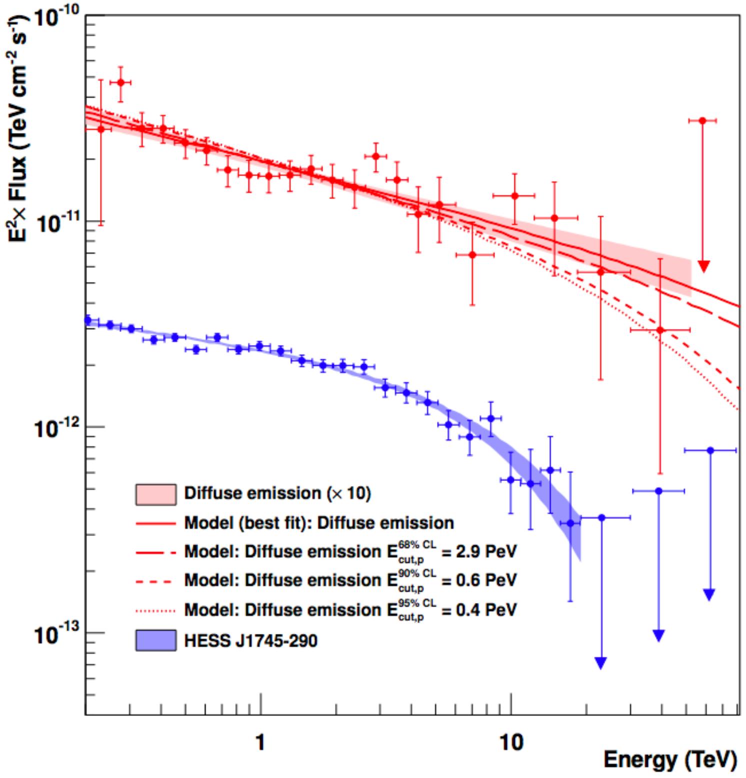

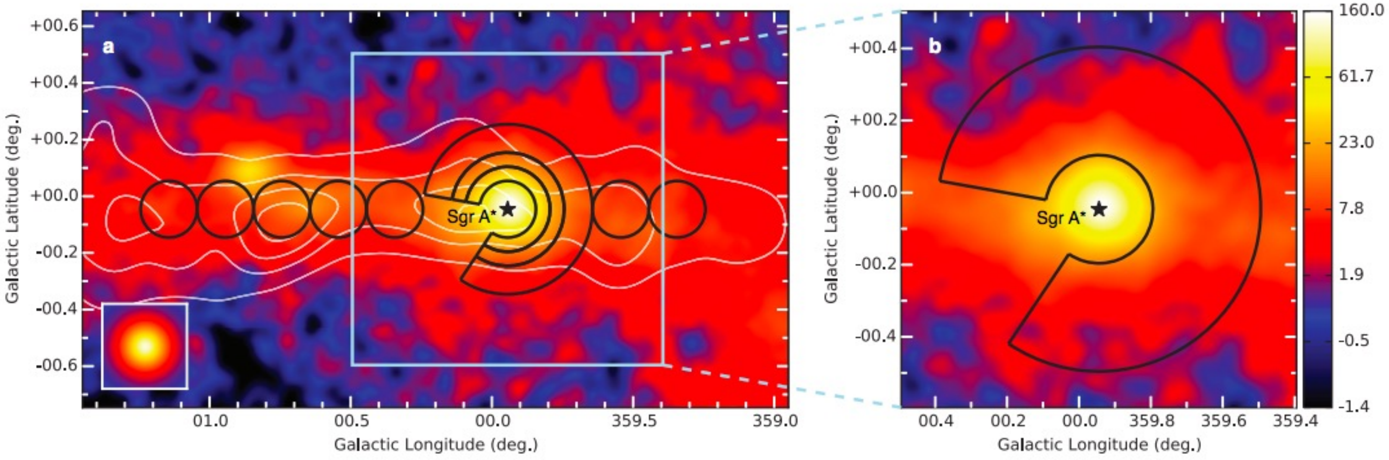

H.E.S.S. Collaboration, Nature **531** (2016) 476-479

$$w_{\mathrm{CR}}(E,r,t) = \frac{\dot{Q}_p(E)}{4\pi D(E) r}\,\mathrm{erfc}(r/r_{\mathrm{diff}})$$

$$r_{diff} \approx \sqrt{4D(E)t}$$

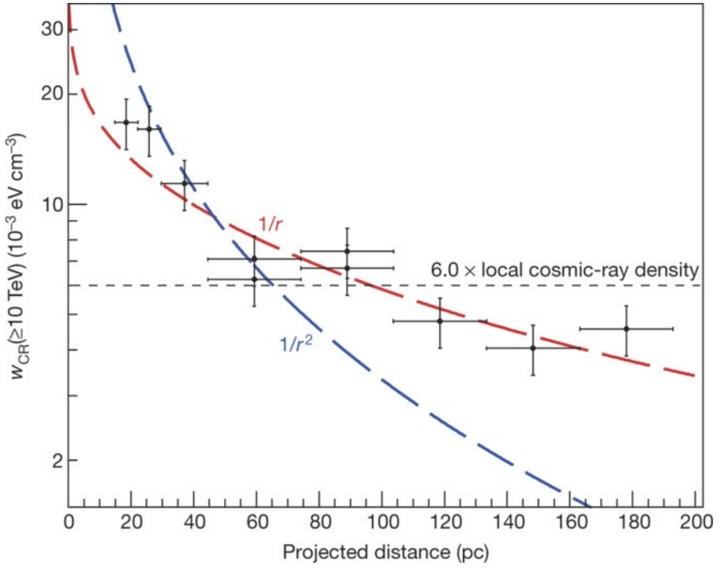

Evidence in the vicinity of the galactic Centre for a former powerful accelerator reaching ~PeV energies

Density profile implies continuous injection into the region

Binary Systems: Microquasars, Colliding wind binaries...

Gamma-ray emitting binaries:

→ Colliding Wind Binaries

→ Gamma-ray binaries

→ Microquasars (solar mass BHs)

→ Novae

Eta Carinae: P ~5.5yr

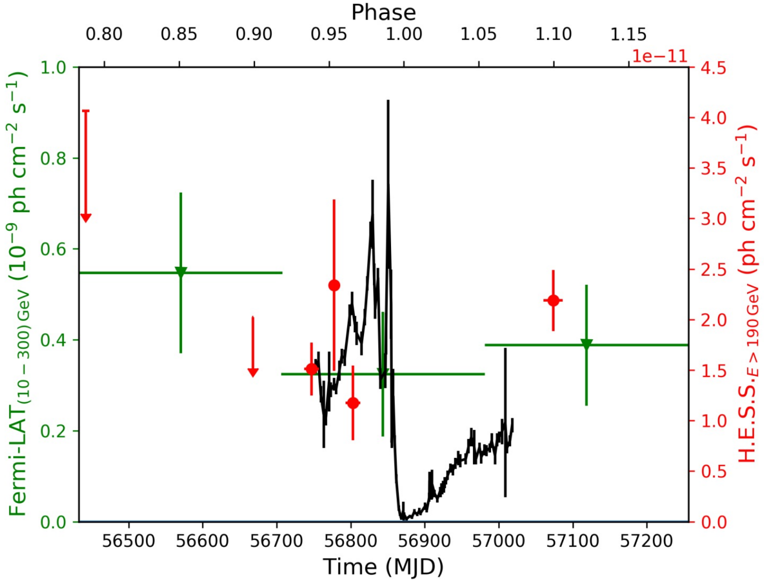

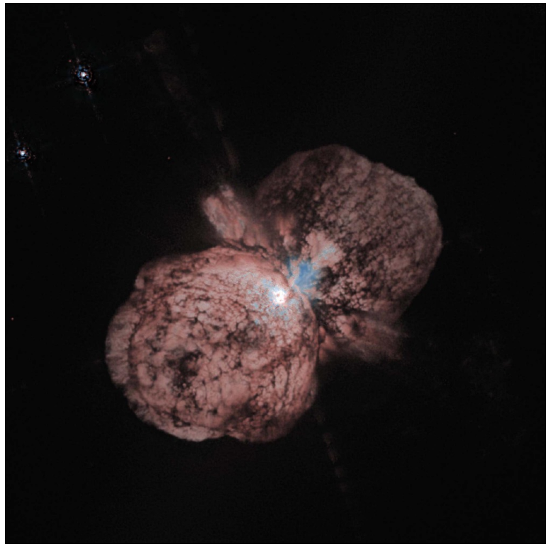

PSR J2032+4127/Be: P ~50yr

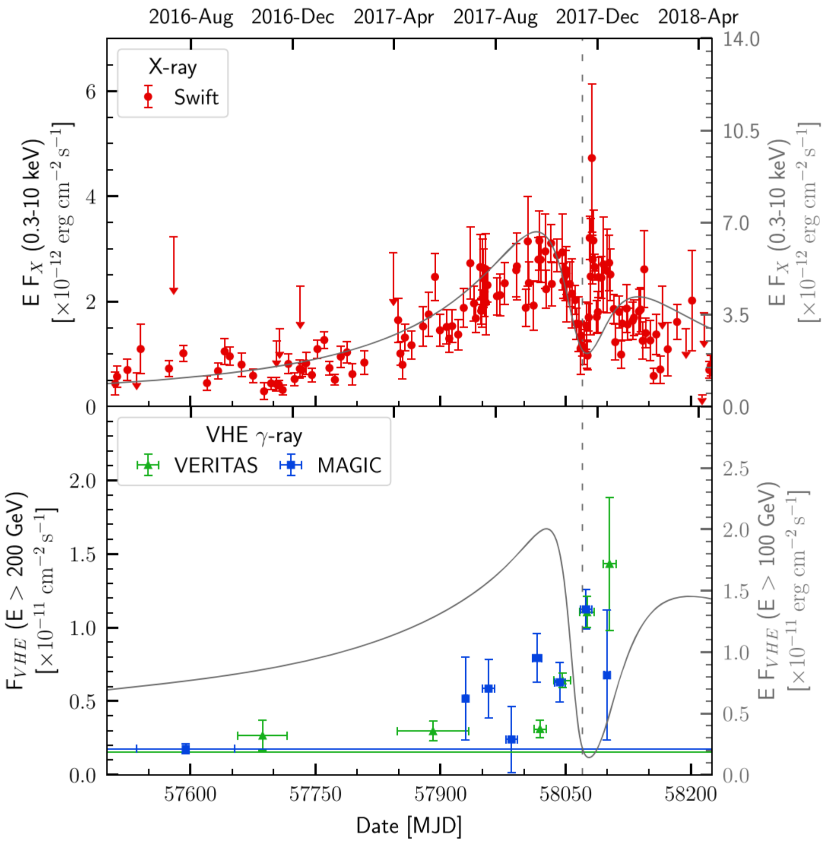

MAGIC & VERITAS Collaborations ApJ **867** L19 (2018)

H.E.S.S. Collaboration A&A **635** A167 (2020) , HST

LS 5039 – binary with 3.9 day period (microquasar?)

Binary system comprised of an O star (~22.9 Msun) and a compact object (Black hole?) ~3.7 Msun.

Lomb-Scargle Periodogram – Fourier Transform to find peak frequency in data

$$P_{LS}(f) = \frac{1}{2}\left\{\left(\sum_n g_n \cos(2\pi f[t_n-\tau])\right)^2 \Big/ \sum_n \cos^2(2\pi f[t_n-\tau]) + \left(\sum_n g_n \sin(2\pi f[t_n-\tau])\right)^2 \Big/ \sum_n \sin^2(2\pi f[t_n-\tau])\right\},$$

where τ is specified for each f to ensure time-shift invariance:

$$\tau = \frac{1}{4\pi f}\tan^{-1}\left(\frac{\sum_n \sin(4\pi f t_n)}{\sum_n \cos(4\pi f t_n)}\right).$$

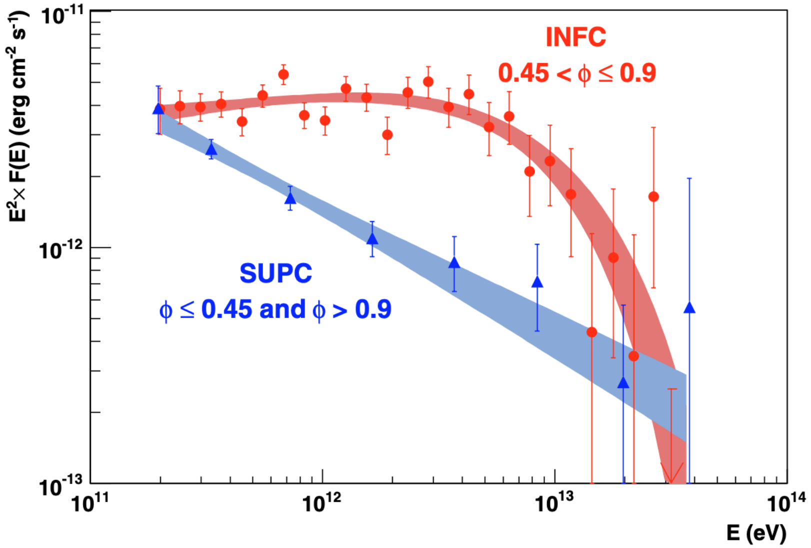

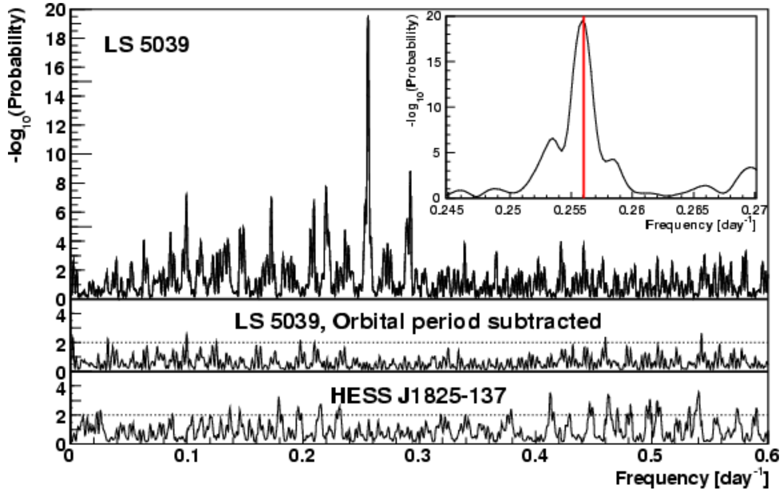

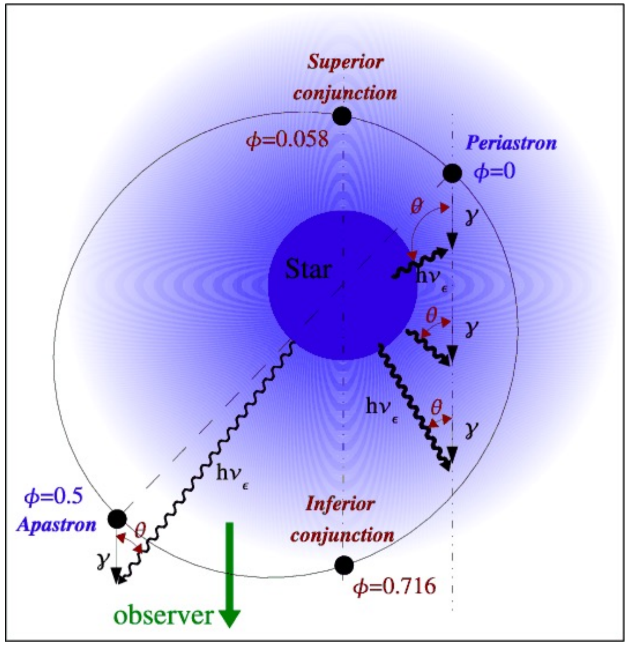

Energy-dependent emission from the jets of SS433

H.E.S.S. Collaboration, Science, **383**, p. 402-406 (2024)

SS 433 microquasar producing powerful jets

H.E.S.S. detection of emission from the outer jets

Indications for an energy-dependence of the emission along the jets

Constrains the particle launch velocity to (0.08 ±0.03)c

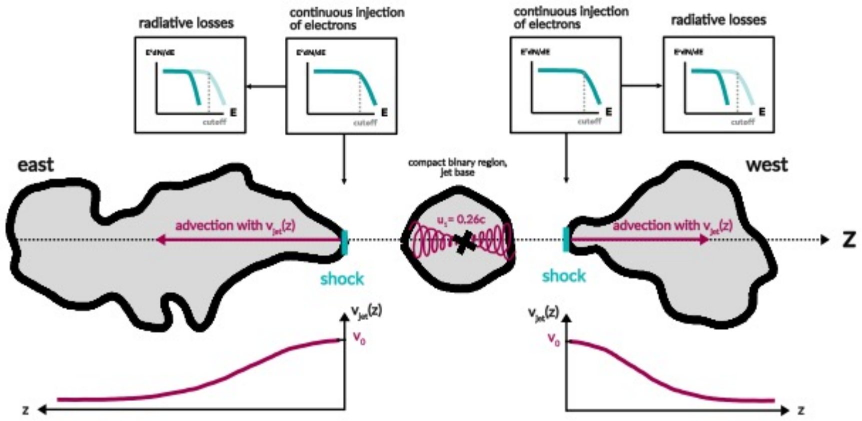

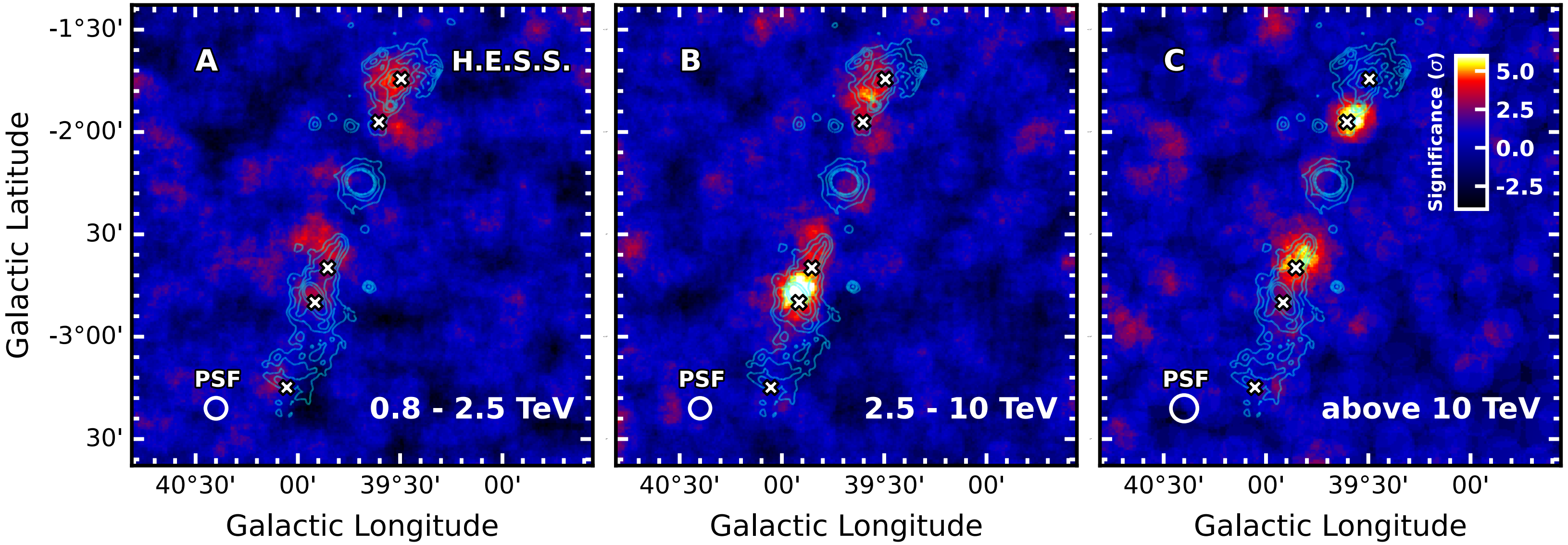

Stellar Novae

Novae – outbursts from accreting binary systems (White Dwarf + massive donor):

- (Classical) Novae → outbursts from cataclysmic variables
- Symbiotic Novae → red giant / “evolved” donor star
- Recurrent Novae → multiple observed outbursts
- Dwarf Novae → mini-outbursts (not thermonuclear)

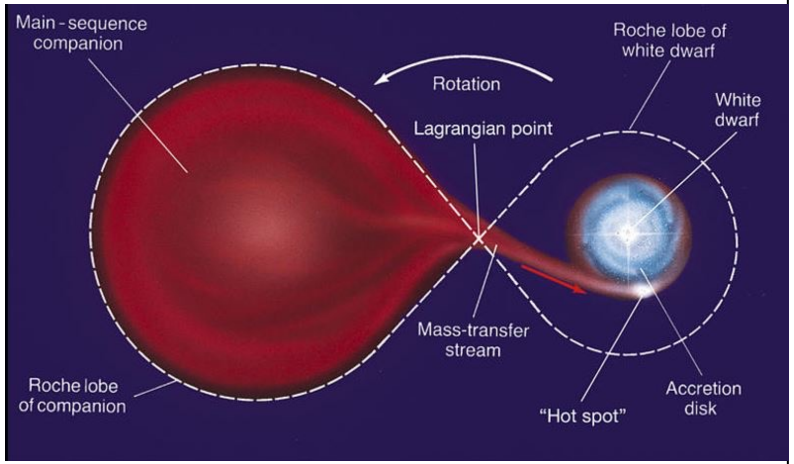

Thermonuclear explosion ignited on surface of white dwarf

Increase in optical brightness $\Delta m_V \sim 8$ to 15

Typical optical duration weeks to months

$$E_{max} = 1.5|Z|\left(\frac{\xi_{esc}}{0.01}\right)\left(\frac{\dot{M} / v_{wind}}{10^{11}\ \mathrm{kg\ m^{-1}}}\right)^{1/2}\left(\frac{u_{sh}}{5000\ \mathrm{km\ s^{-1}}}\right)^{2}\ \mathrm{TeV}$$

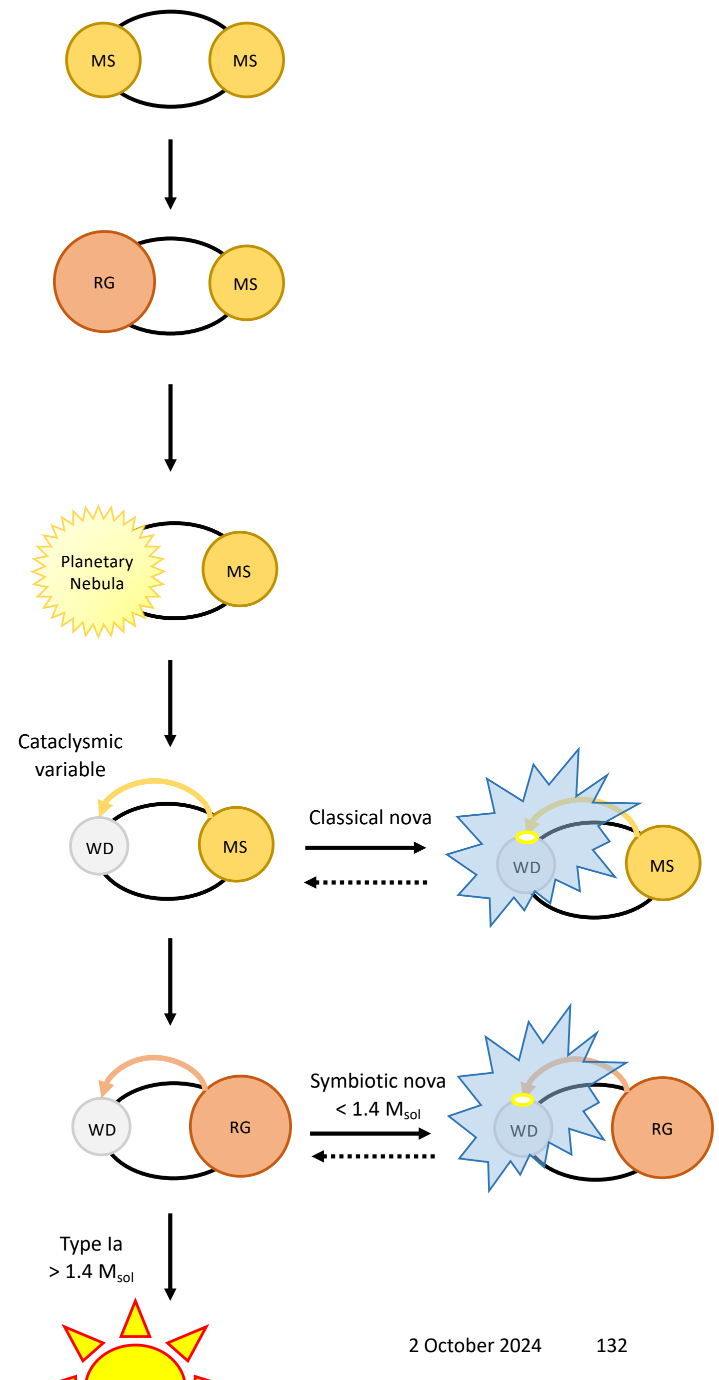

Stellar Novae

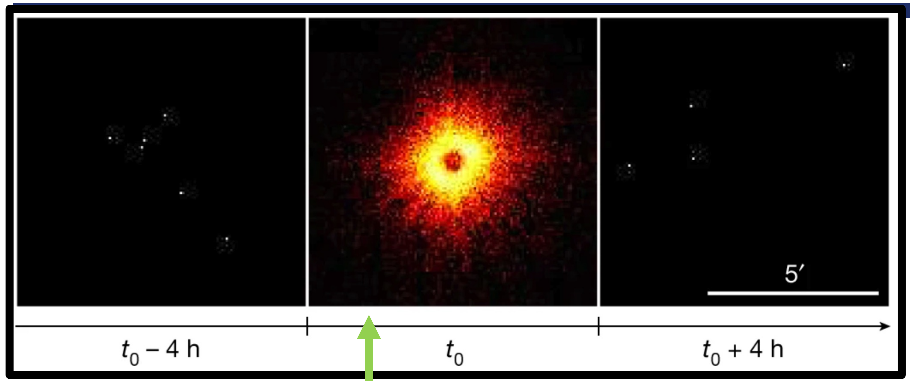


nature

Explore content | About the journal | Publish with us

nature > articles > article

Article | Published: 11 May 2022

X-ray detection of a nova in the fireball phase

Ole König, Jörn Wilms, Riccardo Arcodia, Thomas Dauser, Konrad Dennerl, Victor Doroshenko, Frank Haberl, Steven Hämmerich, Christian Kirsch, Ingo Kreykenbohm, Maximilian Lorenz, Adam Malyali, Andrea Merloni, Arne Rau, Thomas Rauch, Gloria Sala, Axel Schwope, Valery Suleimanov, Philipp Weber & Klaus Werner

Nature **605**, 248–250 (2022) | Cite this article

3807 Accesses | **8** Citations | **516** Altmetric | Metrics

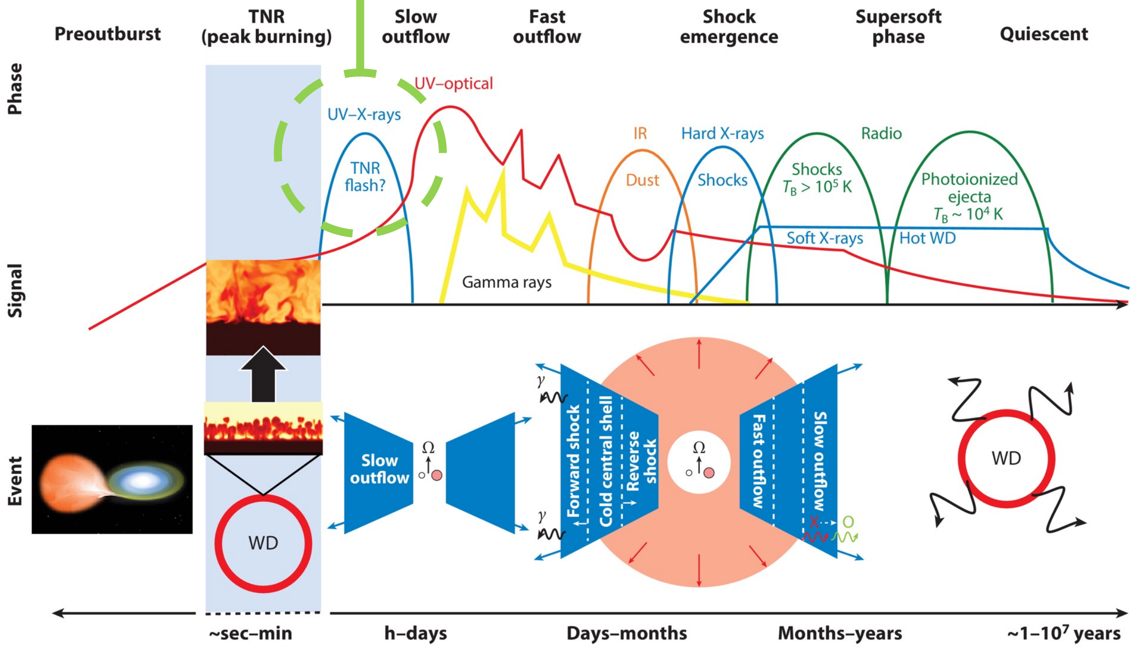

Chomiuk L, et al. 2021
Annu. Rev. Astron. Astrophys. 59:391–444

Initial X-ray flash as thermonuclear burning is ignited

Rapid rise in optical magnitude

Gamma-ray emission from particle acceleration at shocks

Infrared emission from dust

Shock emergence → X-ray emission, no longer gamma-rays

Eventual return to quiescent state

First Nova in VHE gamma-rays: RS Ophiuchi

Binary of white dwarf and red giant

- Binary system comprised of white dwarf and red giant at ~1.4 kpc distance
- Semi-regular explosions observed since 1898
- Last two: 12th February 2006 and **8th August 2021** reaching m_v = 4.6 (cf quiet state m_v = 12.5)

→ Detected by H.E.S.S., MAGIC and LST in VHE gamma-rays (Atel 14844)

Hadronic scenario preferred

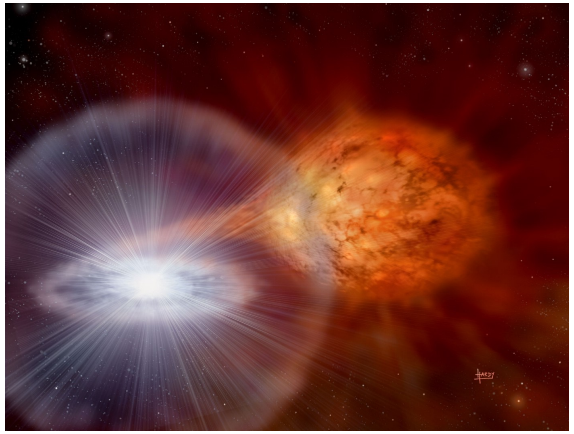

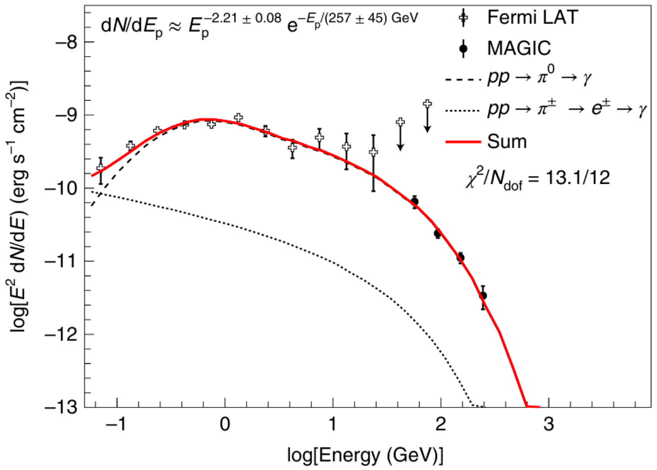

MAGIC collaboration Nat. Astr. **6** (2022) 689-697

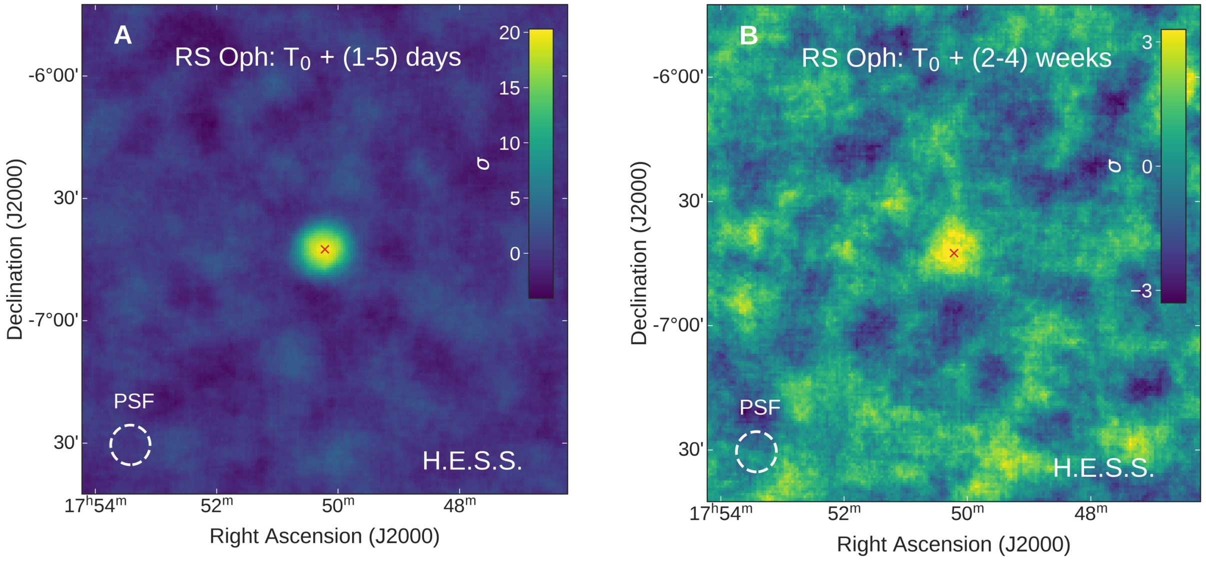

H.E.S.S. collaboration Science **376** (2022) 77-80

Gamma-ray flux decay

Optical peak occurred at T_0 = 59435.25 (MJD)

VHE gamma-ray flux peak seen by H.E.S.S. is delayed with respect to Fermi-LAT

Consistent decay slope after peak flux is attained

It takes time to reach the theoretical maximum energy

Either: cooling limited (leptonic)

Or: confinement limited (hadronic)
until particles become sufficiently energetic to escape the shock

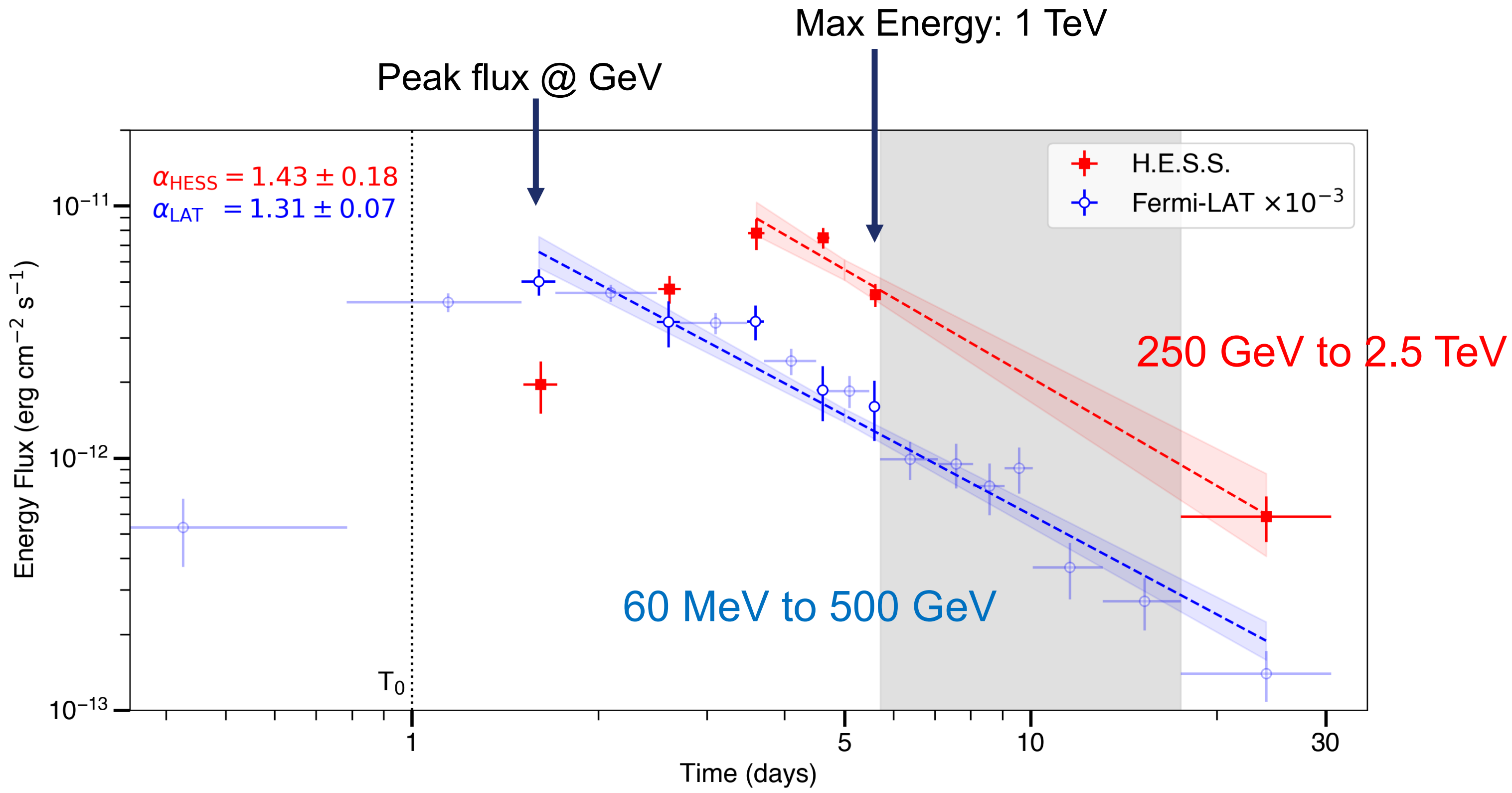

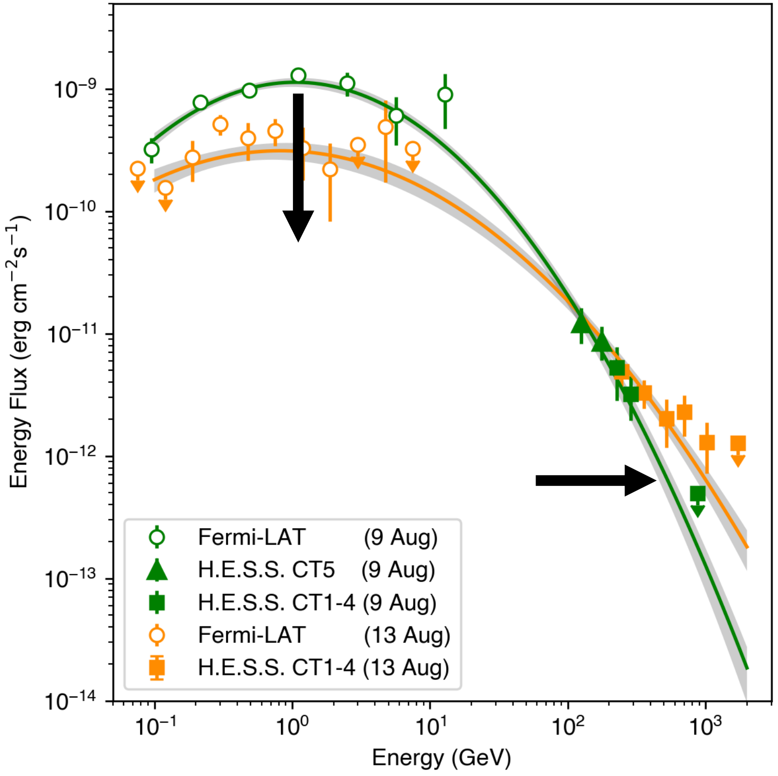

Shock expansion

Find asymmetric expansion & bipolar outflow
(perpendicular to accretion disk)

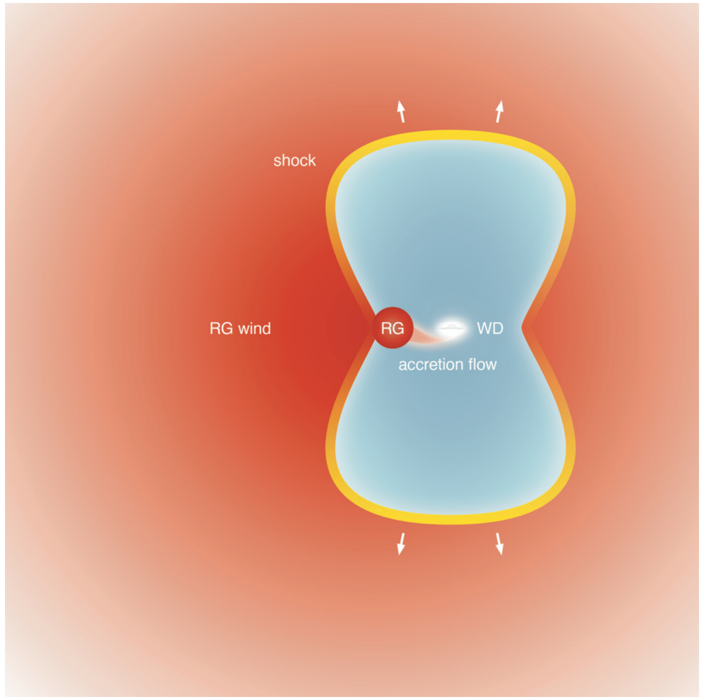

Maximum energy:

$$E_{\max} = 1.5|Z|\left(\frac{\xi_{esc}}{0.01}\right)\left(\frac{\dot{M}/v_{wind}}{10^{11}\ \mathrm{kg\ m^{-1}}}\right)^{1/2}\left(\frac{u_{sh}}{5000\ \mathrm{km\ s^{-1}}}\right)^{2}\ \mathrm{TeV}$$

For RS Oph, E_{max} ~10 TeV for 1% efficiency and $\dot{M}/v_{wind} = 6\times10^{11}\ \mathrm{kg\ m^{-1}}$

i.e. theoretical limit for the maximum energy via diffusive shock acceleration reached in nature
If results scale, this supports SNRs as the origin of PeV cosmic rays

Future observations of novae

It is thought that all novae eventually recur

Yet to date, only a limited number of repeating systems are known

T Coronae Borealis is expected to erupt *imminently* (overdue)

Peak brightness ~ magnitude 2 (naked eye visible)

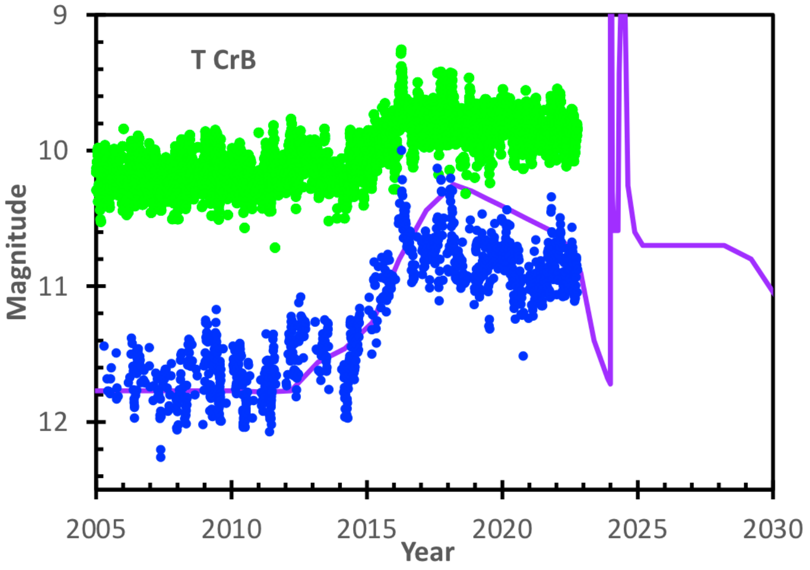

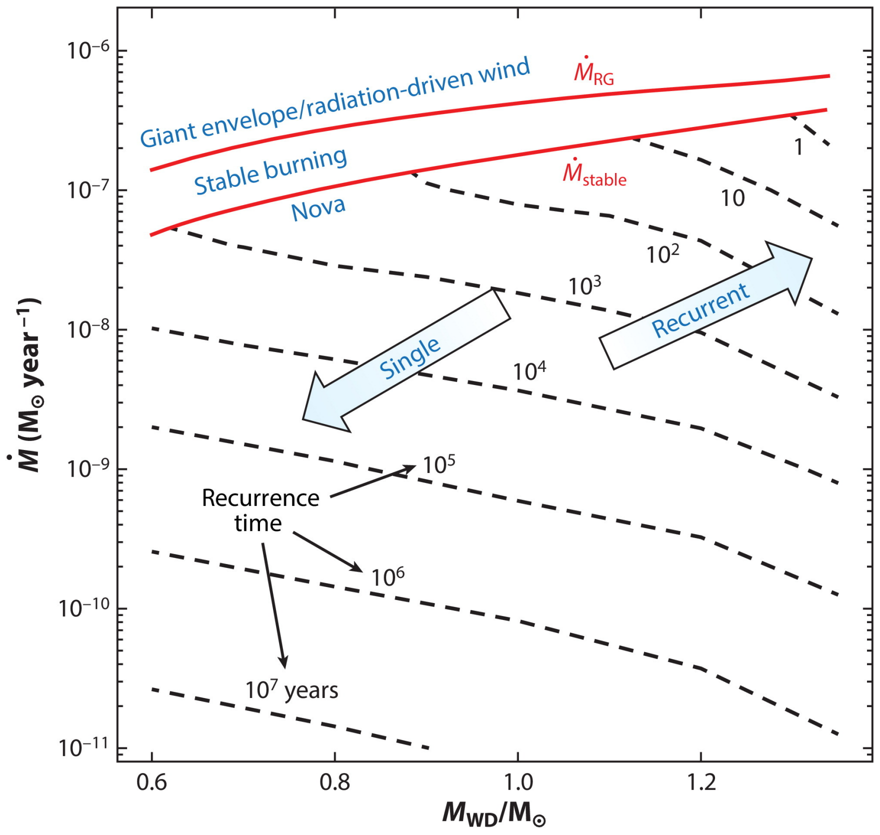

Chomiuk L, et al. 2021
Annu. Rev. Astron. Astrophys. 59:391–444

Friedrich-Alexander-Universität
Erlangen-Nürnberg

Erlangen Centre for Astroparticle Physics

FAU

Gamma-Ray Astronomy

III – Extragalactic Sources and Fundamental Physics

Dr Alison Mitchell
Junior Research Group Leader,
FAU Erlangen-Nürnberg

Astroparticle School, Obertrubach-Bärnfels
13th October 24

Emmy Noether-Programm
DFG Deutsche Forschungsgemeinschaft

Funded by
DFG Deutsche Forschungsgemeinschaft
German Research Foundation

Extragalactic Sources: Large Magellanic Cloud (LMC)?

Satellite galaxy of the Milky Way at ~50 kpc distance

Individual emitters are powerful sources of galactic types:

N132 D – radio-loud SNR
core-collapse SNR, ~6kyr yet maximum energy still in TeV range

N157 B – powerful PWN
Similar spin-down luminosity to the Crab nebula, 4.9×10^{38} erg/s

30 Dor C – superbubble
X-ray synchrotron shell with radius 47 pc → large, yet young (~few kyrs) and powerful with high luminosity

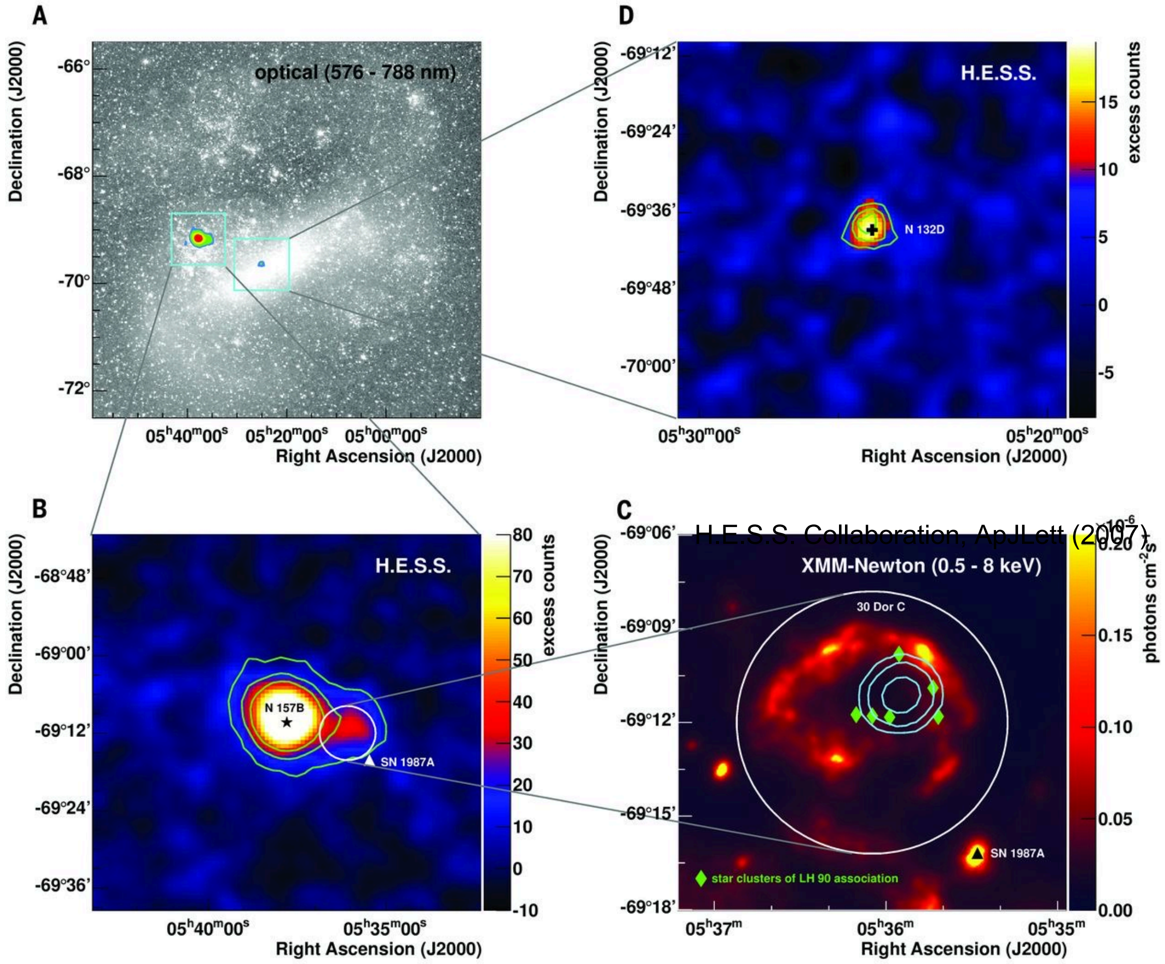

H.E.S.S. Collaboration, Science **347** 406-412 (2015)

Extragalactic Sources: Large Magellanic Cloud (LMC)?

Hadronic vs leptonic scenarios for the TeV emission → both viable for the SNR & superbubble.

However, no TeV emission detected yet from SN 1987 A. Why? Expect flux to be rising over time, at least in early evolutionary stages...

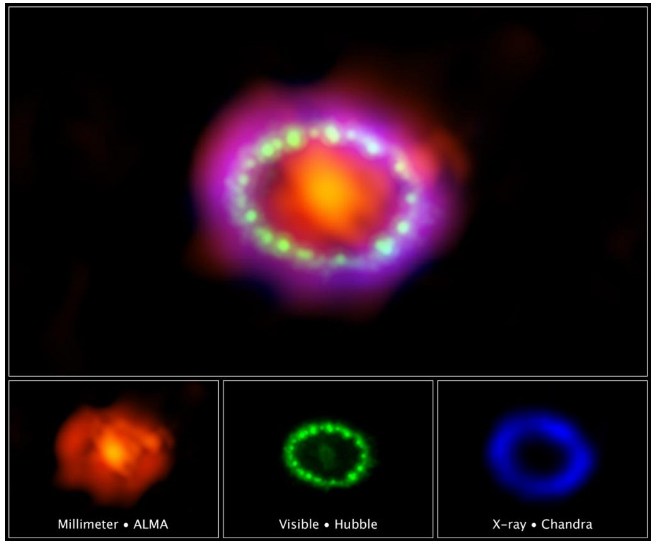

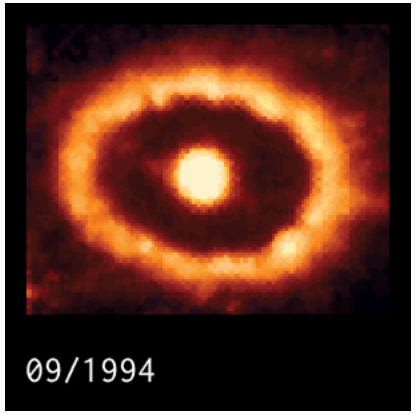

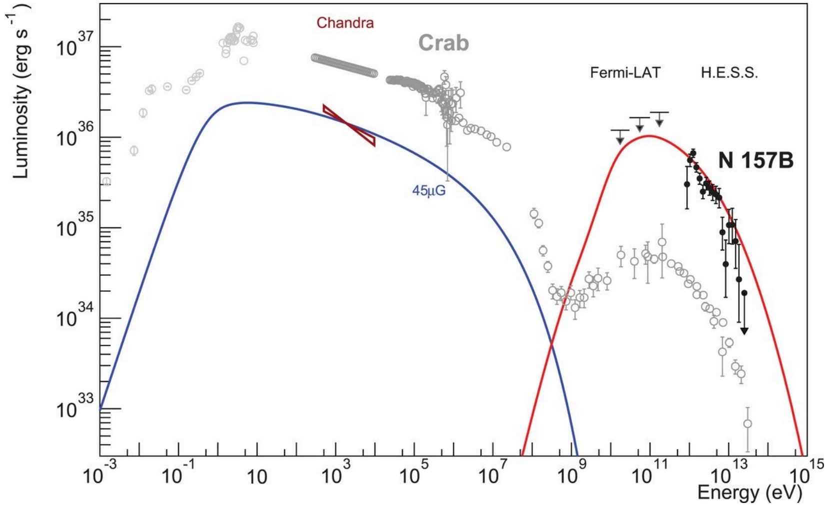

Assuming a constant fraction ~11% of the spin-down power gets injected into the nebula.
B-field ~45μG (cf Crab ~124μG)

H.E.S.S. Collaboration, ApJLett (2007)

TeVCat source distribution

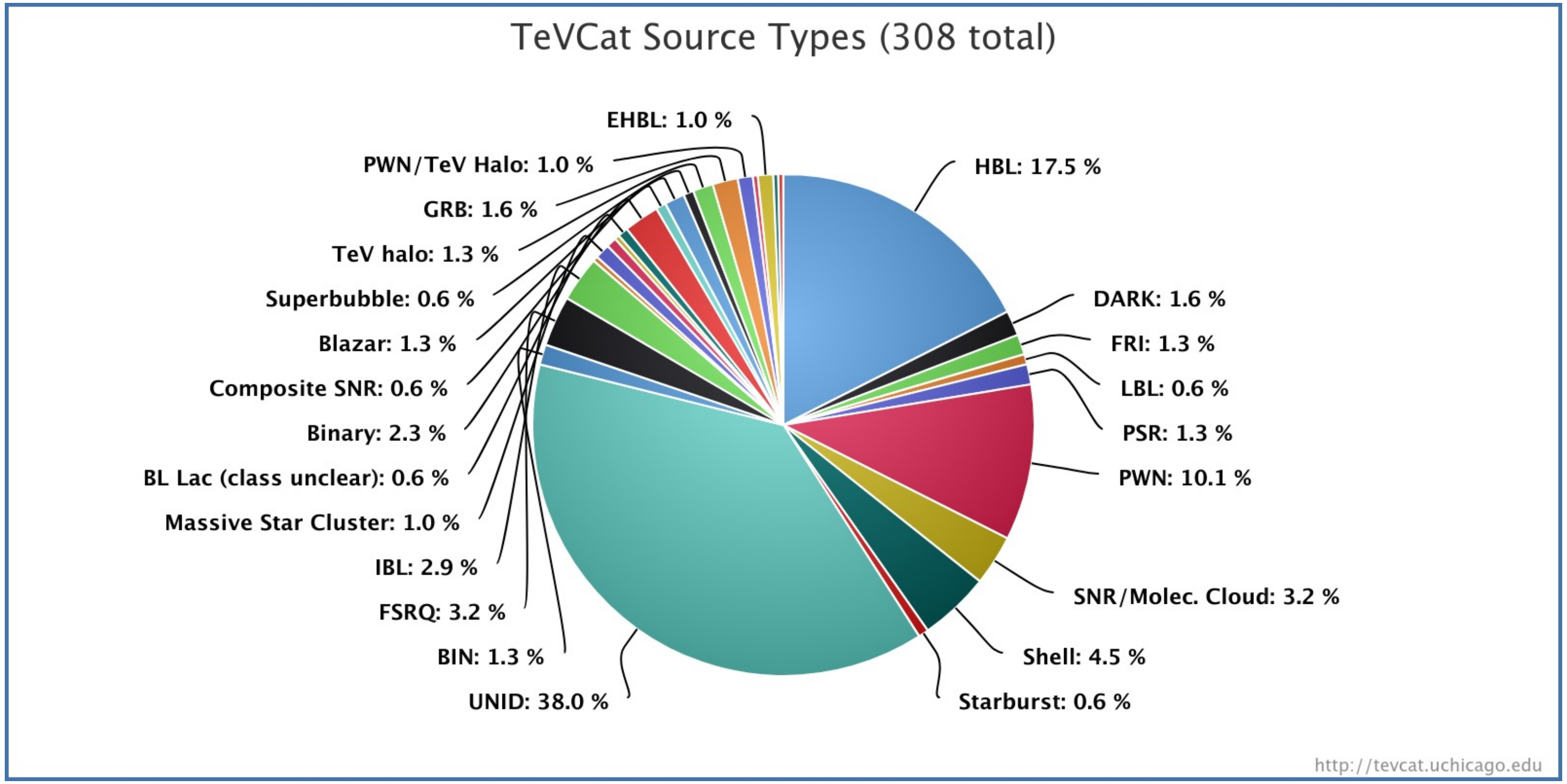

Active Galactic Nuclei (AGN)

Unified model

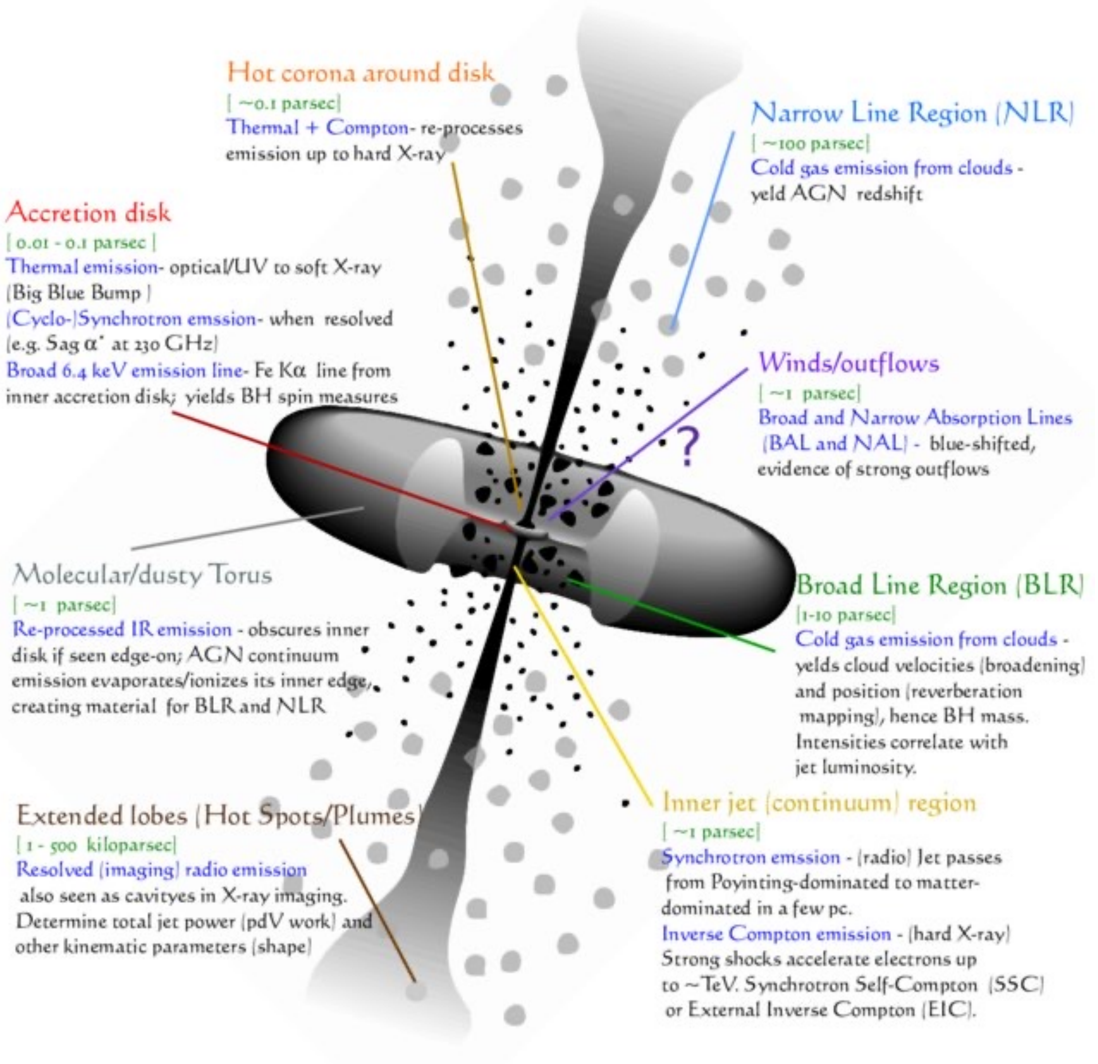

S. Cielo (2015)

Different features dominate depending on the viewing angle

Seyfert 1 – broad and narrow emission lines are present

Seyfert 2 – narrow emission lines are present, but no broad lines

Blazars – orientated such that the observer is looking along the jet "down the barrel of the gun" θ < 15º

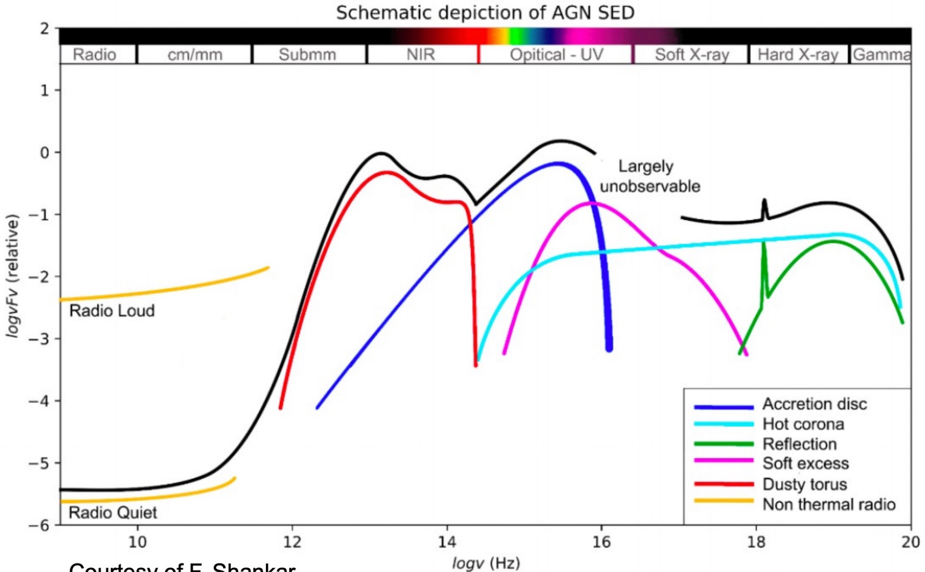

Courtesy of F. Shankar

Active Galactic Nuclei (AGN)

Unified model

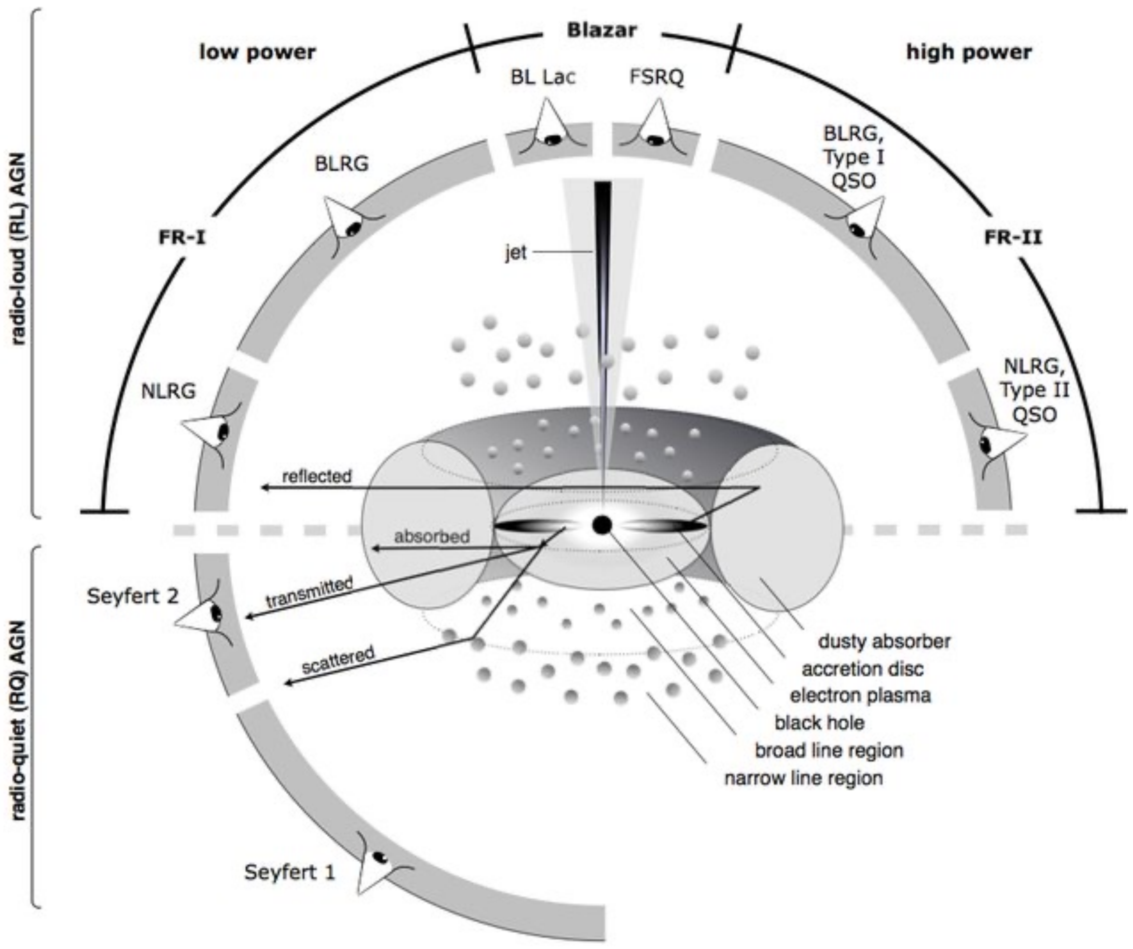

Beckmann & Shrader (2012)

Radio-Loud:

Emission dominated by non-thermal processes (jet-related)

Radio-Quiet:

Emission dominated by thermal processes (multi-band)

$$S_\nu \propto \nu^{-\alpha}$$

Flat spectrum: α < 0.5 (Steep spectrum: α > 0.5)

FSRQ – strong & broad emission lines

BL Lac – weak emission lines

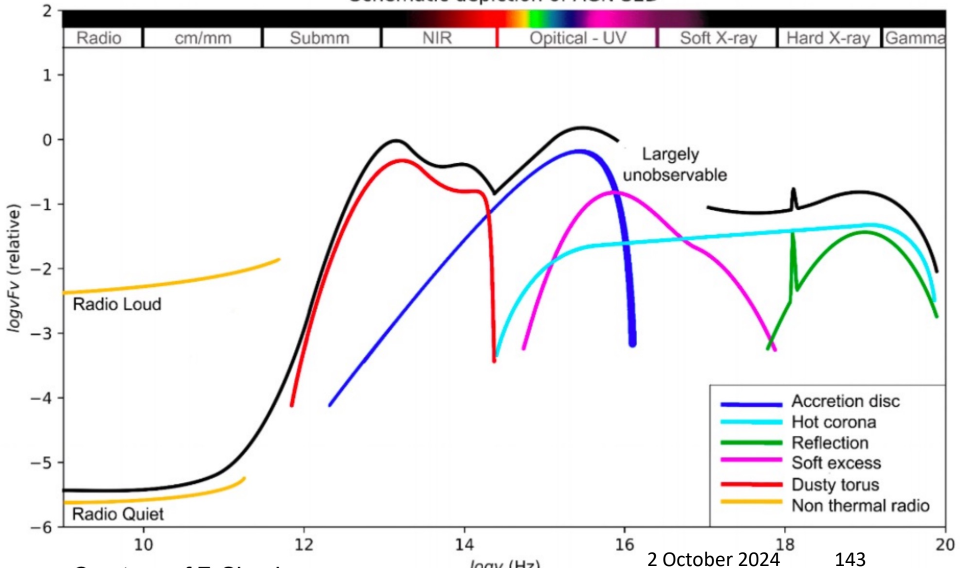

Courtesy of F. Shankar

Extragalactic Background Light (EBL)

Pair-production of gamma-rays interacting with background photon fields yields an energy-dependent gamma-ray horizon.

(where $\tau_{\gamma\gamma} = 1$)

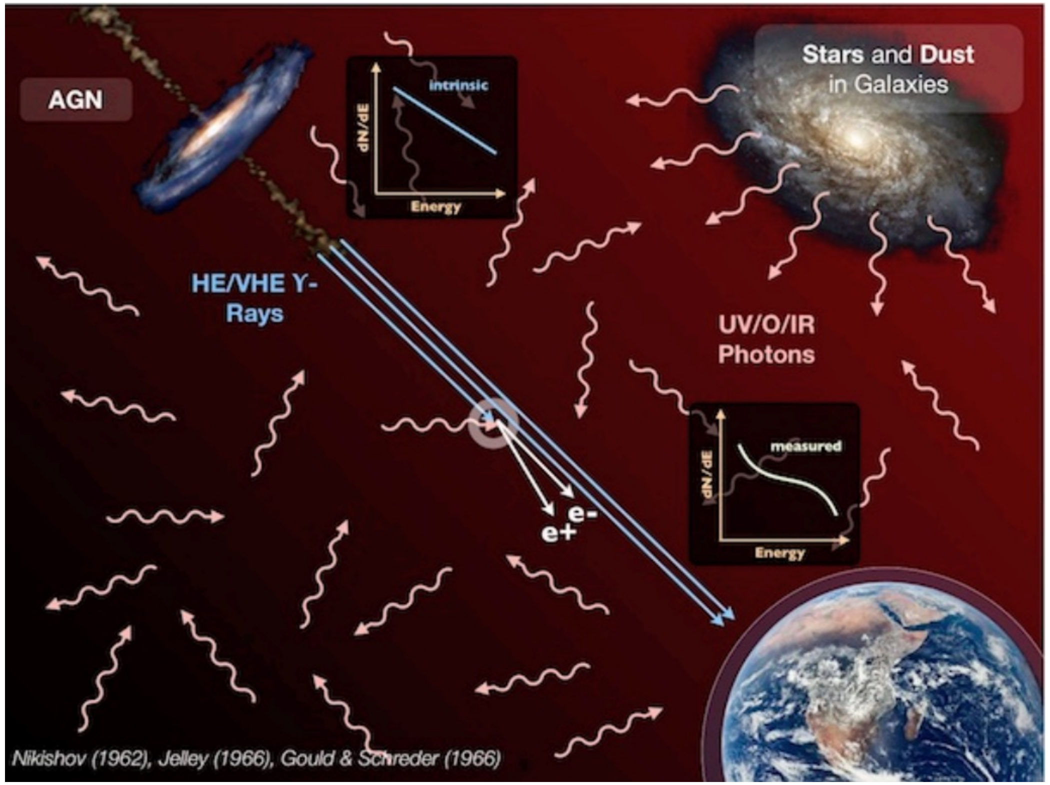

Optically thick: $\tau_{\gamma\gamma} > 1$

Optically thin: $\tau_{\gamma\gamma} < 1$

$$I_\nu(d) = I_\nu(0)e^{-\tau_\nu}$$

Mean free path: $\langle\tau_\nu\rangle = n\sigma_\nu\langle l_\nu\rangle = 1$

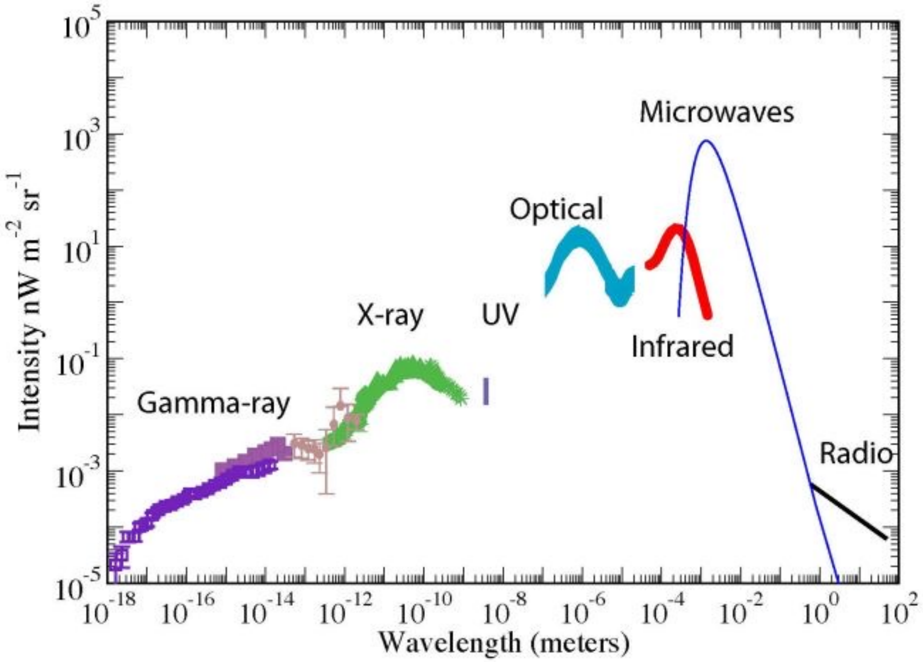

Cooray

Extragalactic Background Light (EBL)

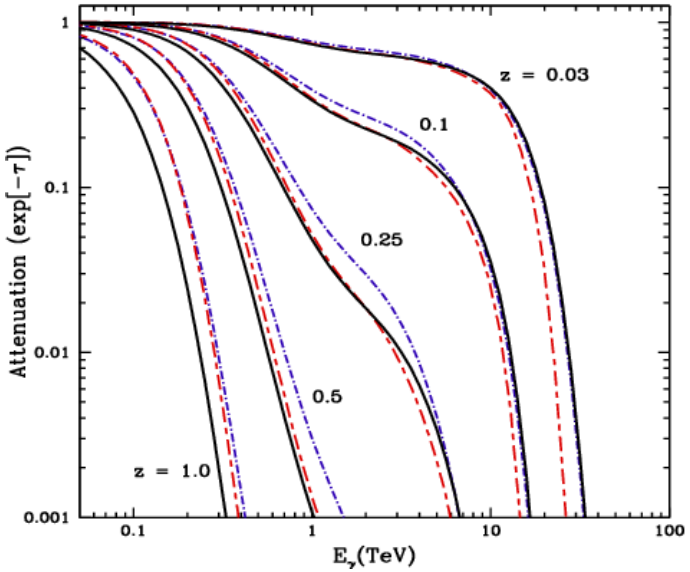

Gamma-ray attenuation must be corrected for in order to recover the true gamma-ray spectrum.

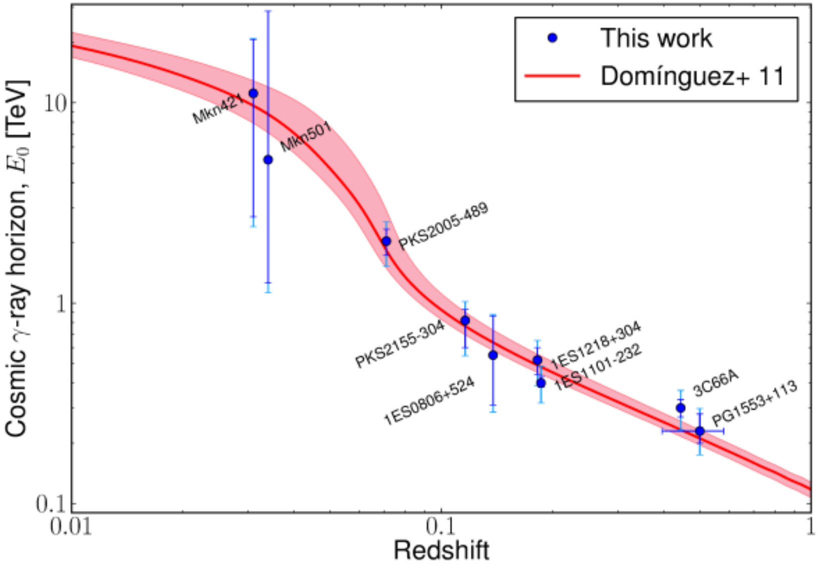

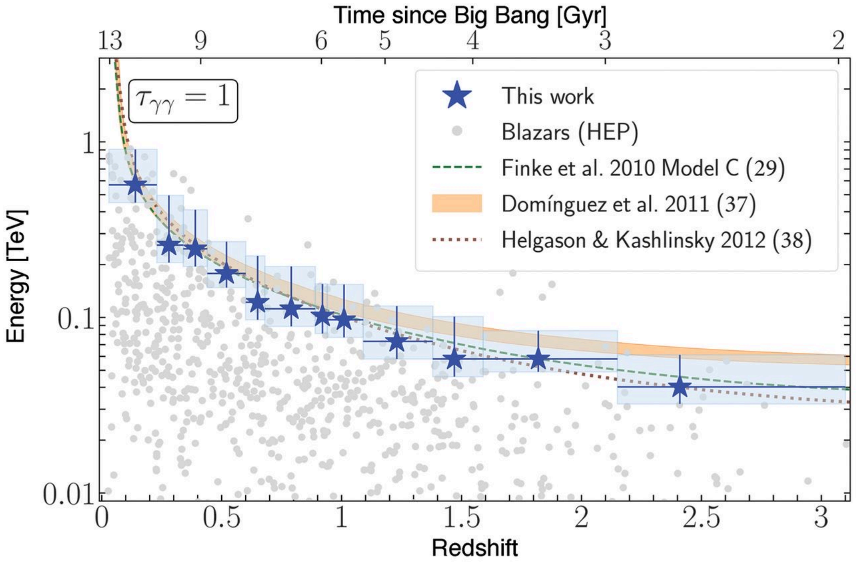

Buson (2016), Dominguez et al. ApJ **770**, 77 (2013), Fermi-LAT collaboration Science **362** (2018) 1031-1034

Galaxies in Gamma-rays
Markarian 421

Bright and highly variable nearby blazar
z = 0.030

Define variability index (Vaughan 2003):

$$F_{var} = \sqrt{\frac{S^2 - \overline{\sigma_{err}^2}}{\bar{x}^2}}$$

For the variability compared to expectation and measurement error in a given frequency band.

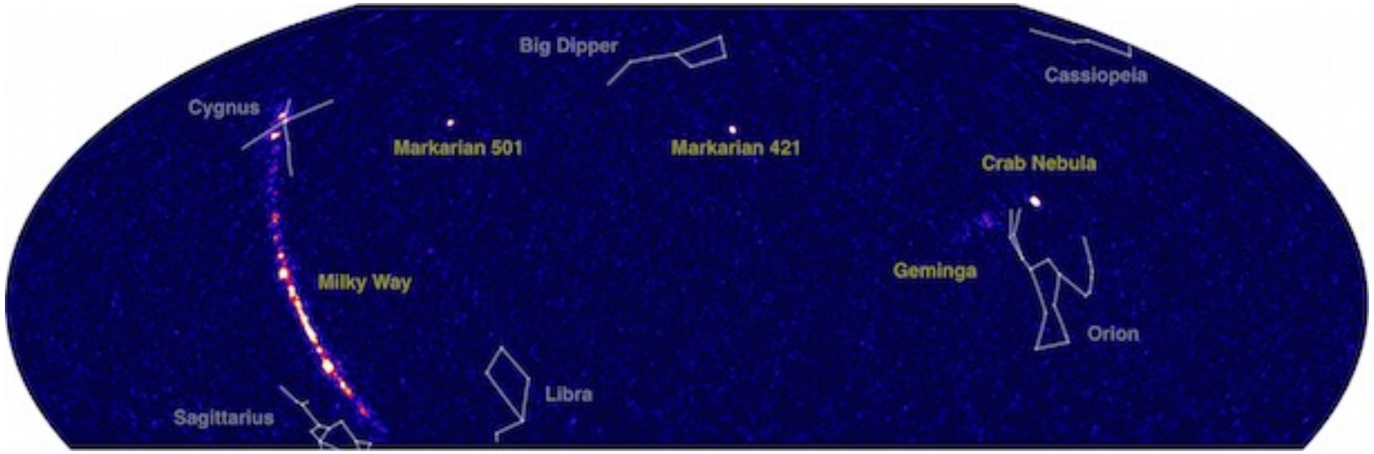

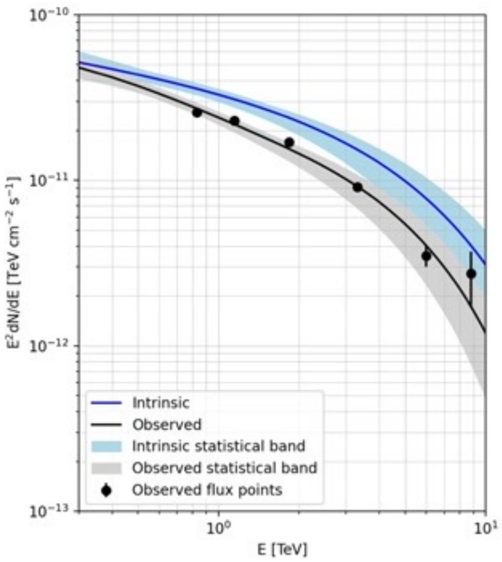

HAWC collaboration *ApJ* **929** 125 (2022)

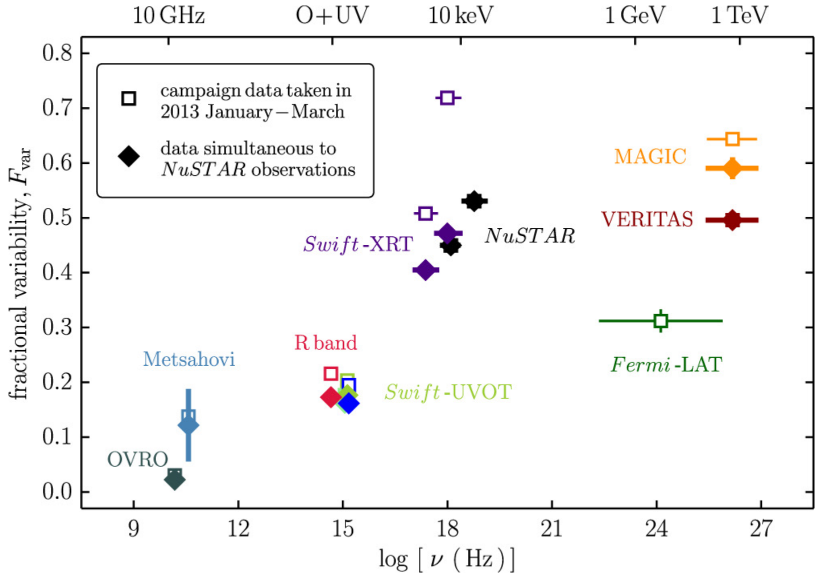

Arbert-Engels et al. A&A **647**, A88 (2021), HESS

Galaxies in Gamma-rays

Markarian 501

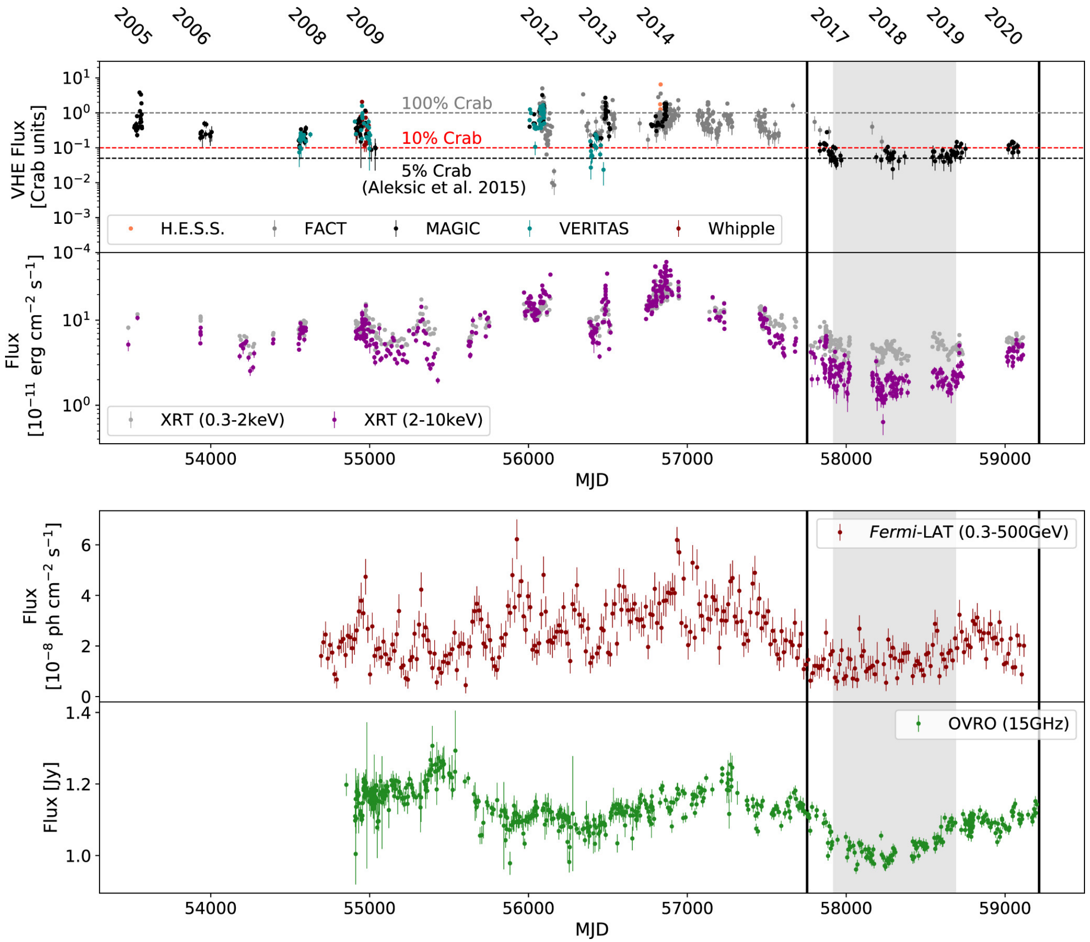

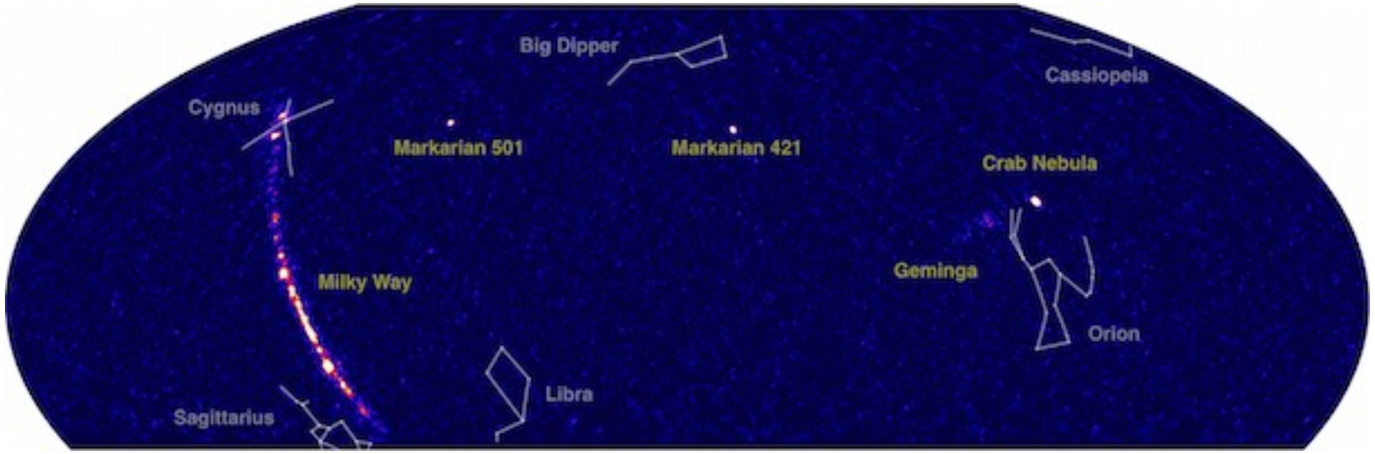

Bright and highly variable nearby blazar

z = 0.034

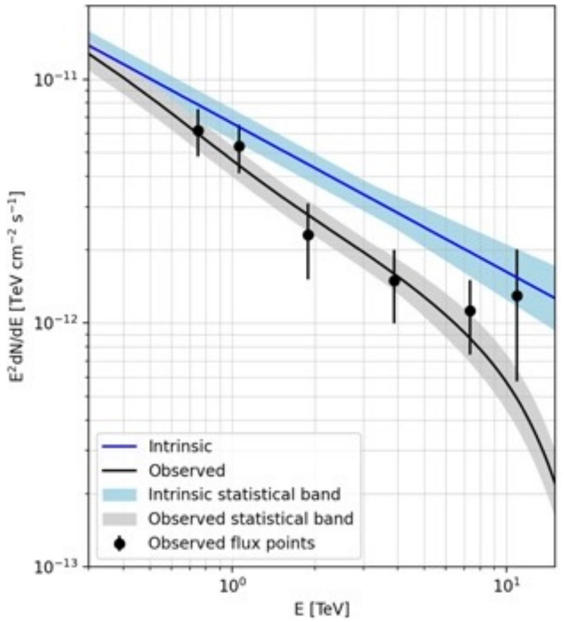

H. Abe *et al* 2023 *ApJS* **266** 37

HAWC collaboration *ApJ* **929** 125 (2022)

AGN population in gamma-rays

Fermi-LAT population distribution

FSRQ = Flat Spectrum Radio Quasar
BL Lac = Blazars reminiscent of BL Lac
LSP, ISP, HSP = Low, Intermediate & High Synchrotron Peaked
BCU = Blazars of unknown type

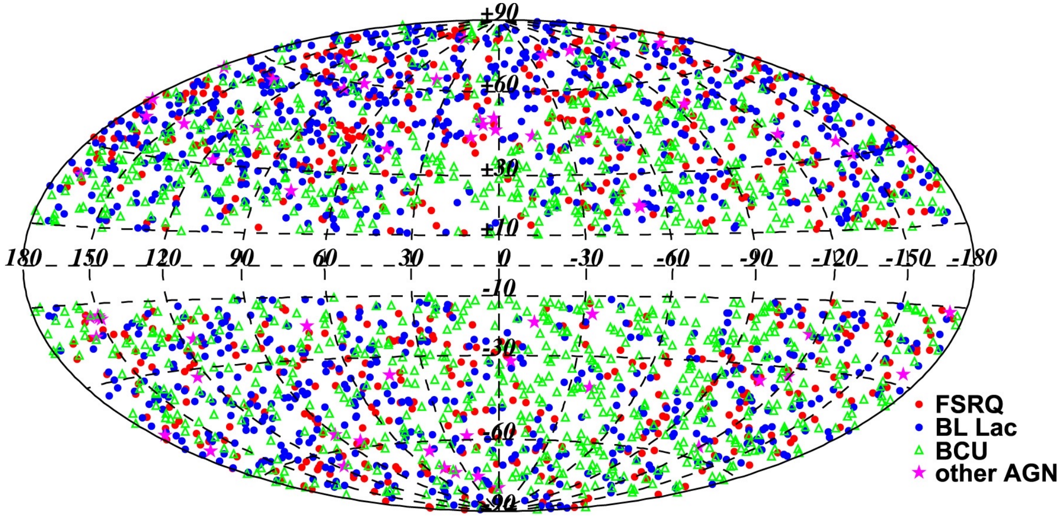

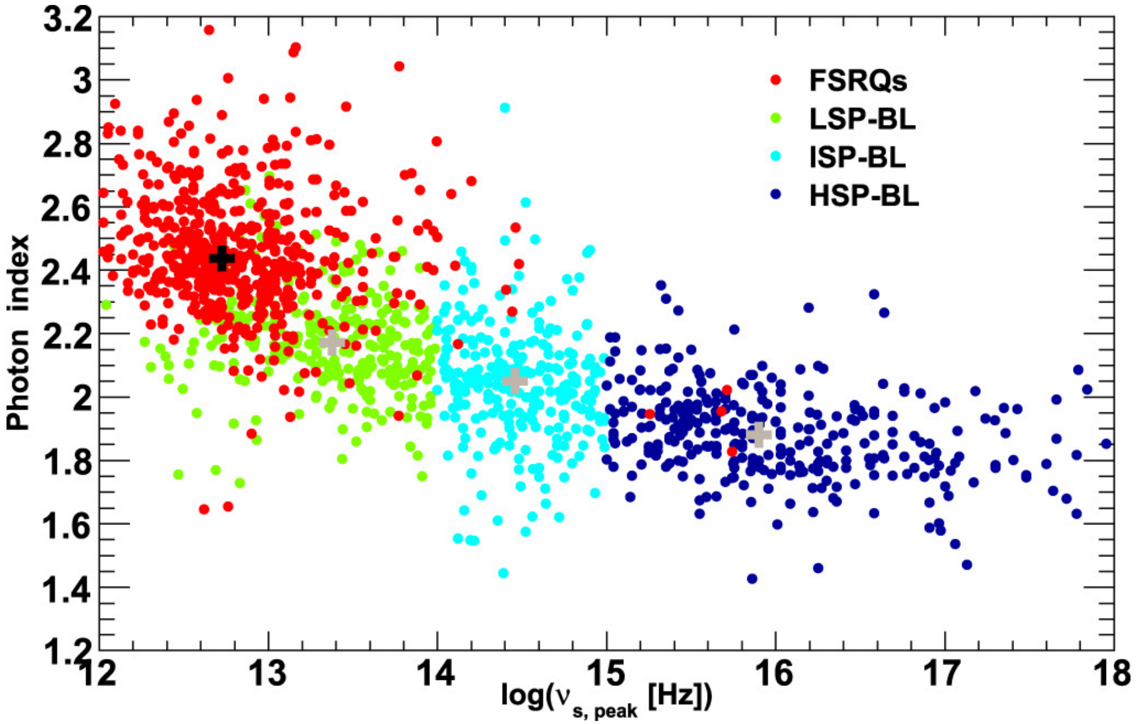

4th AGN catalogue (4LAC), Fermi-LAT collaboration M. Ajello *et al* 2020 *ApJ* **892** 105

Blazars – variability

Many blazars exhibit rapid variability

Places constraints on the origin of the radiation → must originate from a region R smaller than cΔt (light crossing time)

Example: exceptional flare of PKS 2155-304 in 2006

Nearly 50x brighter flux than in its quiescent state

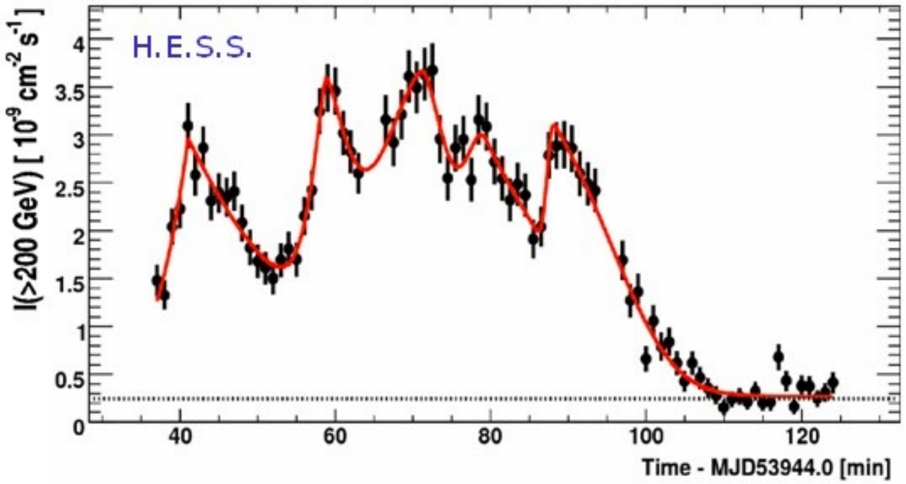

H.E.S.S. Collaboration, ApJLett (2007)

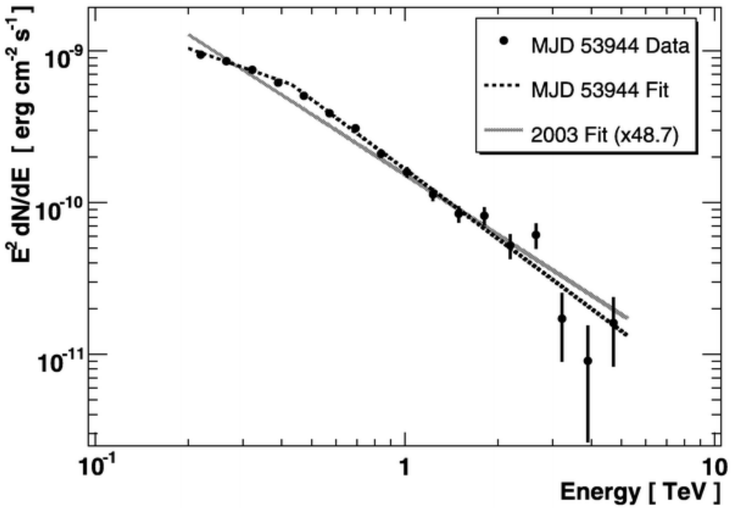

$$\theta_E = \sqrt{\frac{4GM}{c^2}\frac{D_{LS}}{D_L D_S}}$$

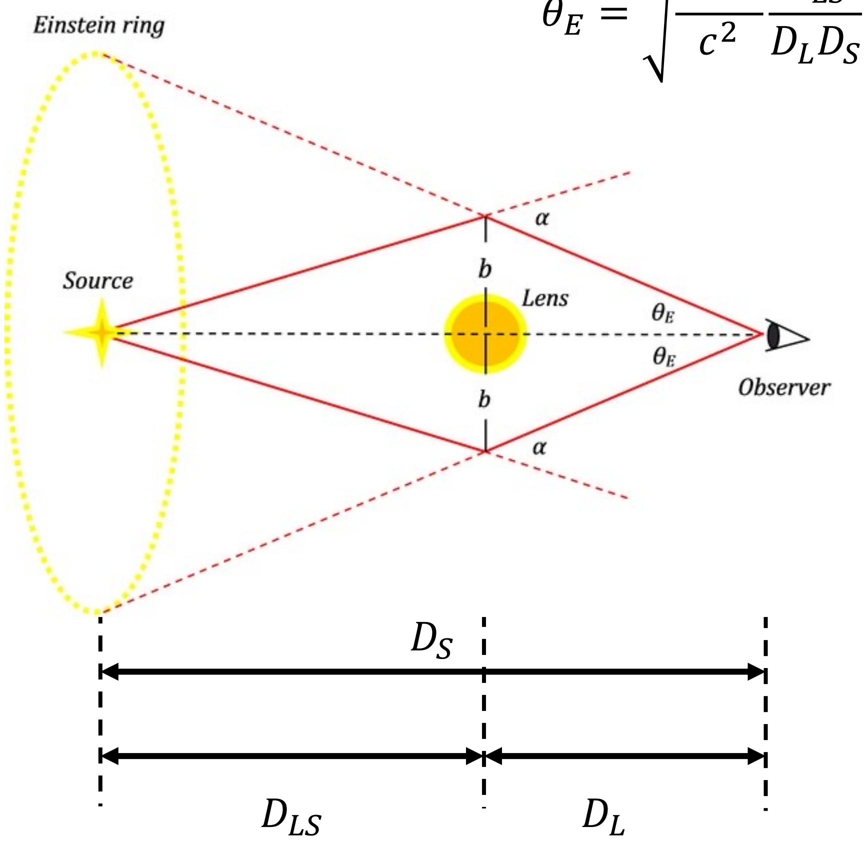

Rays of light follow curved space-time & bent around a massive object.

Causes apparent positions for the observer offset from the true position

If perfectly aligned, can cause a ring-shaped image

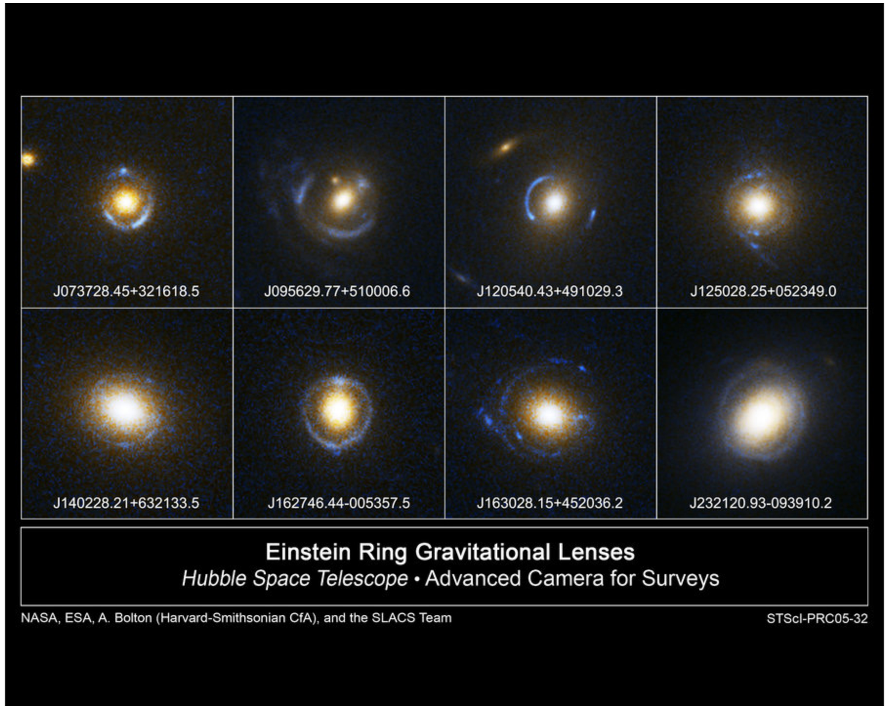

Pinochet (2018)

Gravitationally lensed blazar QSO B0218+357

Due to different path lengths, signal from lensed image is delayed with respect to the main image.

Although MAGIC (IACTs) missed the first event, they were able to catch the second by anticipating when it would occur.

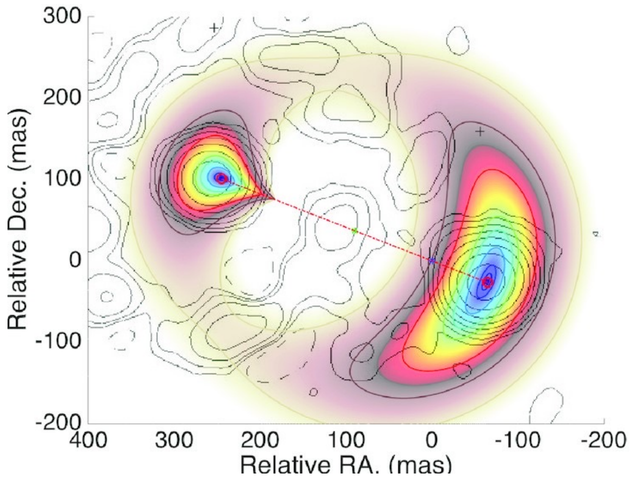

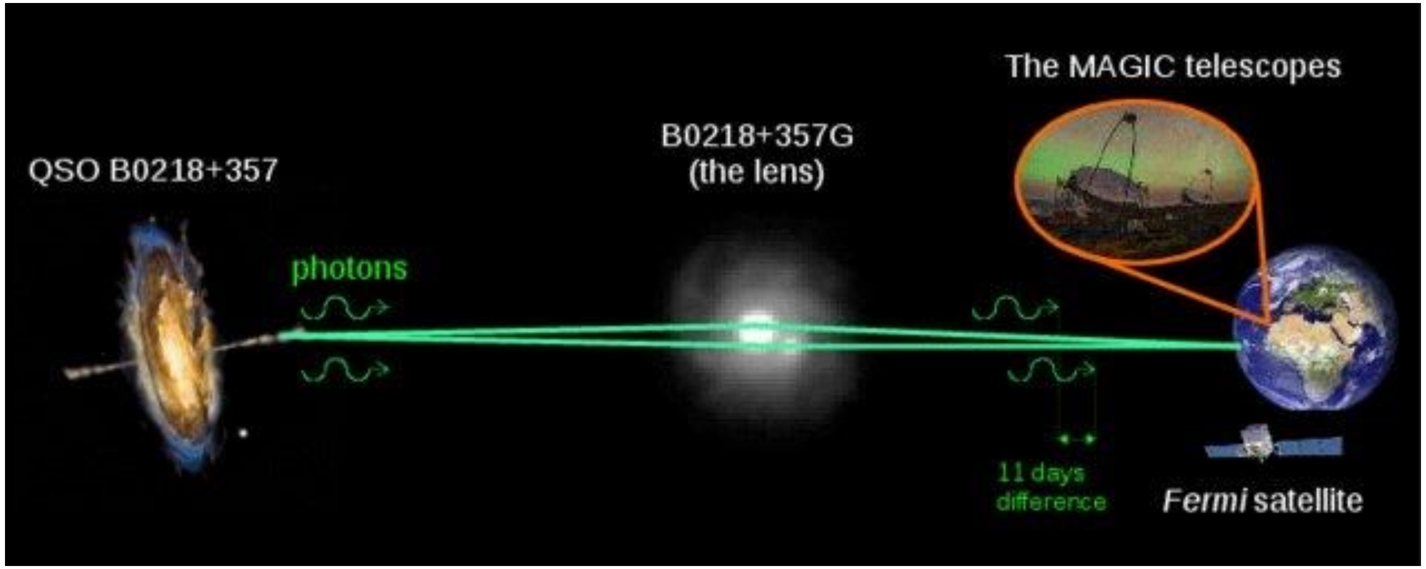

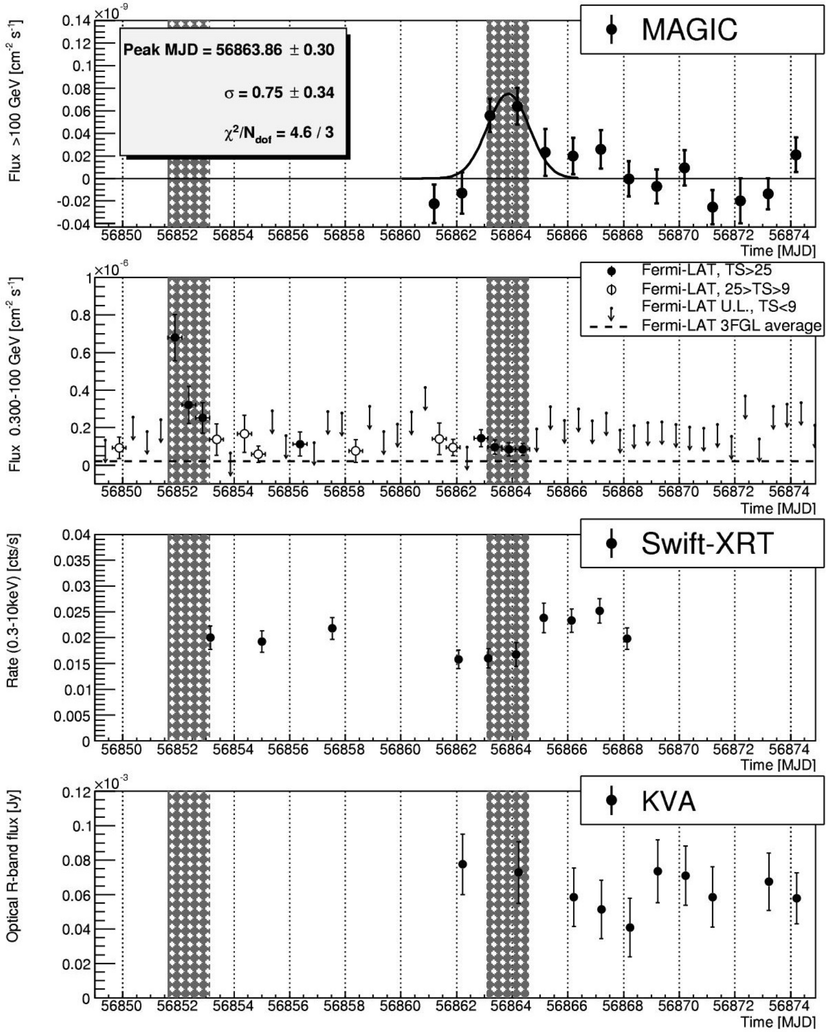

MAGIC Collaboration, A&A **595** (2016) A98

MAGIC Collaboration, MNRAS **510**, 2344–2362 (2022)

Extended Extragalactic Sources

- Resolving extension of Centaurus A jets ≥ 2.2 kpc
- Constraining morphology of M87 and CR pressure in the Virgo cluster
  → radio lobes excluded as associated to VHE gamma-ray emission

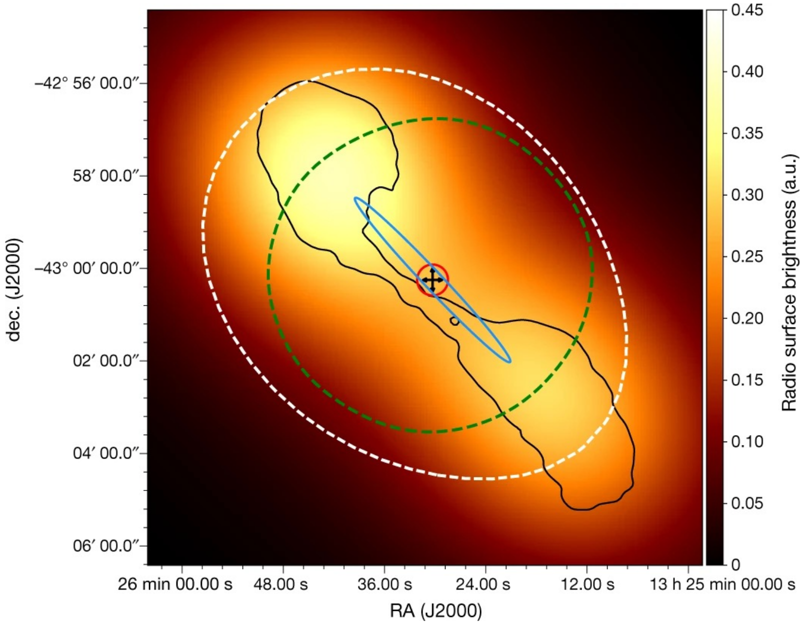

H.E.S.S. collaboration Nature **582** (2020) 356-359

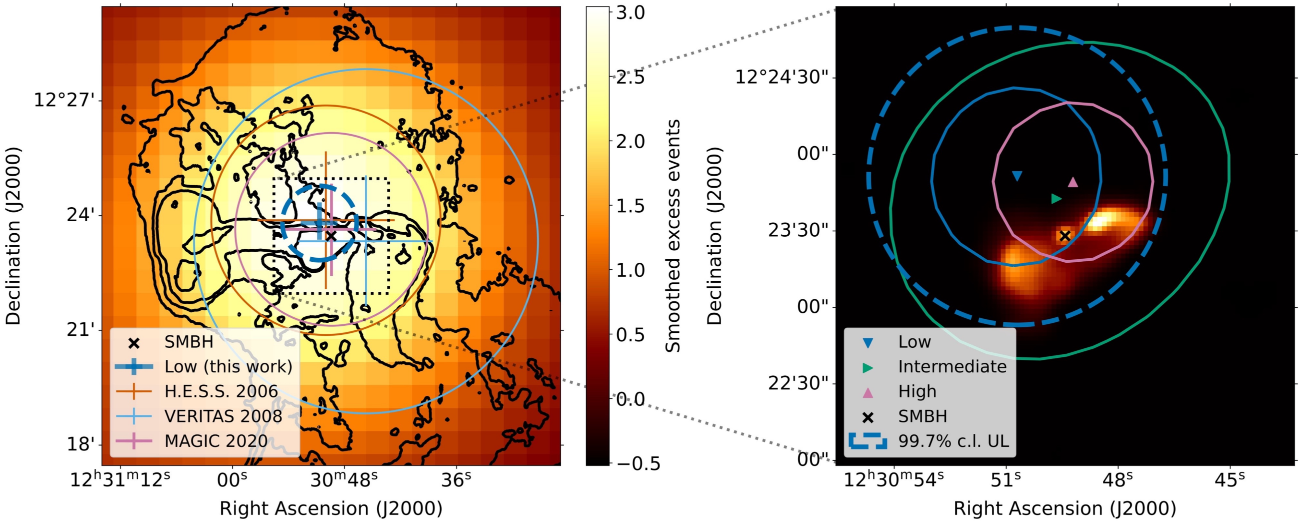

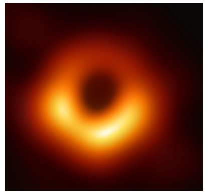

EHT collaboration ApJL **875** (2019) L1

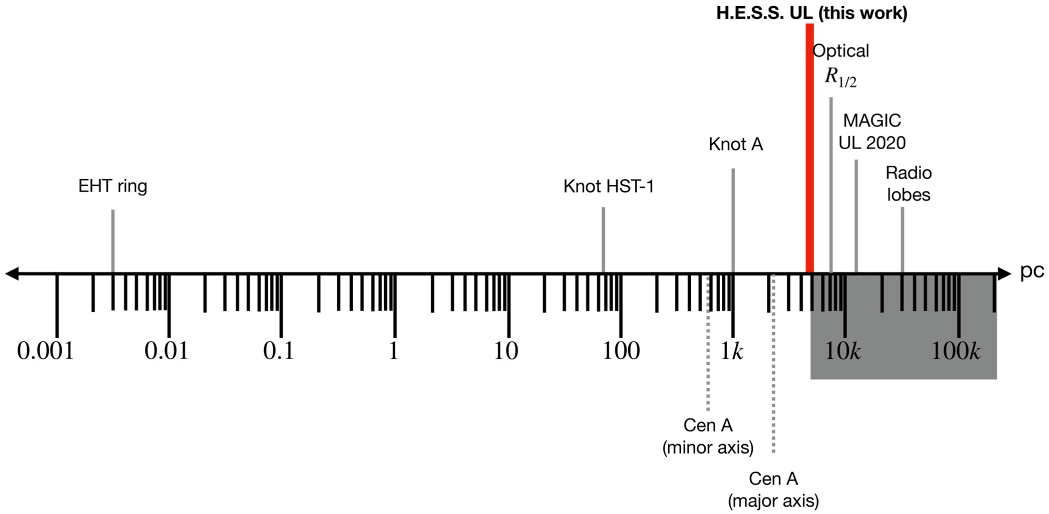

H.E.S.S. collaboration A&A (2023)

Gamma-Ray Bursts

Isotropic distribution on the sky indicated an extragalactic origin.

Characterised as short or long duration, now also by intermediate

Population of GRB events characterised in terms of:

T_{90} – the time during which 90% of the energy is released (from 5% up to 95%)

HR – hardness ratio gives the ratio of flux from a GRB in hard and soft bands

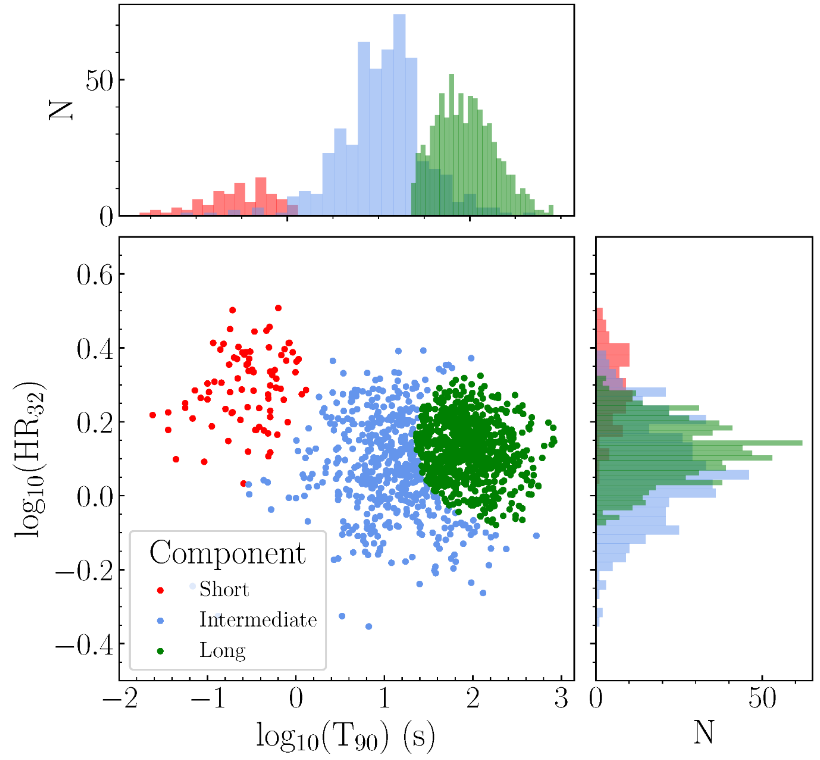

Salmon et al., *Galaxies* **2022**, *10*(4), 77

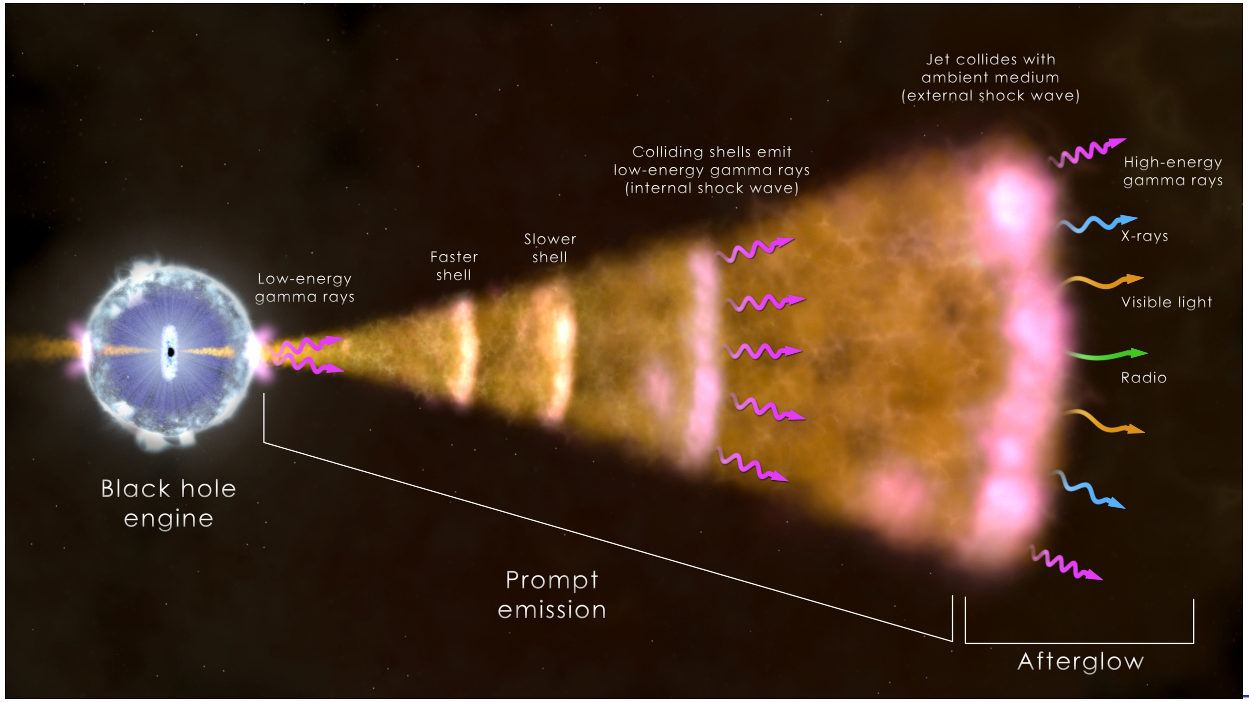

<u>Mechanism:</u>

Short GRBs – binary Neutron Star mergers (or NS-BH)

Long GRBs – massive star collapse (?)

Both – jet launching

Transients: Gamma-Ray Bursts

First four VHE GRBs detected by H.E.S.S. & MAGIC between 2018 – 2020 (long GRBs, detected during afterglow phase)

- GRB 180720B, z ~ 0.654 (H.E.S.S.)
- GRB 190114C, z ~ 0.4245 (MAGIC)
- GRB 190829A, z ~ 0.08 (H.E.S.S.)
- GRB 201216C, z ~ 1.1 (MAGIC)

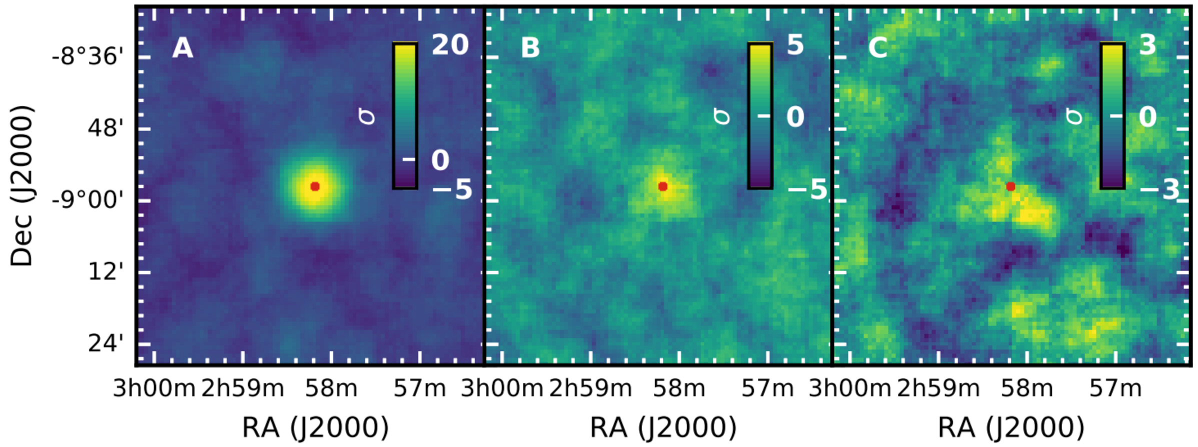

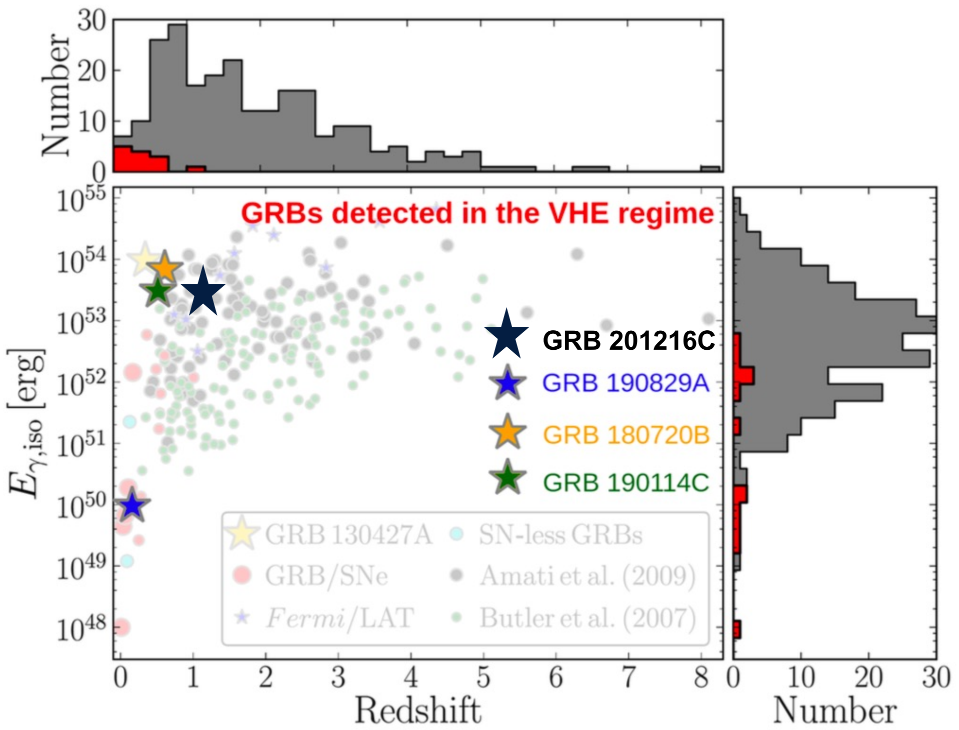

Large distances z ≥ 1 → severe attenuation due to the Extragalactic background light

Interactions with EBL → strongly attenuated spectra

H.E.S.S. collaboration Science **372** (2021) 1081-5

GRB 190114C and EBL absorption

- Synchrotron self-Compton (SSC) component: Necessary or not?
- Absorption by Extragalactic Background Light (EBL)
  → large uncertainties on models
  → Need to correct spectrum

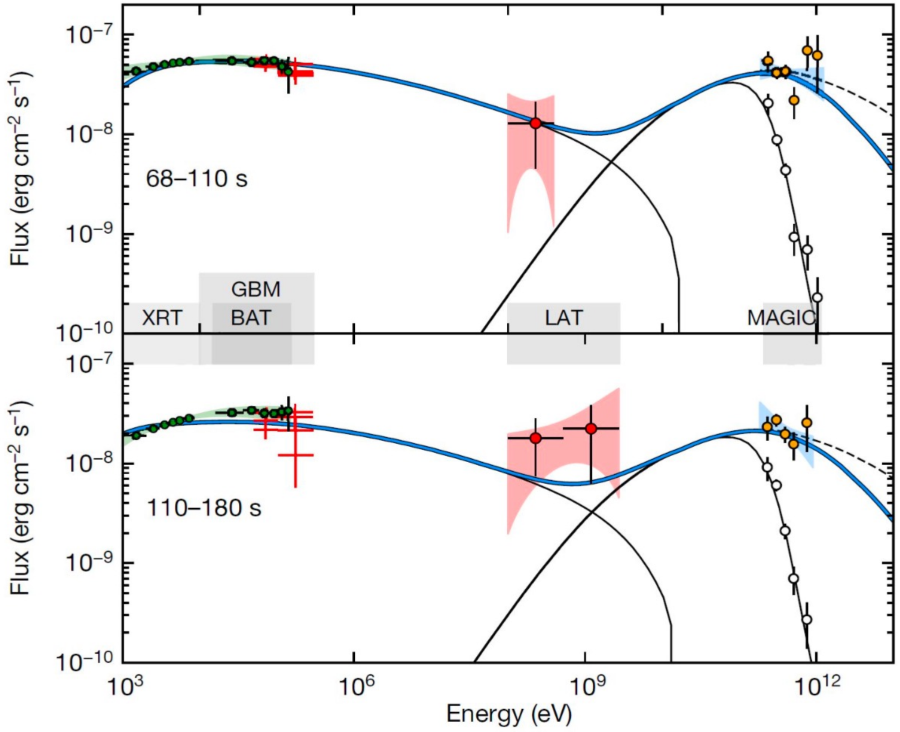

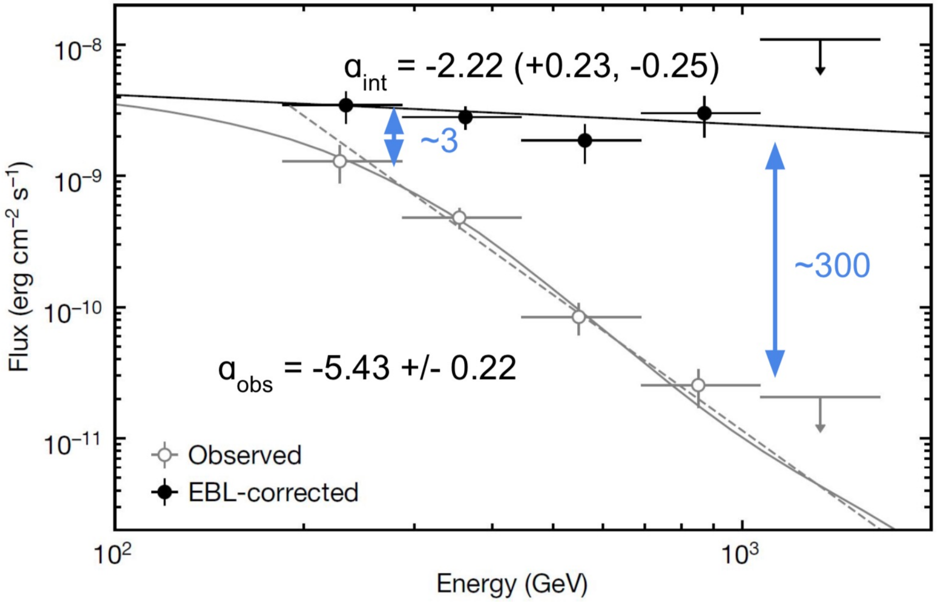

GRB 221009A – The BOAT

Brightest of all time

October 9th 2022 – extremely bright GRB (“once in 10,000 years event”)

Full moon: no IACT detection ☹

Special collection in ApJLett volume **946** (2023)

Saturated detectors (e.g. SWIFT)

LHAASO detection of > 5000 photons between 0.5 and 18 TeV (!!)
GCN 2677

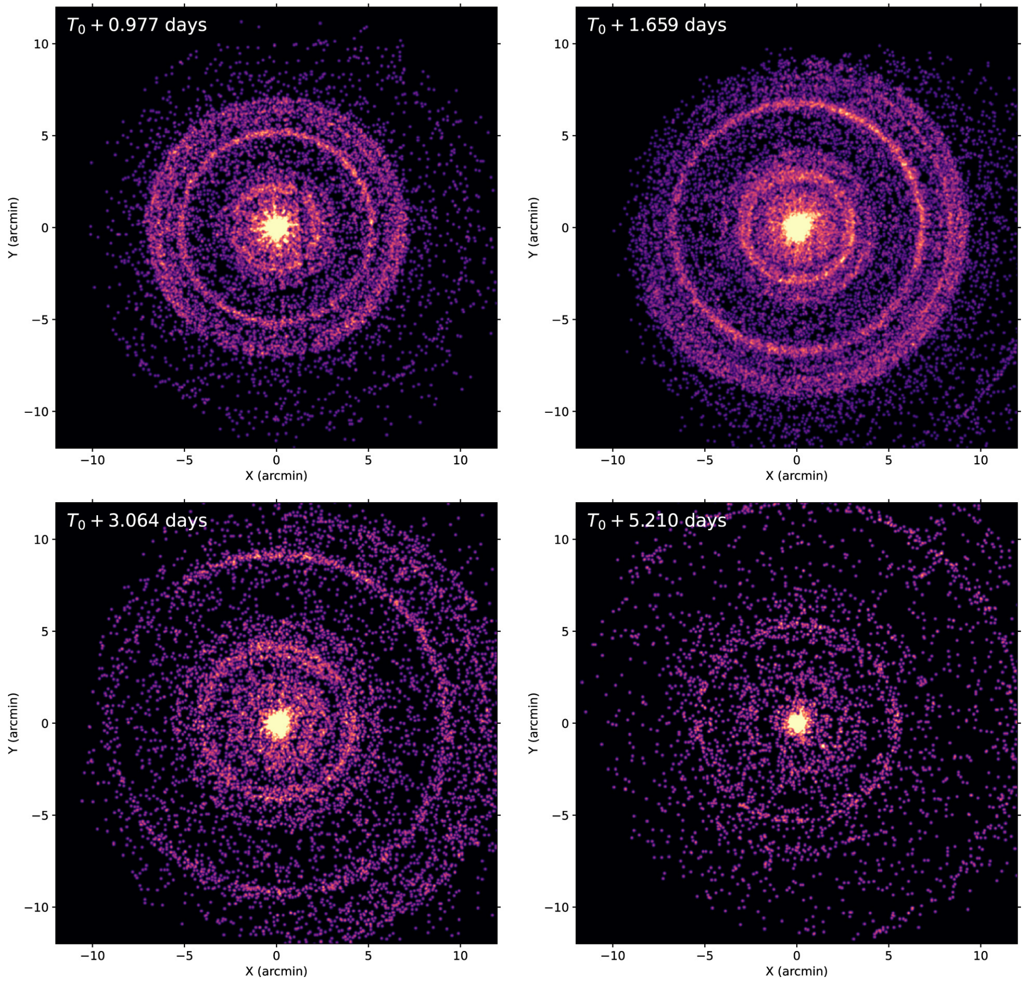

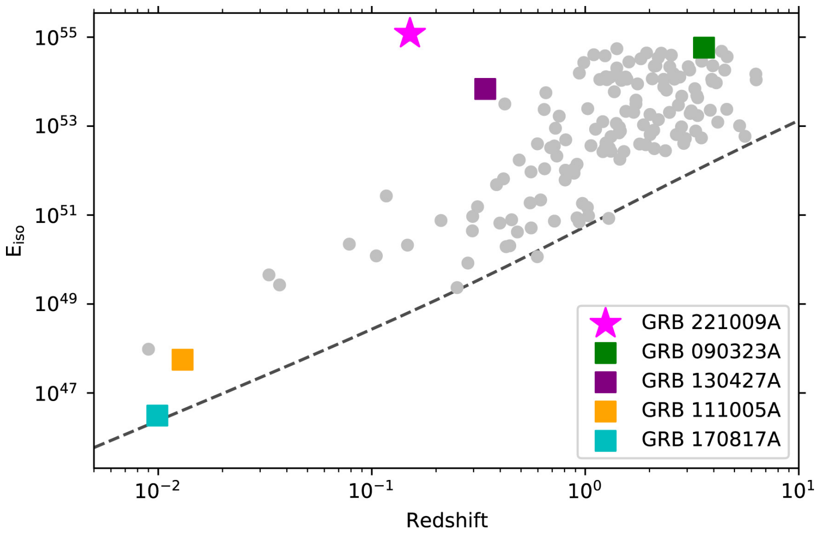

Starburst Galaxies

→ Massive & high star formation rates

→ "starburst" phase is short duration

→ Young stars are overabundant

→ Bright infrared luminosity

Detection of GeV and TeV gamma-ray emission likely from diffuse cosmic rays in the galaxy

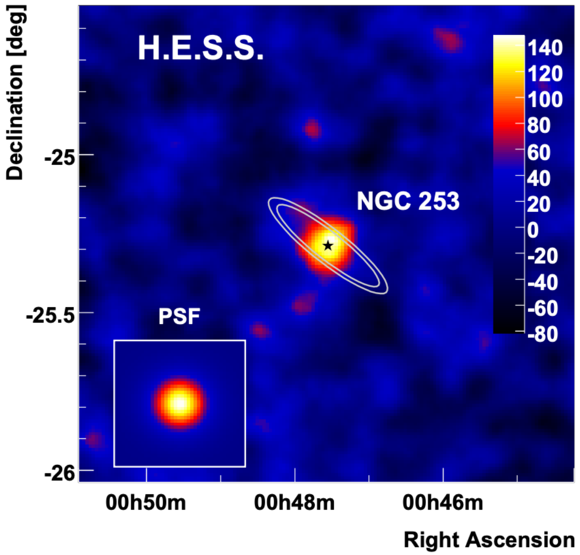

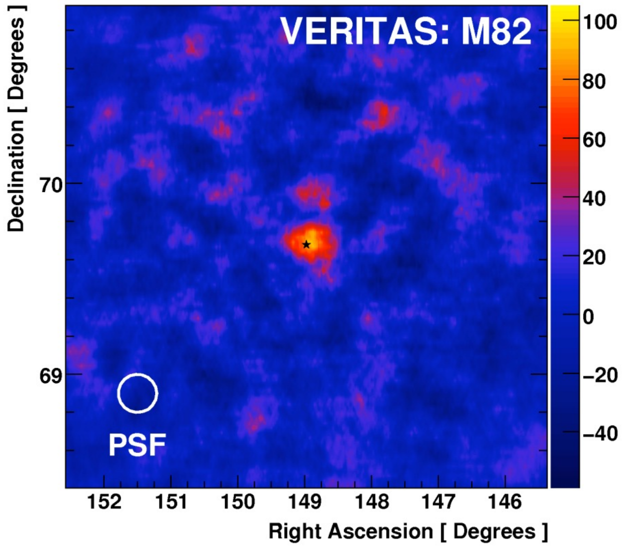

HESS collaboration, Science **326** 1080 (2009), VERITAS collaboration, Nature **462** 770 (2009)

In order of increasing luminosity:
LMC, Milky Way, NGC 253, M82 compared →

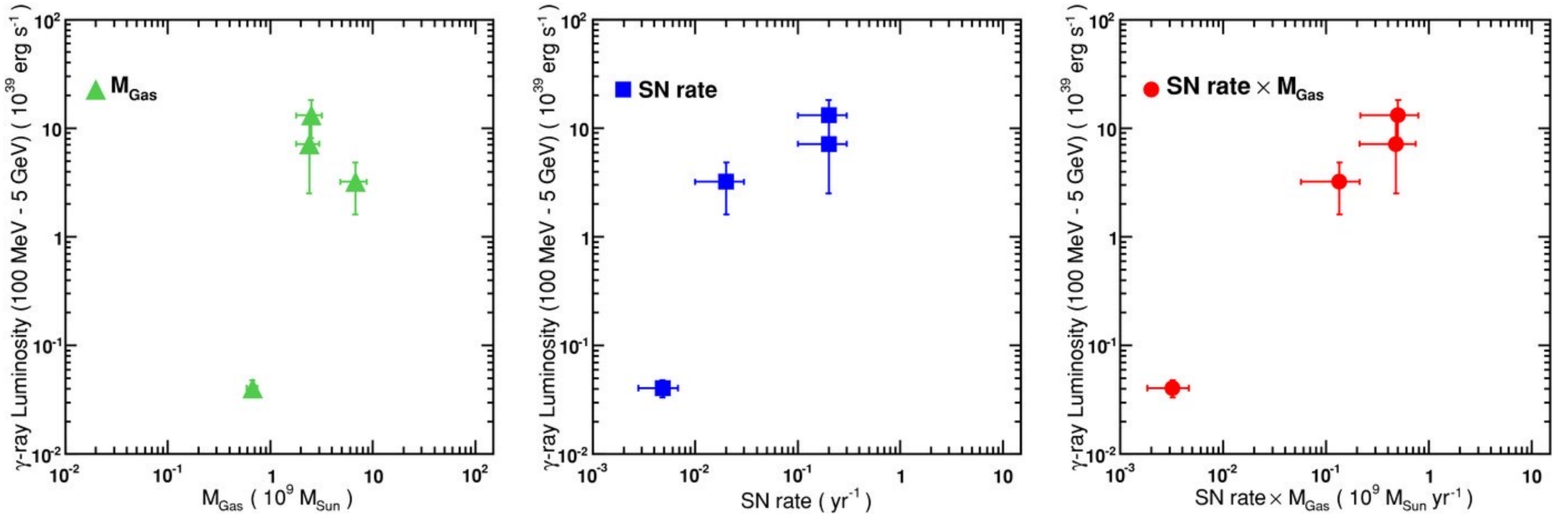

A. A. Abdo *et al* 2010 *ApJL* **709** L152

Searching for Dark Matter

Dark Matter upper limits from observations of dwarf spheroidal galaxies

Combined likelihood more constraining

Other targets: Galactic centre, Galaxy clusters...

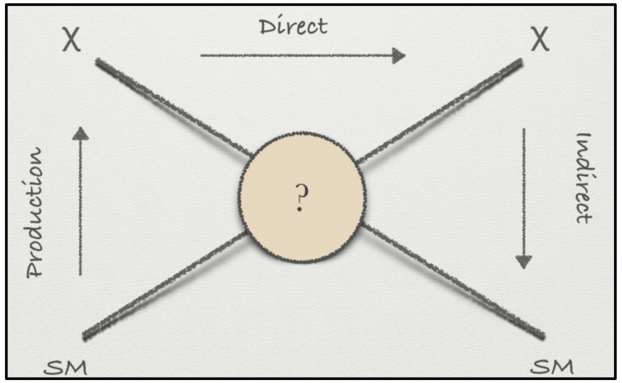

Kerszberg, Gamma2022

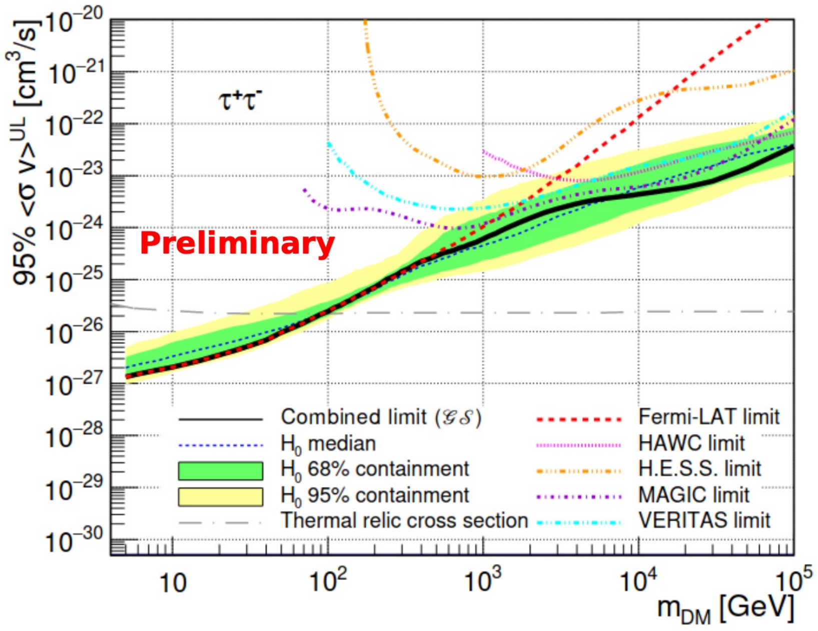

Dwarf Spheroidal Galaxies & Galaxy Clusters

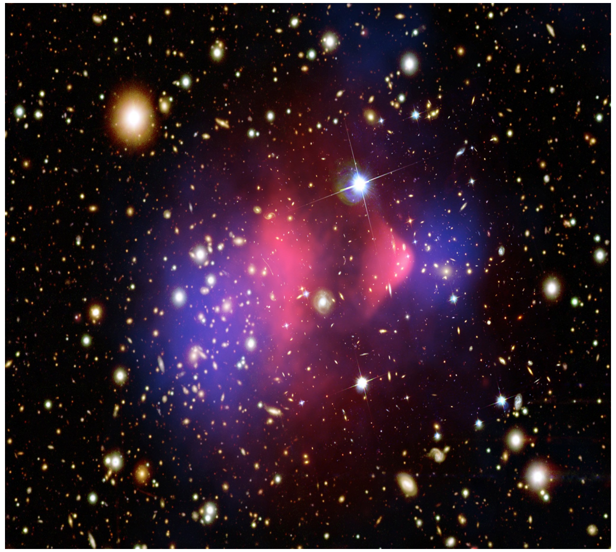

Presence of dark matter inferred in dSphs.

Stellar kinematics & virial theorem to infer mass
→ M/L ~10-1000 much larger than ordinary / spiral galaxies.

Total mass >> visible mass (no gas)

In Galaxy clusters, the mass can be inferred via lensing of background stars & dynamics

Discrepancies between visible mass and measured mass indicates the presence of dark matter

Example: Bullet cluster. Mass distribution (blue) interacts less than the visible (gas / stars) matter distribution following the collision

Gamma-ray observations of dSphs or galaxy clusters can place limits on e.g. the WIMP cross section.

Other DM candidates

Axions, Primordial BHs…

Many more exotic DM candidates

Axions → modify the gamma-ray spectrum from an extragalactic source via a boost at high energies / reduction in EBL absorption

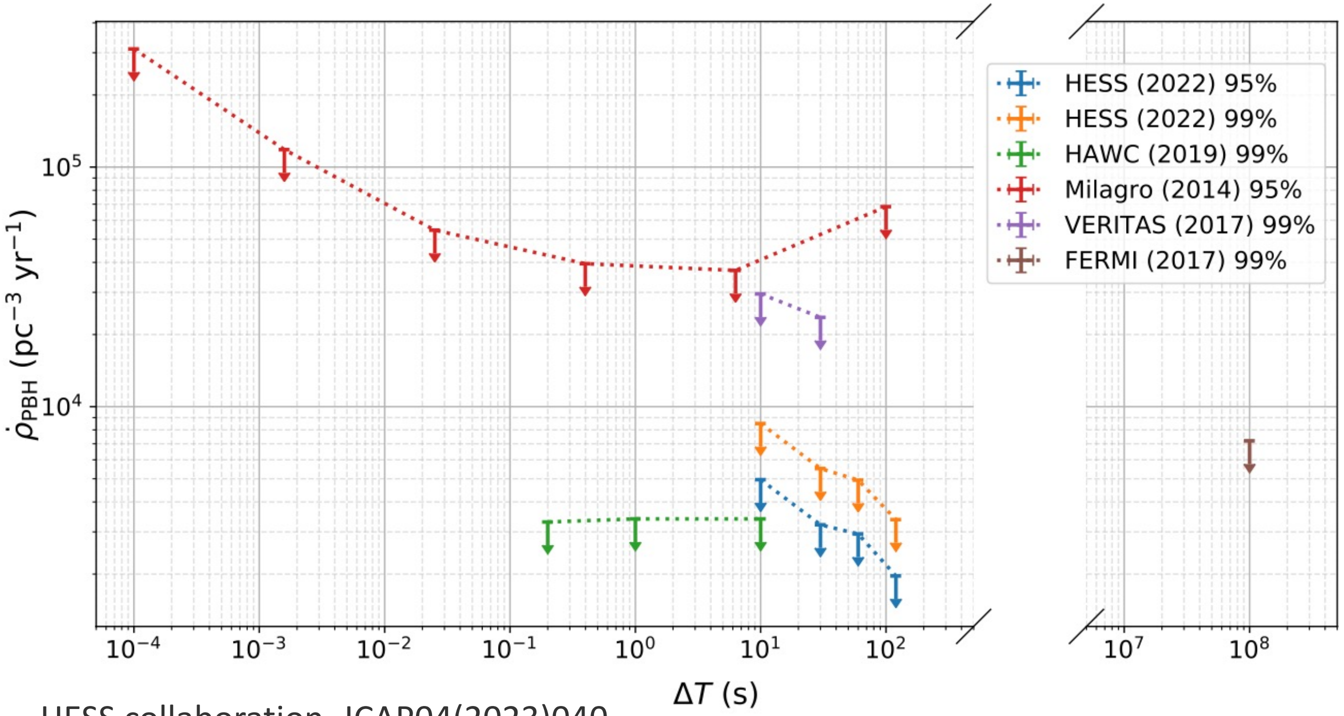

HESS collaboration, JCAP04(2023)040

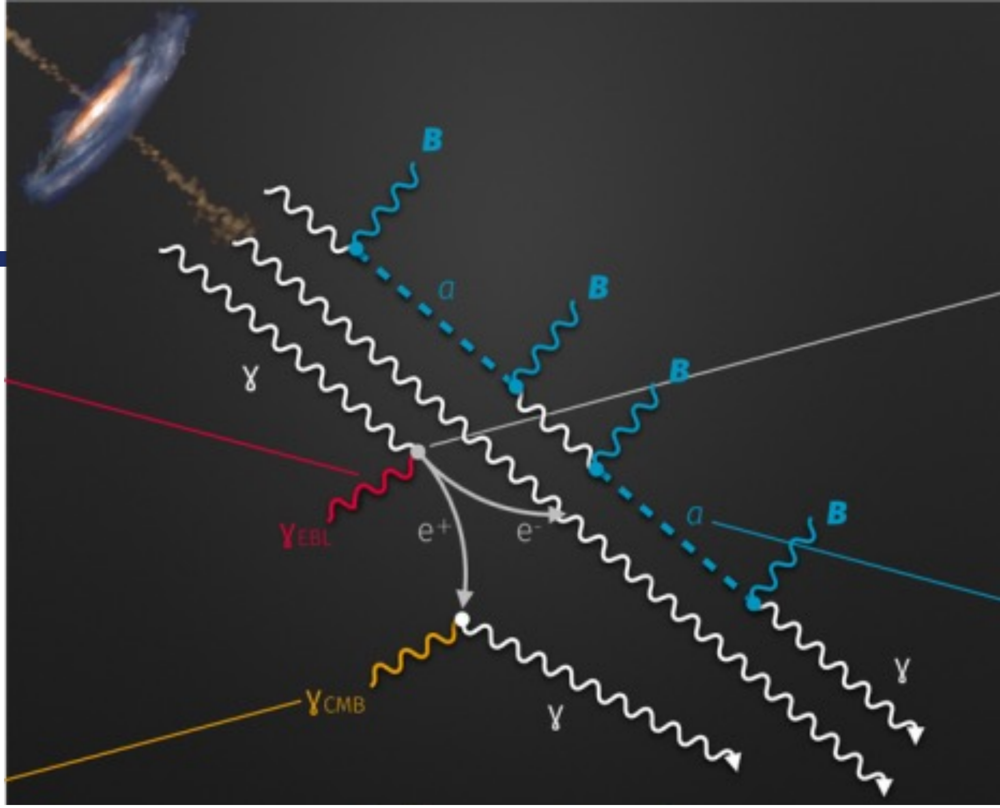

Primordial Black Holes → evaporate via Hawking radiation

For effective temperature $T_{BH} = \frac{M_p^2}{8\pi M_{BH}}$, radiation with wavelength $\lambda = 2\pi/T_{BH}$ cannot be localised within a black hole with $R_{BH} = 2GM_{BH}$ if the radius $R_{BH} \ll \lambda$

Can place limits on the primordial black hole rate.

Biteau & Meyer https://www.cta-observatory.org/what-propogation-of-energetic-light-can-tell-us/

Lorentz Invariance Violation (LIV)

- Many grand unification models and/or high-energy models that extend the validity range of relativity either require or accommodate some level of Lorentz Invariance Violation
- A common effect from this is a change in the **dispersion relation** of particles
- The effect is expected to be suppressed up to high energies
- High energy cosmic rays and gamma-rays can test this effect

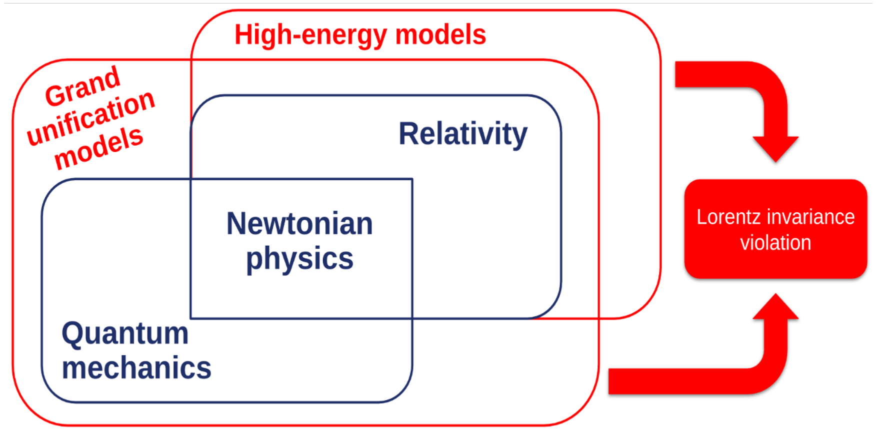

$$E_a^2 = p_a^2 + m_a^2 + \sum_{n=0}^{\infty} \delta_{a,n} E^{(n+2)}$$

Suppressed up to high energies

LIV with gamma-rays

The change in the dispersion relation may lead to several effects that would leave imprints on gamma-ray data:
(and other messengers)

- Energy dependent photon speed
  → GRBs
- Photon decay via highest energy photons
  → Crab
- Change in the interaction kinematics via EBL interactions → extragalactic spectra
- Others…

No LIV signal has been found so far, leading to very restrictive limits on the order of the effect.

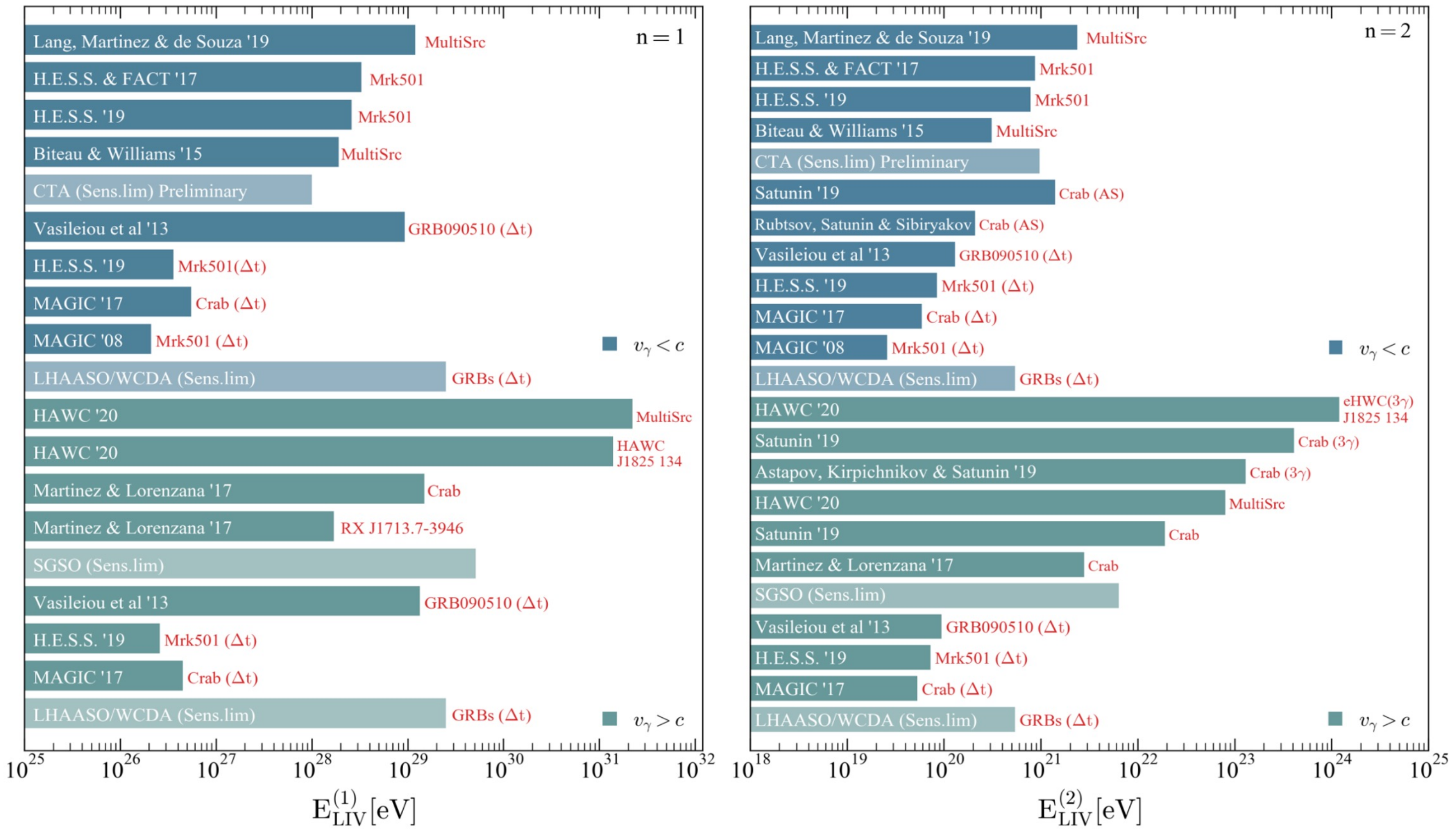

Martínez-Huerta, Lang and de Souza, Symmetry, 2020

Neutrino Astronomy:
flaring activity from AGN & Galactic sources

Majority of extragalactic sources – blazars

First indications of a neutrino source: TXS 0506+056 (z=0.3365)
Associated gamma-ray detection of flaring activity by Fermi-LAT & MAGIC
Chance coincidence disfavoured at ~3 sigma → **Multi-messenger astronomy**

Detection of the Galactic Plane in neutrinos – at 4.5σ in 10 years of IceCube data (June 2023)

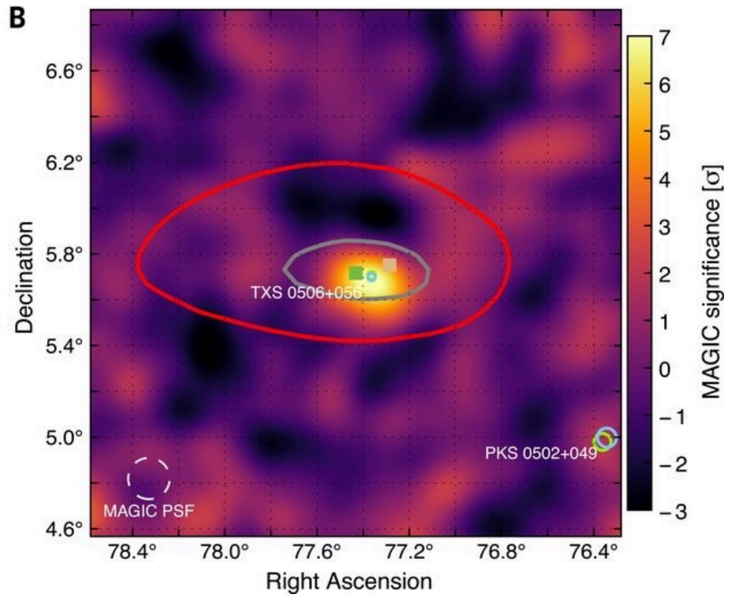

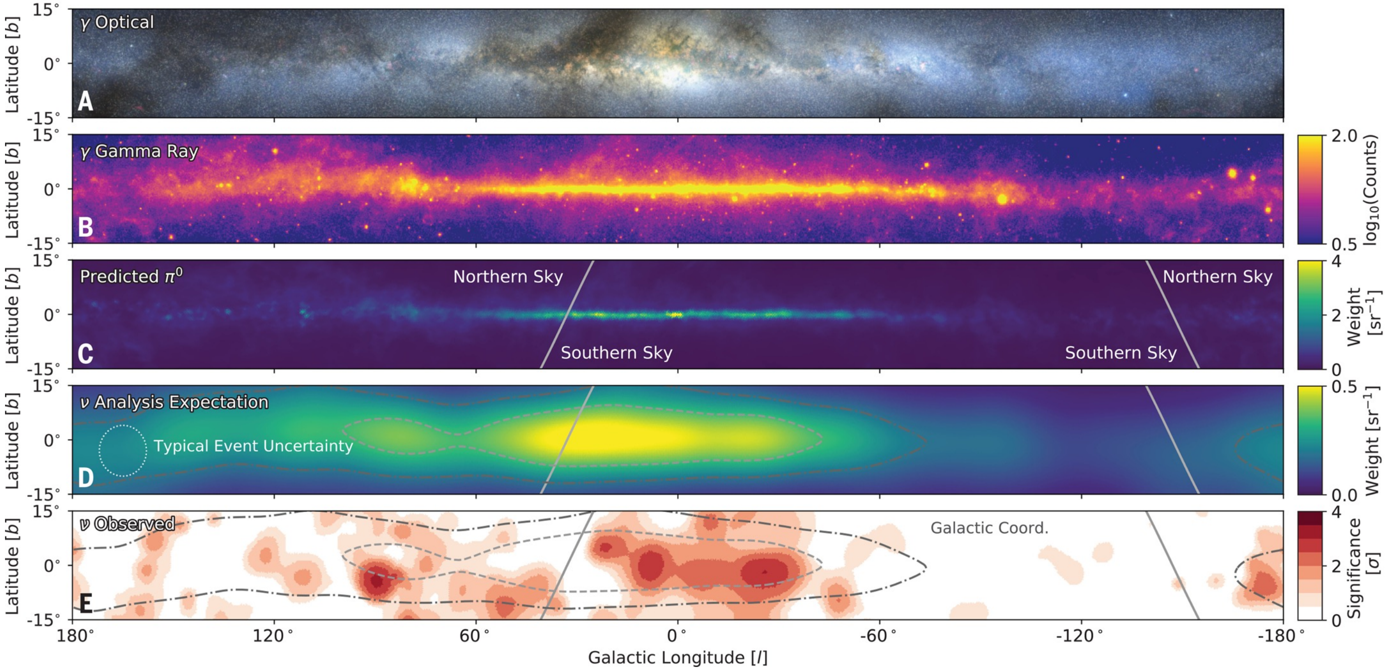

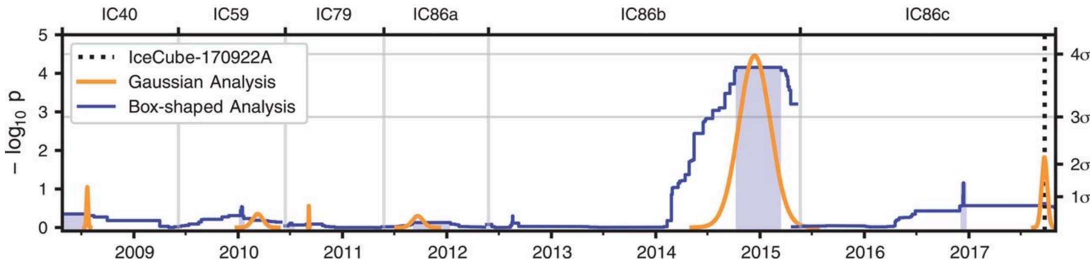

Science **361** (2018) eaat1378 Science **361** (2018) 147-151

Science **380** (2023) 1338-1343

Gravitational Waves

General relativity yields a wave equation for gravity:

$$\phi_{\mu\nu,\alpha}{}^{,\alpha} \equiv \Box\phi_{\mu\nu} \equiv -\left(\frac{1}{c^2}\frac{\partial^2}{\partial t^2} - \nabla^2\right)\phi_{\mu\nu} = -\kappa T_{\mu\nu}$$

$$\Box_\eta \tilde{h}_{\mu\nu} = -\frac{16\pi G_N}{c^4} T_{\mu\nu}$$

Which in the so-called Transverse-traceless gauge has plane-wave solutions:

$$h_{\mu\nu}^{TT} = \begin{pmatrix} 0 & 0 & 0 & 0 \\ 0 & h_+ & h_\times & 0 \\ 0 & h_\times & -h_+ & 0 \\ 0 & 0 & 0 & 0 \end{pmatrix} \cos\left[\omega\left(t - z/c\right)\right]$$

Total strain $h(t) = \frac{\Delta L}{L} = h_+(t)\cos(\omega t) + h_\times(t)\sin(\omega t)$

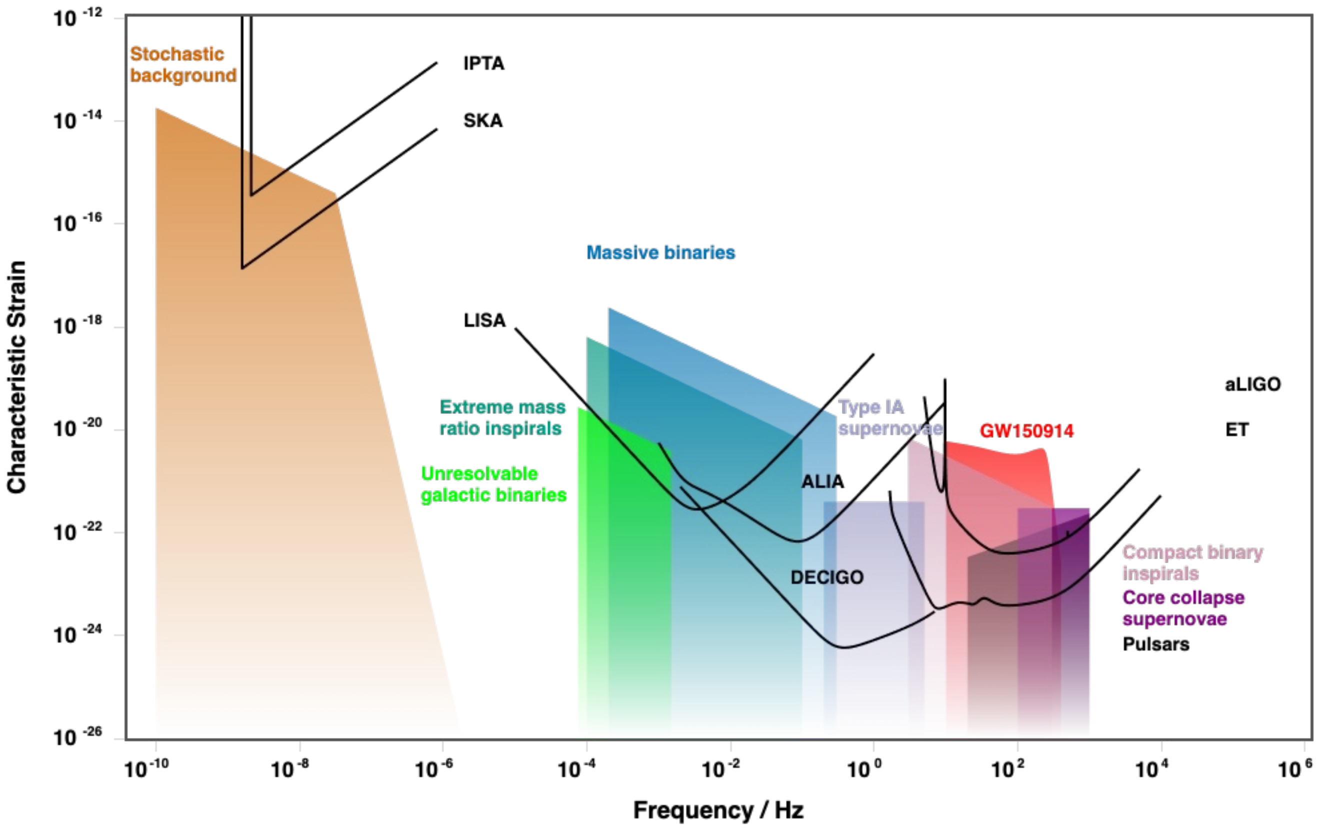

Gravitational Wave alerts

Alerts (to date) from interferometers e.g. LIGO-VIRGO

Uncertainty band from GW localisation is typically larger than IACT field-of-view

Continuously operating ground-based particle detectors can place limits, but less sensitive on short timescales / at higher energies.

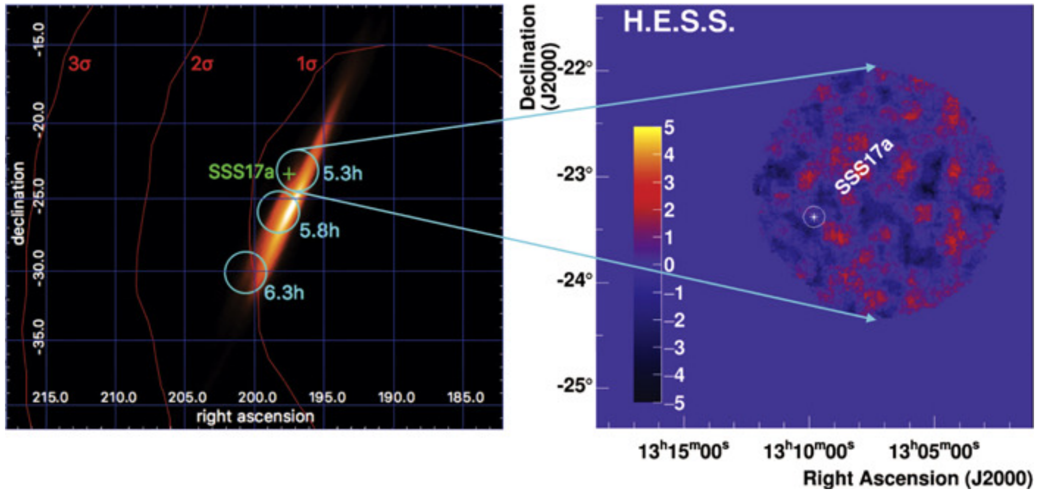

H. Abdalla *et al* 2017 *ApJL* **850** L22

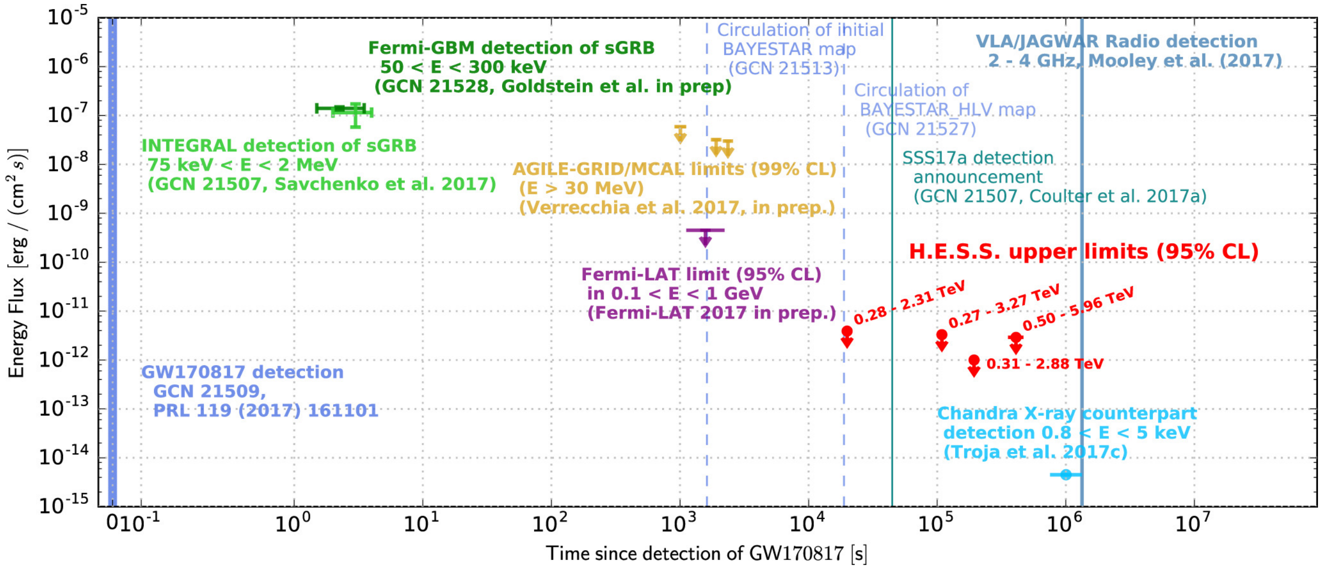

GW170817 – "Multi-messenger observations of a binary neutron star merger" B. P. Abbott *et al* 2017 *ApJL* **848** L12

(~3600 authors, ~3320 citations)

Future (IACT): quickly on target, divergent pointing...

Summary

- Gamma-ray astronomy covers a wide range of energies: 100 keV – PeV   (10 orders of magnitude!)
- Different detection methods: Compton scattering & pair-production satellites, IACTs, WCDs, scintillators...
- Detectors complementary to each other in terms of:
  Energy range, time coverage, sensitivity, resolution...
- Analysis and calibration methods are key to exploiting data fully
- Wide variety of galactic sources:
  SNRs, pulsars, PWNe, pulsar halos, stellar clusters, binary systems, illuminated clouds, unidentified...
- And extragalactic sources:
  AGN - blazars, FSRQs, Seyferts, Starburst galaxies GRBs... But the EBL imposes a horizon.
- Gamma-ray measurements can contribute to fundamental physics & multi-messenger astrophysics:
  Dark matter searches, LIV limits, neutrino & GW alerts
- And things I didn't have time to mention / aren't confirmed:
  Fermi bubbles, Hubble constant, LMXBs, SGRs...

Friedrich-Alexander-Universität
Erlangen-Nürnberg

Erlangen Centre for Astroparticle Physics

FAU

alison.mw.mitchell@fau.de

Emmy Noether-Programm
DFG Deutsche Forschungsgemeinschaft

Funded by
DFG Deutsche Forschungsgemeinschaft
German Research Foundation

Backup